

**Performance and effectiveness of adsorbents prepared from  
lignocellulosic agro-industrial residues on the abatement of leachate  
odor containing ammonia**

**Thalles Perdigão Lima**

*Dissertation submitted to the Escola Superior Agrária de Bragança to obtain the  
Degree of Master in Environmental Technology under the scope of the double diploma  
with the Centro Federal de Educação Tecnológica de Minas Gerais (CEFET-MG)*

Supervised by

**Manuel Feliciano**

**Adriana Alves Pereira Wilken**

**Jose Luis Díaz de Tuesta**

Bragança

2020

**Thalles Perdigão Lima**

**Performance and effectiveness of adsorbents prepared from  
lignocellulosic agro-industrial residues on the abatement of leachate  
odor containing ammonia**

A dissertation presented to the Escola Superior Agrária de Bragança in partial fulfillment of the requirements for the degree of Master of Science in Environmental Technology in cooperation with the Centro Federal de Educação Tecnológica de Minas Gerais (CEFET-MG) under the double diploma programme.

Supervisors:

Manuel Feliciano (IPB)

Adriana Alves Pereira Wilken (CEFET-MG)

Jose Luis Díaz de Tuesta (IPB)

Bragança

2020

## ACKNOWLEDGMENTS

Thank you, Lord, for your great love, care, mercy, and grace. During all difficulties, when I was weak, then you made me strong in you, Jesus. Thank you, mom and dad, for your unconditional love, always there for me even 8.000 km away. I thank my grandmas, cousins, uncles, aunts, and friends for sharing love, encouragement, and prayers. I thank my sister Ingrid for being supportive during the final stage of this work. I am grateful to Marina for being by my side and cheer me up in challenging times.

I want to thank my supervisors Feliciano, Adriana, and Jose, as well as professor Helder, for accepting the challenge of starting a new line of research. I am grateful to professor Feliciano for having seen potential in me and for assisting and trusting. I thank Dr. Jose for knowledge sharing, help, encouragement, and patience. I thank professor Adriana for her contributions to my formation in the past few years and for accepting the challenge of distance supervising. I am also grateful to Dr. Stephen (McCord Environmental Inc.) for supporting me since 2015 and for his valuable contribution to thoroughly reviewing this document.

I am very grateful to my colleagues Adriano, Fernanda, Gabriel, Leonardo Delgado, Leonardo Fürst, and Yago to have supported the work carried out in the laboratories and to Maria João for being always willing to help and host various laboratory tests at the Chemical Process Laboratory. I also would like to thank the volunteers for dedicating time to participate in the sensorial analysis.

I am very appreciative to the *Centro Federal de Educação Tecnológica de Minas Gerais* for the scholarship and support, in particular the professors of the *Departamento de Ciência e Tecnologia Ambiental* and staff of the *Secretaria de Relações Internacionais*. Special thanks to the Portuguese people for your welcome and to the *Instituto Politécnico de Bragança*, in particular the professors, researchers, and staff, for the outstanding support that made this work to be completed.

I am grateful to the Foundation for Science and Technology (FCT Portugal) for financial support by national funds FCT/MCTES to CIMO (UIDB/00690/2020).



For the Lord gives wisdom; from his mouth come  
knowledge and understanding.  
Proverbs 2:6

*Pois o Senhor é quem dá sabedoria; de sua boca  
procedem o conhecimento e o discernimento.  
Provérbios 2:6*

## ABSTRACT

This work aimed to prepare different adsorbent materials (bioadsorbent, pyrochar, hydrochar, and activated carbon), using olive stone and malt bagasse as feedstock and evaluating its performance and effectiveness in the adsorption of ammonia ( $\text{NH}_3$ ), deriving from composting leachate. A lab-scale adsorption system was assembled for the adsorption tests. The performance and effectiveness of the adsorbents on  $\text{NH}_3$  adsorption were evaluated objectively, by chemical analytical measurement, and subjectively by olfactometric assessment using the human sense of smell. The materials' preparation was studied to assess the biomass loss and the carbon released into the liquid phase during the hydrothermal carbonization process. Besides, resultant adsorbents were characterized to study their surface chemistry, elemental analysis, and textural properties. Saturated adsorbents were regenerated using water and subsequently re-used in the adsorption of  $\text{NH}_3$  coming from the leachate to assess their adsorption capacities after a sorption-desorption cycle. The hydrochar derived from olive stone, prepared by hydrothermal carbonization assisted by sulfuric acid ( $\text{H}_2\text{SO}_4$ ), was found as the best adsorbent for  $\text{NH}_3$  removal produced in this work since it has the lowest height of mass transfer zone (0.315 - 0.520 cm) and the highest  $\text{NH}_3$  adsorption capacity (9.445 - 11.421  $\text{mg g}^{-1}$ ). The bioadsorbent prepared only by milling and drying olive stones was also capable of adsorbing  $\text{NH}_3$ , showing a height of mass transfer zone of 0.484 - 0.565 cm, and an adsorption capacity of 0.975 - 1.455  $\text{mg g}^{-1}$ ; besides the advantage of being environmentally-sound since it requires low energy expenditure, and no chemicals are used in its preparation. The olfactometric evaluations confirmed that the adsorbents mentioned above, prepared by olive stone, can reduce odor annoyance of the gases derived from leachate. Finally, the regeneration process using water delivered adsorbents capable of being used in one  $\text{NH}_3$  sorption-desorption cycle, with satisfactory performance ( $>70\%$  of the mean  $\text{NH}_3$  adsorption capacity of its respective first-generation adsorbents), leading to increasing the materials' resource-use efficiency.

Keywords: adsorption, agro-industrial waste, biomass, leachate, ammonia.

## RESUMO

Este trabalho teve como objetivo preparar diferentes materiais adsorventes (bioadsorvente, pyrochar, hydrochar e carvão ativado), utilizando caroço de azeitona e bagaço de malte como matéria-prima e avaliar seu desempenho e eficácia na adsorção de amoníaco ( $\text{NH}_3$ ), proveniente do lixiviado de compostagem. Um sistema de adsorção em escala de laboratório foi montado para os testes de adsorção. O desempenho e eficácia dos adsorventes na adsorção de  $\text{NH}_3$  foram avaliados objetivamente, por medição analítica química, e subjetivamente, por avaliação olfatométrica usando o sentido do olfato humano. A preparação dos materiais foi estudada para avaliar a perda de biomassa e o carbono liberado na fase líquida durante o processo de carbonização hidrotermal. Além disso, os adsorventes resultantes foram caracterizados para estudar sua química de superfície, sua análise elementar e suas propriedades texturais. Adsorventes saturados foram regenerados com água e posteriormente reutilizados na adsorção de  $\text{NH}_3$  proveniente do lixiviado para avaliar sua capacidade de adsorção após um ciclo de sorção-dessorção. O hydrochar derivado de caroço de azeitona, preparado por carbonização hidrotermal assistida por ácido sulfúrico ( $\text{H}_2\text{SO}_4$ ), foi apontado como o melhor adsorvente para remoção de  $\text{NH}_3$  produzido neste trabalho, por apresentar a menor altura de zona de transferência de massa (0,315 - 0,520 cm) e a maior capacidade de adsorção de  $\text{NH}_3$  (9,445 - 11,421  $\text{mg g}^{-1}$ ). O bioadsorvente preparado apenas pela moagem e secagem do caroço da azeitona também foi capaz de adsorver  $\text{NH}_3$ , apresentando uma altura de zona de transferência de massa de 0,484 - 0,565 cm e uma capacidade de adsorção de 0,975 - 1,455  $\text{mg g}^{-1}$ ; além da vantagem de ser ambientalmente adequado, uma vez que requer baixo gasto de energia e nenhum produto químico é utilizado em sua preparação. As avaliações olfatométricas confirmaram que os adsorventes citados acima, preparados a partir de caroço de azeitona, podem reduzir a incomodidade do odor dos gases derivados do lixiviado. Por fim, o processo de regeneração com água forneceu adsorventes capazes de serem utilizados em um ciclo de sorção-dessorção de  $\text{NH}_3$ , com desempenho satisfatório (> 70% da capacidade média de adsorção de  $\text{NH}_3$  de seus respectivos adsorventes de primeira geração), levando ao aumento da eficiência de utilização dos materiais.

Palavras-chave: adsorção, resíduo agro-industrial, biomassa, lixiviado, amônia.

## TABLE OF CONTENTS

ABSTRACT .....	vi
RESUMO .....	vii
List of Tables .....	xi
List of Figures.....	xiii
List of Abbreviations, Acronyms and Units of Measure.....	xvi
1 INTRODUCTION .....	1
1.1 Background.....	1
1.2 Objectives .....	4
1.2.1 General Objective .....	4
1.2.2 Specific Objectives .....	4
1.3 Organization of the thesis .....	5
2 LITERATURE REVIEW .....	7
2.1 Organic waste .....	7
2.1.1 Agro-industrial residues .....	7
2.1.2 Legal framework on solid organic waste.....	11
2.2 Carbonaceous adsorbents.....	16
2.2.1 Carbonaceous materials.....	16
2.2.2 Adsorbent carbonaceous materials .....	17
2.2.3 Adsorbents derived from biomass .....	24
2.2.4 Regeneration of adsorbents .....	30
2.3 Odorous air emissions.....	30
2.3.1 Pollutants and sources of pollution.....	30
2.3.2 Measuring, prevention, and control.....	35
2.3.3 Adsorption of gaseous odorous pollutants .....	36
2.3.4 Legal framework on odorous air emissions.....	39

3	MATERIALS AND METHODS .....	44
3.1	General methodology.....	44
3.2	Materials and equipment.....	45
3.3	Preparation of the adsorbents.....	47
3.3.1	Bioadsorbents .....	47
3.3.2	Pyrochars .....	48
3.3.3	Hydrochars .....	49
3.3.4	Activated carbon.....	51
3.4	Carbon and mass balance.....	51
3.4.1	Biomass loss .....	51
3.4.2	TOC of the liquid effluent obtained by HTC .....	51
3.4.3	Elemental analysis .....	52
3.5	Characterization of the adsorbents.....	52
3.5.1	Surface chemistry characteristics .....	52
3.5.2	Ashes determination .....	53
3.5.3	Textural properties.....	54
3.5.4	Void fraction characteristics.....	55
3.6	Set-up of the lab-scale system .....	56
3.7	NH <sub>3</sub> concentration and adsorption.....	59
3.7.1	Evaluation of zero-air and gases derived from leachate.....	60
3.7.2	Objective evaluation of NH <sub>3</sub> adsorption.....	60
3.7.3	Subjective evaluation of NH <sub>3</sub> adsorption.....	63
3.8	Regeneration of saturated adsorbents .....	67
3.8.1	Experimental procedure.....	67
3.8.2	TOC, conductivity, and pH of the liquid phase.....	69
4	RESULTS AND DISCUSSION.....	70
4.1	Carbon and mass balance.....	70



4.1.1	Biomass loss .....	70
4.1.2	TOC of the liquid effluent obtained by HTC .....	71
4.1.3	Elemental analyses and ashes determination.....	72
4.2	NH <sub>3</sub> concentration and adsorption.....	73
4.2.1	NH <sub>3</sub> concentration in zero-air .....	73
4.2.2	NH <sub>3</sub> concentration in feed stream from leachate.....	74
4.2.3	Chemical analysis of NH <sub>3</sub> adsorption.....	76
4.2.4	Olfactometric analysis of NH <sub>3</sub> adsorption.....	79
4.3	Characterization of the adsorbents.....	82
4.3.1	Surface chemistry characteristics .....	82
4.3.2	Textural properties.....	84
4.3.3	Void fraction characteristics.....	86
4.4	Regeneration of saturated adsorbents .....	87
4.4.1	NH <sub>3</sub> adsorption with regenerated samples.....	87
4.4.2	Biomass loss .....	90
4.4.3	TOC, conductivity, and pH of the liquid phase.....	90
5	CONCLUSIONS AND RECOMMENDATIONS FOR FUTURE WORK .....	93
5.1	Conclusions.....	93
5.2	Recommendations for future work .....	94
	LIST OF REFERENCES .....	96
	APPENDIX A .....	108
	APPENDIX B.....	109
	APPENDIX C.....	110
	COMMUNICATIONS .....	113

## List of Tables

Table 1. Proximate and ultimate analysis of various agricultural waste (Yahya et al., 2015).....	8
Table 2. Lignocellulosic compositions of agricultural residues. Based on Razi et al. (2018), Yahya et al. (2015), Blanco López et al. (2002), Cagnon et al. (2009) and González et al. (2009).....	9
Table 3. Surface area values ( $\text{m}^2.\text{g}^{-1}$ ) for physically activated carbons (ACs) obtained from different lignocellulosic precursors. Adapted from González-García (2018) .....	25
Table 4. Surface area values ( $\text{m}^2.\text{g}^{-1}$ ) for chemically activated carbons (ACs) obtained from different lignocellulosic precursors. Adapted from González-García (2018) .....	27
Table 5. Characteristics and detection thresholds of the main odoriferous compounds.	34
Table 6. Types of adsorbent, process of preparation, feedstock, and sample label of the adsorbents prepared. ....	47
Table 7. Sample labeling and regeneration operating conditions.....	68
Table 8. Biomass loss (B.L) of samples prepared in this work. ....	70
Table 9. Total Organic Carbon (TOC) of the liquid phase resulting from the $\text{H}_2\text{SO}_4$ -assisted HTC processes. ....	71
Table 10. Elemental composition of the adsorbents.....	72
Table 11. Values of the mass of adsorbent ( $m$ ) and height of the adsorption bed ( $Z$ ), and the results of $\text{NH}_3$ inlet concentration ( $C_0$ ), breakthrough time ( $t_b$ ), stoichiometric time ( $t_{\text{sto}}$ ), saturation time ( $t_{\text{sat}}$ ), height of mass transfer zone ( $H_{\text{MTZ}}$ ), and dynamic adsorption capacity ( $q_a$ ). ....	77
Table 12. Acidity and basicity of the surface of fresh and saturated first-generation adsorbents. ....	83

Table 13. Textural properties of the adsorbents: specific surface area ( $S_{BET}$ ), external surface area ( $S_{ext}$ ), micropore surface area ( $S_{mic}$ ), micropore volume ( $V_{mic}$ ), total pore volume ( $V_{total}$ ), and average pore diameter ( $W_{mic}$ ). .....	85
Table 14. Void fraction characteristics determination: volume of adsorbent material ( $V_m$ ), volume of distilled water ( $V_w$ ), total volume ( $V_t$ ), void volume ( $V_{void}$ ), and void fraction ( $V_{oid}$ ). .....	86
Table 15. Values of the mass of adsorbent regenerated ( $m$ ), regeneration temperature ( $T$ ), volume of ultrapure water ( $V_{UPw}$ ), mass of regenerated adsorbent in the fixed-bed column ( $FB_m$ ), height of the adsorption bed ( $Z$ ), and the results of $NH_3$ inlet concentration ( $C_0$ ), breakthrough time ( $t_b$ ), stoichiometric time ( $t_{sto}$ ), saturation time ( $t_{sat}$ ), height of mass transfer zone ( $H_{MTZ}$ ), and dynamic adsorption capacity ( $q_a$ ). .....	89
Table 16. Parameters of the regeneration processes and biomass loss: regeneration temperature ( $T$ ), volume of ultrapure water ( $V_{UPw}$ ), initial and final mass of adsorbent, and biomass loss (B.L). .....	90
Table 17. Parameters of the regeneration processes and liquid phase characteristics: mass of adsorbent before regeneration ( $m$ ), temperature ( $T$ ), volume of ultrapure water ( $V_{UPw}$ ), TOC, and conductivity and pH of the liquid phase (before and after the regeneration). .....	92

## List of Figures

Figure 1. Waste hierarchy (European Union, 2008b).....	15
Figure 2. Representation of a carbonaceous adsorbent: (a) amorphous form; (b) porous structure with adsorbate; (c) aromatic clusters. Based on Celzard et al. (2007). .....	18
Figure 3. Schematic of pyrochar structure development under many temperature ranges (Lehmann et al., 2009).....	20
Figure 4. Hydrochar formation by hydrothermal carbonization (HTC) (Jain et al., 2016). .....	21
Figure 5. Preparation of AC by HTC, followed by chemical activation (Jain et al., 2016). .....	24
Figure 6. Ideal breakthrough curve: fixed-bed dynamic behavior in which gas is injected at a constant concentration of a particular pollutant at the column entrance. Adapted from Ang et al. (2020) and Tan et al. (2017). .....	38
Figure 7. Schematic diagram of the stages of this work.....	45
Figure 8. The feedstock (a) OS and (b) MB.....	45
Figure 9. The centrifugal mill and ring sieve with trapezoid holes used to mill the olive stones. ....	48
Figure 10. The bioadsorbents (a) OS-M and (b) MB prepared in this work. ....	48
Figure 11. The horizontal tube furnace used to perform the pyrolysis.....	49
Figure 12. The pyrochars (a) OS-M-P and (b) MB-P prepared in this work. ....	49
Figure 13. The high-pressure batch reactors used to perform the H <sub>2</sub> SO <sub>4</sub> -assisted HTC.....	50
Figure 14. The hydrochars (a) OS-M-HTC, and (b) MB-HTC prepared in this work... ..	50
Figure 15. Filtration and washing of the HTC's solid product.....	50
Figure 16. TOC analyzer used to assess the carbon released in the liquid phase.....	51

Figure 17. The flasks containing the mixture of adsorbent and solution placed in the orbital shaker. ....	52
Figure 18. The furnace used in the ash analysis. ....	54
Figure 19. Main types of physisorption isotherms established by IUPAC (Thommes et al., 2015). ....	55
Figure 20. Schematic of the set-up of the lab-scale system for evaluating: (a) zero-air (za), (b) leachate off-gases, and (c) the performance and effectiveness of the adsorbents. ....	58
Figure 21. Photo of the lab-scale system assembled. In detail: source of odor (SO), upstream gas for subjective evaluation (ugs), fixed-bed (FB) column, downstream gas for objective evaluation (dgo), downstream gas for subjective evaluation (dgs), and multi-gas analyzer (MGA). ....	59
Figure 22. Monitoring station containing the air temperature sensor and the data logger. ....	60
Figure 23. Schematic of the fixed-bed column: (1) cap, (2) glass wool, (3) mesh, and (4) adsorbent. ....	61
Figure 24. Illustration of the integration calculation using the Peak Analyzer tool in a real breakthrough curve obtained in an adsorption test performed in this work. ....	63
Figure 25. Pictures of sampling and storing steps: (a) empty sample bag, (b) sample being taken from the adsorption test, and (c) bags filled with samples stored. ....	64
Figure 26. Schematic representation of downstream samples on the breakthrough curve. $SE_{Clean}$ - at maximum removal capacity; $SE_{Break}$ - between breakthrough and stoichiometric times; $SE_{Stoic}$ - between stoichiometric and saturation times; and $SE_{Sat}$ - right after saturation. ....	65
Figure 27. Odor (a) intensity and (b) hedonic tone scales. Based on (VDI, 1992a). ....	66
Figure 28. Set-up of the olfactometric analysis: (a) olfactometer and (b) the sniffing ports in detail. ....	66
Figure 29. Set-up of the adsorbents' regeneration process. ....	68

Figure 30. Concentrations of $\text{NH}_3$ in the zero-air (za). .....	74
Figure 31. Tests that lasted 8 h: (a) temperature during the tests and (b) concentration of $\text{NH}_3$ emitted from leachate.....	75
Figure 32. Tests that lasted 24 h: temperature during the tests and concentration of $\text{NH}_3$ emitted from leachate. (a) Test 1, and (b) Test 2.....	76
Figure 33. Normalized breakthrough curves of the adsorption tests performed in this work.....	77
Figure 34. Evaluation of odor hedonic tone of samples derived from adsorption tests using (a) OS-M and (b) OS-M-HTC.....	80
Figure 35. Evaluation of odor intensity of samples derived from adsorption tests using (a) OS-M and (b) OS-M-HTC. ....	81
Figure 36. $\text{N}_2$ adsorption-desorption isotherms of the adsorbents at 77 K.....	85
Figure 37. Normalized breakthrough curves of adsorption tests using regenerated (R_X_OS-M and R_X_OS-M-HTC) and first-generation (OS-M and OS-M-HTC) samples. (A) bioadsorbents and (B) hydrochars.....	87
Figure 38. Possible improvement of the stages of this work after future studies.....	95

## List of Abbreviations, Acronyms and Units of Measure

### Abbreviations and Acronyms

<b>AC</b>	activated carbon
<b>B.L</b>	biomass loss
<b><i>dgo</i></b>	downstream gas for objective evaluation
<b><i>dgs</i></b>	downstream gas for subjective evaluation
<b><i>eo</i></b>	effluent outlet
<b>FB</b>	fixed-bed
<b>FC</b>	flow control
<b>FM</b>	flow meter
<b>HTC</b>	hydrothermal carbonization
<b>IUPAC</b>	International Union of Pure and Applied Chemistry
<b>MB</b>	malt bagasse
<b>MGA</b>	multi-gas analyzer
<b>MTZ</b>	mass transfer zone
<b>OFGs</b>	oxygenated functional groups
<b><i>og</i></b>	odorous gas
<b>OS</b>	olive stone
<b>PM<sub>10</sub></b>	airborne particles of equivalent aerodynamic diameter less than 10 $\mu\text{m}$
<b>PM<sub>2.5</sub></b>	airborne particles of equivalent aerodynamic diameter less than 2.5 $\mu\text{m}$
<b>SDGs</b>	United Nations Sustainable Development Goals
<b>SE<sub>Clean</sub></b>	sample taken downstream the FB, at maximum removal capacity
<b>SE<sub>Break</sub></b>	sample taken downstream the FB, between breakthrough and stoichiometric points
<b>SE<sub>Feed</sub></b>	gas sample taken upstream the FB
<b>SE<sub>Stoic</sub></b>	sample taken downstream the FB, between stoichiometric and saturation points

<b>SE<sub>Satur</sub></b>	sample taken downstream the FB, right after saturation point
<b>SO</b>	source of odor
<b>SP1</b>	sniffing port providing neutral air
<b>SP2</b>	sniffing port providing odor stimulus
<b>TOC</b>	Total Organic Carbon
<b>ugs</b>	upstream gas for subjective evaluation
<b>UPw</b>	ultrapure water
<b>VOCs</b>	volatile organic compounds
<b>Void<sub>f</sub></b>	void fraction
<b>WHO</b>	World Health Organization
<b>za</b>	zero-air
<b>ZAG</b>	zero-air generator

### Units of Measure

<b><math>C_o</math></b>	initial concentration of adsorbate [ppm]
<b><math>FB_m</math></b>	mass of regenerated adsorbent in the fixed-bed column [g]
<b><math>H_{MTZ}</math></b>	height of mass transfer zone [cm]
<b><math>m</math></b>	mass of adsorbent [g]
<b><math>q_a</math></b>	dynamic adsorption capacity [mg g <sup>-1</sup> ]
<b><math>Q</math></b>	gas flow rate [L min <sup>-1</sup> ]
<b><math>S_{BET}</math></b>	BET specific surface area [m <sup>2</sup> ]
<b><math>S_{ext}</math></b>	external surface area [m <sup>2</sup> g <sup>-1</sup> ]
<b><math>S_{mic}</math></b>	micropore surface area [m <sup>2</sup> g <sup>-1</sup> ]
<b><math>t_b</math></b>	breakthrough time [min]
<b><math>t_{sat}</math></b>	saturation time [min]



$t_{sto}$	stoichiometric time [min]
$V_m$	volume of adsorbent material [mL]
$V_w$	volume of distilled water [mL]
$V_{mic}$	micropore volume [mm <sup>3</sup> g <sup>-1</sup> ]
$V_{total}$	total pore volume [mm <sup>3</sup> g <sup>-1</sup> ]
$V_{void}$	volume of voids in the bed [mL]
$W_c$	weight of the crucible [g]
$W_{ci}$	weight of the crucible + weight of inorganic material [g]
$W_m$	weight of adsorbent material [g]
$W_{mic}$	average pore diameter [nm]
$Z$	height of the adsorption bed [cm]

## 1 INTRODUCTION

### 1.1 Background

Odorous pollutants may result directly or indirectly from human activities (*e.g.*, composting plants, landfills, and wastewater treatment plants). They may cause adverse effects, including various undesirable reactions, ranging from annoyance to documented health effects. In residences and workplaces exposed to odors resulting from gaseous emissions, even though the affected individuals may not immediately appear diseased or infirm, there certainly is not an atmosphere of complete mental, social, or physical well-being (Nicell, 2009).

Despite contributing to proper waste management, landfill facilities and compost plants typically are sources of odor pollution (Rincón et al., 2019). A study carried out by Cheng et al. (2019) showed that both waste treatment facilities mentioned above have  $\text{NH}_3$  as one of the most critical offensive odorants that should be considered on health risk assessment.

Agro-industrial solid waste is mostly composed of organic matter, known as biomass, that comes from plants. The biomass stores chemical energy in the form of carbohydrates (Sansaniwal et al., 2017). It is the only renewable source of carbon that can be transformed into a solid, liquid, and gaseous products through various conversion processes (Mohamed et al., 2010). Among the appropriate destinations of the biomass residue produced in agro-industrial activities is converting this inexhaustible, low-cost, and non-hazardous biomass into carbonaceous materials (Mohtashami et al., 2018).

Research is underway in the field of agricultural waste valorization as potential adsorbent materials for pollution control since they have a porous structure and a macromolecular matrix that consists of polymer chains which contain numerous polyvalent functional groups (such as carboxylic and hydroxylic reactive groups) (Calero et al., 2010). Efforts are being made to achieve sustainable production of carbonaceous materials derived from biomass. Sustainable production of these adsorbents requires proper management of biomass, water, energy, chemicals, and appropriate residuals management (Daramola & Ayeni, 2020).

Olive-based products are primary elements in the EU's southern countries' agricultural economy, with about 5 million hectares of plantations and more than €7 billion in production value every year (Rossi, 2017). The EU accounts for 70 to 75 % of the world production of olive oil. More than half of the olive plantation areas in the EU are located in Spain, and most of it is used for olive oil production (Rossi, 2017). The main byproduct generated during the processing of olives for oil production is a residue named olive cake, consisting of a mixture of crushed stones (also known as pits), seeds, peel, and pulp (Sanginés et al., 2015). The production of olives for oil and table use in the EU was about 10.5 million tons in the 2018-2019 harvesting year (Eurostat, 2020). It is estimated that olive stone (OS) ranges from 8 to 15% of the weight of the olives (Pattara et al., 2010), so that about 0.8 to 1.6 million tons of OS may have been generated during the processing of olives in the EU in 2018-2019.

Brazil is the third-largest beer producer globally, after China and EUA, and has produced 13.3 billion liters of the product in 2016 (SINDICERV, 2020). Malte bagasse (MB) is considered the most crucial residue of the beer production process (Mello & Mali, 2014). That residue is generated in the cereals' filtration used in the brewing process (Nadolny et al., 2020). It is estimated that approximately 17 to 20 kg of MB is generated to produce 100 liters of beer (Franciski et al., 2018), so that about 2.3 to 2.7 million tons of bagasse may have been generated during beer production in Brazil in 2016.

The valorization of agro-industrial biomass as a precursor of adsorbents is a practical manner to increase resource-use efficiency. It keeps natural resources in use for as long as possible, which is the principle of the circular economy (Baldikova et al., 2019). Also, it may contribute to reducing the use of non-renewable resources in the commercial production of adsorbents. Bioadsorbent, pyrochar, hydrochar, and activated carbon (AC) are types of adsorbent materials synthesized from biomass, thus producing environmentally sound adsorbents for pollutant removal (Chen et al., 2017; Eslami et al., 2018).

Bioadsorbent consists of low-cost organic matter with a natural affinity for inorganic and organic pollutants (Fomina & Gadd, 2014; Safarik et al., 2018). Pyrochar is the solid char remaining from the organic matter's thermal decomposition under an inert atmosphere, a high-carbon material with good porosity and surface area (Ioannidou & Zabaniotou, 2007). The thermal treatment removes the moisture and the volatile matter

contents of the biomass (Lehmann & Joseph, 2009; Mohamed et al., 2010). Hydrochar is a material obtained by hydrothermal carbonization (HTC), a thermo-chemical process, which uses water, heat, and high pressure to convert biomass into carbonaceous materials through fractionation of the feedstock (Daramola et al., 2020; Jain et al., 2016; Ok et al., 2016). According to the International Union of Pure and Applied Chemistry (IUPAC), AC is “a porous carbon material, a char which has been subjected to reaction with gases, sometimes with the addition of chemicals, before, during or after carbonization in order to increase its adsorptive properties” (IUPAC, 1997).

Agricultural biomass waste could be the basis of a low-cost  $\text{NH}_3$  adsorbent, allowing the recycling of residues and the abatement of air pollutants simultaneously (Kastner et al., 2009). In the literature, many studies have focused on producing adsorbents derived from biomass and their assessment of adsorption tests of gaseous pollutants derived from commercial bottles. This work presents a different approach focused on bioresource technology to produce adsorbents and their application in emission control of an odor's actual source.

Based on the three fundamental pillars of sustainability, this work seeks to improve environmental, economic, and social spheres: organic matter recycling, air pollution abatement, resource-use efficiency, environmentally sound technology development, health and well-being, and safety. As part of the 2030 Agenda for Sustainable Development, the United Nations Sustainable Development Goals (SDGs) consists of seventeen global goals for the next eleven years in areas of critical importance for humanity and the planet (United Nations, 2015). This work is directly aligned with four SDGs, as shown below.

Goal 3 (Good Health and Well-being) has included targets for air pollution prevention and control to ensure healthy lives and promote the well-being of all. The definition of “health” given by the World Health Organization (WHO) is “a state of complete physical, mental and social well-being and not merely the absence of disease or infirmity”. Given the above, the importance of controlling odorous gas emissions is noticeable because even the odor annoyance can affect well-being.

Goal 9 (Industries, Innovation, and Infrastructure) includes targets for increased resource-use efficiency and greater adoption of clean and environmentally sound technologies and industrial processes. Agro-industrial biomass's valorization as a

precursor of adsorbents is a practical manner to increase resource-use efficiency, producing an environmentally sound technology for pollutant removal. Additionally, re-using this recovered product reduces non-renewable material on commercial adsorbents' production.

Goal 11 (Sustainable Cities and Communities) includes targets for reducing adverse per capita environmental impact of cities and communities by paying particular attention to air quality and municipal and other waste management. Once again, the importance of controlling gas emission is evident, including the odorous ones, and besides the proper management of agro-industrial waste, not to mention the agricultural biomass.

Goal 12 (Responsible Consumption and Production) includes targets for the environmentally sound management of chemicals and all wastes throughout their life cycle by reducing their release to air, water, and soil to minimize their adverse impacts on human health and the environment. This goal also includes targets for substantial waste generation abatement through prevention, reduction, recycling, and re-use. Reiteratively recycling organic biomass by converting it into new materials reduces waste released into the environment, reducing its adverse impacts.

## 1.2 Objectives

### 1.2.1 General Objective

This thesis aims at preparing adsorbent materials using olive stone and malt bagasse as feedstock and evaluates its performance and effectiveness in the adsorption of  $\text{NH}_3$ , deriving from leachate originated from a composting line of mechanical and biological treatment of municipal organic wastes, by using an experimental system developed for this purpose.

### 1.2.2 Specific Objectives

The specific objectives of this research are to:

- I. provide a literature review about agro-industrial residues, carbonaceous adsorbents and odorous air emissions;

- II. prepare adsorbent materials using agro-industrial organic residues as feedstock;
- III. characterize the materials produced;
- IV. set-up an experimental adsorption system;
- V. evaluate the odorous pollutant  $\text{NH}_3$ , generated from zero-air generator and leachate, regarding emission rates;
- VI. evaluate the performance and effectiveness of the materials in the adsorption of  $\text{NH}_3$  by chemical analytical measurement;
- VII. prepare a low-cost olfactometer to access the olfactory analysis;
- VIII. evaluate the performance and effectiveness of the materials in the adsorption of  $\text{NH}_3$  by olfactometric assessment;
- IX. evaluate the regeneration of adsorbents saturated with  $\text{NH}_3$  by an environmentally sound process.

### 1.3 Organization of the thesis

Chapter 1 introduces the thesis. Firstly, it presents the background of the central themes, including the emission and negative impacts of odorous pollutants, agro-industrial organic waste production and valorization, the adsorption of odorous pollutants, and the sustainable approach of this work confirmed by its alignment with the United Nations Sustainable Development Goals (SDGs). The background is followed by the presentation of the general and specific objectives of this work.

Chapter 2 presents relevant literature regarding organic waste, carbonaceous adsorbents, and odorous emissions. The first topic presents the characteristics of lignocellulosic residues, its different applications, and the Brazilian and Portuguese legal frameworks on this theme. The second topic presents the various applications of carbonaceous materials, the types and characteristics of adsorbents derived from biomass, and the regeneration processes for re-use. Lastly, the third topic presents the pollutants and sources of odor, the prevention and methods of measuring and controlling odorous emissions, the methods of adsorption of odorous pollutants, and the Brazilian and Portuguese legal frameworks on this theme.

Chapter 3 covers the detailed methodology of this work, which was developed based on the literature. The materials and equipment used are presented. The methods of preparation of four types of adsorbents are described. The methods to determine the biomass loss, the total organic carbon in the liquid effluent, and elemental analysis of the adsorbents are presented. The methods of characterization of the adsorbents regarding surface chemistry characteristics, ashes, textural properties, and void fraction are presented. The setting-up of the lab-scale system assembled to run adsorption tests is explained. The evaluation methods of zero-air and leachate off-gases, and the objective and subjective evaluation of  $\text{NH}_3$  adsorption are detailed. Lastly, it presents the regeneration method of the adsorbents saturated with  $\text{NH}_3$  using water and the characteristics of this process's liquid effluent.

Chapter 4 presents the results obtained after the development of the steps explained in Chapter 3.

Finally, Chapter 5 presents the conclusions and recommendations for future work.

## 2 LITERATURE REVIEW

This literature review chapter begins with organic waste, presenting the lignocellulosic residues' characteristics, its different applications, and the Brazilian and Portuguese legal frameworks on this theme. The following topic presents the various applications of carbonaceous materials, the types and characteristics of adsorbents derived from biomass, and the regeneration processes for re-use. The final topic presents the pollutants and sources of odor, the prevention and methods of measuring and controlling odorous emissions, specifies the adsorption method, and the Brazilian and Portuguese legal frameworks on this theme.

### 2.1 Organic waste

#### 2.1.1 Agro-industrial residues

The European Commission defines waste as “any substance, material, or object which the holder discards or intends or is required to discard” (European Union, 2008b), and therefore, is no longer useful for the holder (Islas et al., 2019). Solid waste is any waste in the solid and semi-solid state resulting from industrial, domestic, hospital, commercial, agricultural, or municipal activities (ABNT, 2004). The waste may be divided into two main groups: organic waste (composed of organic matter); and non-organic waste (composed essentially of inorganic matter).

Agro-industrial solid waste is mostly composed of organic matter, known as biomass, that comes from plants. The biomass stores chemical energy in carbohydrates by combining solar energy and carbon dioxide using the photosynthesis process (Sansaniwal et al., 2017). It is considered the only renewable source of carbon that can be transformed into a solid, liquid, or gaseous products through diverse processes (Mohamed et al., 2010).

The OS, MB, and other agricultural organic waste are considered non-hazardous, which means that, because of its physical, chemical, and infectious properties, it does not pose risks to human health, either to the environment when properly managed (ABNT, 2004). However, many developing countries produce immense biomass waste and



destroy or burn them inefficiently, causing pollution of the environment (Bhatnagar et al., 2016).

Most agricultural wastes are considered carbon-containing lignocellulosic materials (Uçar et al., 2009). The high amounts of carbon (C), oxygen (O), and hydrogen (H) present in this type of waste are related to the three major structural polymers present in lignocellulosic feedstock: cellulose, hemicellulose, and lignin (González-García, 2018). Table 1 presents the composition of various agricultural wastes, by proximate and ultimate analysis, based on a scientific literature review carried out by Yahya, Al-Qodah, & Ngah (2015).

*Table 1.* Proximate and ultimate analysis of various agricultural waste (Yahya et al., 2015).

Agricultural waste	Proximate analysis (% w/w)			Ultimate analysis (% w/w)				
	Moisture	Ash	Volatiles	C	H	N	S	O
Palm shell	7.96	1.10	72.47	50.01	6.90	1.90	0.00	41.00
Palm stem	6.06	4.02	72.39	45.56	5.91	0.82	-	47.71
Grape stalk	15.69	10.16	51.08	46.14	5.74	0.37	0.00	36.60
Bamboo	-	3.90	80.60	43.80	6.60	0.40	0.00	-
Coconut shell	8.21	0.10	73.09	48.63	6.51	0.14	0.08	44.64
Olive mill	<5.0	<1.0	-	45.64	6.31	1.42	-	-
Almond shell	10.00	0.60	80.30	50.50	6.60	0.20	0.01	42.69
Walnut shell	11.00	1.30	71.80	45.10	6.00	0.30	0.00	48.60
Almond tree pruning	10.60	1.20	72.20	51.30	6.50	0.80	0.04	41.36
Olive stone	10.40	1.40	74.40	44.80	6.00	0.10	0.01	49.09
Bamboo	2.44	6.51	69.63	45.53	4.61	0.22	-	-
Durian shell	11.27	4.84	-	39.30	5.90	1.00	0.06	53.74
Chinese fir sawdust	4.88	0.32	79.92	48.95	6.54	0.11	0.00	39.20
Banana empty fruit bunch	5.21	15.73	78.83	41.75	5.10	1.23	0.18	51.73
<i>Delonix regia</i> fruit pods	0.22	2.80	92.03	34.22	4.50	1.94	0.42	58.91
Corn cob	4.30	0.90	78.70	46.80	6.00	0.90	-	46.30
Pomegranate seed	5.38	1.83	78.71	49.65	7.54	4.03	0.65	38.13
Birch	4.40	0.18	-	48.40	5.60	0.20	-	45.80
Salix	7.30	0.75	-	48.80	6.20	1.00	-	43.40
Sugarcane bagasse	6.20	0.90	-	47.30	6.20	0.30	-	46.20
Wheat straw	3.30	3.23	-	46.50	6.30	0.90	-	46.30
Bagasse	-	6.20	83.30	41.55	5.55	0.03	-	52.86
Rice husk	-	16.70	67.50	36.52	4.82	0.86	-	41.10
Cassava peel	11.40	0.30	59.40	59.31	9.78	2.06	0.11	28.74
Rice stalk	14.17	14.93	66.33	40.79	7.66	1.17	0.49	49.89
Woody birch	6.60	0.20	81.20	48.40	5.60	0.20	-	45.80

In the case of OS, elemental analysis has shown the composition weight percentages (%wt): 43.1 – 52.34 C; 5.9 – 7.11 H; 0.03 - 1.0 nitrogen (N); 0.01 – 0.8 sulfur (S); 40.47 – 49.1 O, and 0.37 – 4.4 ash (Cagnon et al., 2009; Ghouma et al., 2015; González et al., 2009; Martín-Lara et al., 2013). The amount of elemental C of OS is considered one of the highest among various stone fruits (Saleem et al., 2019). On the other hand, MB elemental analysis has shown the %wt: 46.84 C; 8.18 H; 3.86 N; 0.38 S; 40.74 O, and 2.78 ash (Franciski et al., 2018; Mello et al., 2014).

All three major structural polymers (cellulose, hemicellulose, and lignin) play an essential role in the porosity of the chars and ACs. The lignin has been identified as the main component responsible for high values of the external area and good porosity characteristics (Cagnon et al., 2009; González et al., 2009; Williams & Besler, 1993). Table 2 shows the lignocellulosic composition of a variety of agricultural wastes based on scientific literature reviews.

*Table 2.* Lignocellulosic compositions of agricultural residues.  
Based on Razi et al. (2018), Yahya et al. (2015), Blanco López et al. (2002), Cagnon et al. (2009) and González et al. (2009).

<b>Agricultural waste</b>	<b>Lignin (%)</b>	<b>Cellulose (%)</b>	<b>Hemicellulose (%)</b>
Almond shell	24.8	32.5	25.5
Almond tree pruning	25.0	33.7	20.1
Apple pulp	21.0	16.0	16.0
Banana empty fruit bunch	19.06	8.3	21.23
Cassava waste	2.2	18.47	6.01
Cocoa pods	0.95	41.92	35.26
Coconut husk	3.54	0.52	23.7
Coconut shell	30.1-50.0	14.0-19.8	32.0-68.7
Flamboyant fruit pod	23.36	13.9	24.13
Kola nut pod	21.29	38.72	40.41
Lemon waste	7.22	18.49	6.07
Olive stone	32.6-50.45	11.82-30.8	15-24.16
Palm shell	53.4	29.0	47.7
Plantain peel (ripe)	1.63-1.75	13.87	15.07
Plantain peels (unripe)	1.75	10.15	11.38
Plum pulp	39.0	6.5	14.5
Plum stone	49.0	23.0	20.0

(continued)

*Table 2.* Lignocellulosic compositions of agricultural residues.  
Based on Razi et al. (2018), Yahya et al. (2015), Blanco López et al. (2002), Cagnon et al. (2009) and González et al. (2009).

<b>Agricultural waste</b>	<b>Lignin (%)</b>	<b>Cellulose (%)</b>	<b>Hemicellulose (%)</b>
Pomegranate seed	39.67	26.98	25.52
Soft wood	30.5	36.0	18.5
Sugarcane bagasse	18.0-24.0	42.2-55.0	20.0-36.0
Walnut shell	18.2	40.1	20.7

OS is composed predominantly of lignin with approximately 32.6 – 50.45% lignin; 11.82 – 30.8 % cellulose; and 15.0 – 24.16% hemicellulose, thus making it ideal as precursors for adsorbents (Blanco López et al., 2002; Cagnon et al., 2009; Razi et al., 2018; Saleem et al., 2019; Yahya et al., 2015). On the other hand, MB is approximately 24.05 – 26.13% lignin; 11.35 – 12.29 % cellulose; and 23.41 – 28.97% hemicellulose, also ideal as a precursor for adsorbents (Mello et al., 2014).

Several lignocellulosic wastes are potential feedstock for bioenergy production, as liquid biofuels (via pyrolysis) or solid fuels (biomass pellets) (Volpe et al., 2018). Biofuel can be produced from several food crops, including grains (maize, sorghum, and wheat), sugar crops (sugarcane, sugar beet), starch crops (cassava), oilseed crops (canola/rape, soybean, and oil palm), and olive crops (olive stones) (Bordonal et al., 2018). Despite savings in greenhouse gases emissions, by substituting fossil fuels, the combustion of biomass usually results in other atmospheric pollutants that may also be detrimental to the environment and human health (*e.g.*, volatile organic compounds (VOCs), carbon monoxide (CO), nitrogen oxides (NO<sub>x</sub>), and particulates (soot and ash)) (Sanginés et al., 2015).

Thanks to the development of various waste recycling technologies, an increasing number of technological solutions for agricultural waste are emerging (Spalvins et al., 2018). Among the technological approaches, it is the extraction of high value-added products such as enzymes, single-cell oil, building block chemicals, single-cell protein (Spalvins et al., 2018), nanocellulose (Rajinipriya et al., 2018); and supercritical carbon dioxide extraction of waxes from waste (Al Bulushi et al., 2018). In the construction sector, oil palm shells have been found useful as coarse aggregate in structural concrete (Mannan & Ganapathy, 2004). Various agricultural waste has been found helpful in

developing bricks (Raut et al., 2011). Treuer et al. (2017) observed a good synergism between orange peels and pulp, tropical forest restoration, and carbon sequestration in Costa Rica.

Adsorption has been successfully employed to remove inorganic and organic pollutants in the environment in general (Dai et al., 2018). The use of biomass waste for this purpose reduces the environmental waste burden and achieves the effect of treating pollution with waste (Y. Y. Huang, 2017).

## 2.1.2 Legal framework on solid organic waste

### 2.1.2.1 Brazilian Approach

The Brazilian *Política Nacional de Resíduos Sólidos* (National Policy on Solid Waste), established by Law nº 12.305, of 02 August 2010 (Brasil, 2010), provides guidelines on integrated management of solid waste, the responsibilities of the waste producers and public authorities, and the applicable economic instruments. The approval of Law nº 12.305 has initiated joint work between the public spheres, the productive sector, and civil society to search for solutions to solid waste problems.

In conformity with Article 6, the sustainable development and the recognition of reusable and recyclable solid waste as an economic good of a social value stand out as principles of the abovementioned Policy. In accordance with Article 7, essential objectives of this law are (II) the non-generation, reduction, re-use, recycling, and treatment of solid waste, as well as environmentally appropriate final disposal of waste; and (IV) the adoption, development, and improvement of clean technologies as a means of minimizing negative environmental impacts.

Article 8 brought among the policy's essential instruments the scientific and technological research. Article 14 presented a critical plan, the *Plano Nacional de Resíduos Sólidos* (National Plan on Solid Waste), which covers the many types of waste generated in the country, possible waste management alternatives, as well as corresponding goals and actions for various scenarios.

Law nº 12.305 mentions the term “organic waste” only once in Article 36 as a shared responsibility (V) implementing a composting system for organic waste and

articulating ways of using the produced compost. Although the above exposed, based on the definition of “recycle” given by Article 3 as “waste transformation processes that involve chemical, physical-chemical or biological changes, in view of producing inputs or new products”, recycling of organic waste should not be only by biological processes but also by chemical and physical-chemical processes.

It was possible to verify many Brazilian legal texts regulating the production and use of biofertilizers derived from organic waste (e.g., Law nº 6.894/80, Decree nº 4.954/04); however, no legal documents discuss other applications of recycled organic waste.

Regarding the local legal framework, the *Política Estadual de Resíduos Sólidos* (State Policy on Solid Waste) of Minas Gerais, established by Law nº 18.031 (Minas Gerais, 2009), of 12 January 2009, provides guidelines on integrated management of solid waste in the state of Minas Gerais. Article 51 mentions organic waste just twice. A public financial incentive is offered for initiatives that use municipal and rural organic waste for energy production and rural organic waste recovery from intensive livestock. Law nº 21.557 (Minas Gerais, 2014), of 22 December 2014, adds to Law nº 18.031 the prohibition of using incineration technology as the final destination of municipal waste, including the organic fraction.

It was observed that, as well as the federal legal documents, the local legislation in Minas Gerais does not cover the incentive or application of technologies for recycling organic waste.

#### 2.1.2.2 European and Portuguese approach

Directive 2008/98/EC (European Union, 2008b) of the European Parliament and the European Council, of 19 November 2008, also called Waste Framework Directive, defines key concepts such as waste, recovery, and disposal. It also establishes the requirements for managing waste, including the obligation for an establishment or undertaking carrying out waste management operations to obtain a permit or be registered and an obligation for the Member States to formulate waste management plans. Those plans shall, alone or in combination, cover the entire geographical territory of the EU's States.

The directive mentioned above brings important definitions in Article 3. First, “treatment” is defined as “recovery or disposal operations, including preparation before recovery or disposal”. This definition brings the word “recovery”, which is defined as “any operation the principal result of which is waste serving a useful purpose by replacing other materials which would otherwise have been used to fulfill a particular function, or waste being prepared to fulfill that function, in the plant or the wider economy”. Annex II sets out a non-exhaustive list of recovery operations, among which is the R3 – Recycling/reclamation of organic substances which are not used as solvents (including composting and other biological transformation processes). It includes preparing for re-use, gasification, and pyrolysis using the components as chemicals and recovery of organic materials in the form of backfilling. The term “recycling” pointed before is defined as “any recovery operation by which waste materials are reprocessed into products, materials or substances whether for the original or other purposes. Based on the definitions and processes presented above, reprocessing of organic material, which includes processing and use of agricultural biomass waste as a precursor of adsorbents, it is a recycling treatment, but the energy recovery and the reprocessing into materials that are to be used as fuels or for backfilling are not.

Nonetheless, Article 2 excludes from the scope of the Directive 2008/98/EC “...straw and other natural non-hazardous agricultural or forestry material used in farming, forestry, or to produce energy from such biomass through processes or methods which do not harm the environment or endanger human health”. As Annex III does not cover the agricultural biomass waste, it is characterized as natural non-hazardous waste.

Despite the exclusion of agricultural waste from its scope, the Directive 2008/98/EC includes food processing plants as “bio-waste”, according to its Article 3. It also demonstrates that promoting the separate collection and adequate treatment of bio-waste is fundamental to produce environmentally safe compost and other bio-waste-based materials.

There are no specific legal EU documents regarding agro-industrial organic waste production and destination. However, the European Waste List, established by Decision 2014/955/UE, of 18 December 2014 (European Union, 2014), presents the list of waste referred to in Article 7 of Directive 2008/98/CE. It is a harmonized list of waste that considers the origin and composition of the waste. The waste from agriculture,

horticulture, aquaculture, forestry, hunting, and fishing is defined by the four-digit code 0201. OS and MB are included in the abovementioned group as a plant-tissue waste, represented by the six-digit code 020103.

Directive 2018/851/EC (European Union, 2018) of the European Parliament and the European Council, of 30 May 2018, introduced an amendment to Directive 2008/98/CE on solid waste. The first topic of Directive 2018/851/EC presents the need to improve and transform “waste management” into “sustainable material management” to protect, preserve, and improve the environment’s quality. Another critical point of this amendment concerns improving resource use, valuing waste, reducing dependence on imported raw materials, and facilitating the transition to more sustainable material management and a circular economy model. The amendment takes measures on sustainable production and consumption by focusing on the whole life cycle of products to preserve resources and closes the loop to make the economy truly circular.

Considering the circular economy approach’s inclusion as an essential matter in waste management, recycling materials to use them for technological applications can improve the environment’s quality. The use of recycled agricultural biomass as adsorbents of pollutants contributes twice to the environmental quality improvement once it reinserts the material in the process, as proposed by the circular economy, and simultaneously contributes to pollution control.

Portuguese Decree-Law n° 73/2011(Portugal, 2011), of 17 July 2011, introduced the third amendment to Decree-Law n° 178/2006, of 05 September 2006, with changes in the general regulation of waste management and transposed Directive 2008/98/CE. Under the Member States’ obligation to draw up waste management plans, imposed by Directive 2008/98/EC, Portugal elaborated the *Plano Nacional de Gestão de Resíduos* (National Solid Waste Management Plan) 2014-2020. This plan established national strategic guidelines for waste prevention policy and waste management and the guiding rules ensuring the coherence of specific waste management instruments. One topic covered in this plan is the Green Economy, which has policies that point to a circular economy. The circular economy proposes that the waste generated in a production/consumption process should recirculate as input in the same or another process.

Complementarily Portugal also established specific strategic plans according to the source of waste. The *Plano Estratégico dos Resíduos Agrícolas* (Strategic Plan on

Agricultural Solid Waste) should be the one to cover plans for agricultural waste; however, it is still being developed. Thus, the *Plano Estratégico dos Resíduos Industriais* (Strategic Plan on Industrial Solid Waste), approved by Decree-Law nº 89/2002 (Portugal, 2002), includes agricultural waste in its scope but does not mention agro-industrial solid waste not once.

According to the European Commission (2018), waste management means “the collection, transport, recovery (including sorting), and disposal of waste, including the supervision of such operations and the after-care of disposal sites, and actions taken as a dealer or broker”. It also mentions it as an essential process that should be improved and transformed into sustainable material management, ensuring prudent, efficient, and rational utilization of natural resources, promoting the circular economy’s principles. Proper waste management shall follow a hierarchy or order of priority, as shown in the schematic pyramid in Figure 1, which consists of prevention, preparing for re-use, recycling, other recovery (energy), and final disposal environmentally appropriate (Brasil, 2010; European Union, 2008b; Portugal, 2011).

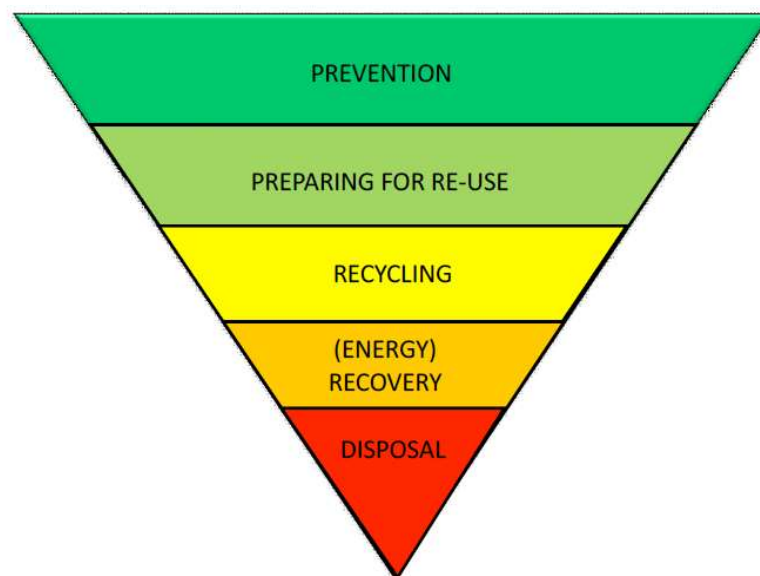


Figure 1. Waste hierarchy (European Union, 2008b).

Waste prevention is considered the most environmentally preferred strategy because it consists of non-production and reduced production, reducing waste at the source (European Union, 2008b). It can be done by buying in bulk, reducing packaging,



or redesigning products. Waste prevention may save natural resources, conserve energy, and reduce other types of pollution (*e.g.*, air and water pollution).

Preparing for re-use consists of re-use of products or components that are not waste for the same purpose they will be conceived, and it is also a source reduction (European Union, 2008b). It can be done by re-using plastic bags, jars, containers, etc., and donating old clothes and furniture. Re-use also may save natural resources, conserve energy, and reduce other types of pollution (*e.g.*, air and water pollution).

Recycling consists of recovery operations by which waste is reprocessed into products, materials, or substances, whether for the original or other purposes (European Union, 2008b). It also includes the recovery of organic matter (*e.g.*, composting and producing carbonaceous materials from biomass). Recycling helps reduce the overall amount of waste sent for disposal and conserve natural resources by replacing the need for virgin materials (US EPA, 2009a).

Other recovery consists mostly of energy recovery (European Union, 2008b). It includes converting materials into heat, electricity, or fuel through various processes, including combustion, gasification, pyrolyzation, anaerobic digestion, and landfill gas recovery (US EPA, 2009a).

Final disposal consists of operations that are not recovery, even when the process has a secondary effect of substances or energy reclamation. The most common form of proper waste disposal is landfill. Methane gas, a byproduct of decomposing waste, can be collected and used as fuel to generate electricity. Another residue of decomposing waste is the leachate, which needs to be collected and treated (US EPA, 2009a).

## 2.2 Carbonaceous adsorbents

### 2.2.1 Carbonaceous materials

A variety of light-weight, relatively low-cost, and environmentally friendly materials with various microtextures (powders, fibers, fabrics, foams, glassy carbon, and composites) contain carbon (Kurzweil, 2009). With multiple chemical bonding possibilities, carbon can be found in many allotropes. Diamond, graphite, nanotubes, and fullerenes are among the carbon-based materials (Nudrat et al., 2018).

AC, pyrochar, hydrochar, carbon black (furnace soot, thermal black), carbon fibers (polyacrylonitrile, phenol resin, pitch), glassy carbon (polymer-based), and carbon foam (nanomaterials, polymer-based) are examples of various materials composed of carbon. Most carbon materials' key features are high surface area, tailored pore geometry, pore size distribution, wettability, and conductivity (Kurzweil, 2009).

Carbonaceous materials have been widely used for capacitor electrodes in aqueous and aprotic solutions. Powdered graphitic materials usually conduct better than powdered amorphous carbon (*e.g.*, activated carbons, biochar). Porous carbonaceous materials have been widely used in catalysis, energy storage (supercapacitors and Li-ion batteries), energy production (electrocatalysts or electrocatalyst support for fuel cells), gas storage (water (H<sub>2</sub>O), methane (CH<sub>4</sub>), carbon dioxide (CO<sub>2</sub>)) and the removal of contaminants (*e.g.*, heavy metals, gaseous pollutants, dyes) (Sevilla & Fuertes, 2016).

## 2.2.2 Adsorbent carbonaceous materials

According to IUPAC (2015), adsorption is defined as the enrichment of molecules, atoms, or ions in an interface's vicinity. In gas-solid systems, the interface material is a solid surface, called adsorbent, and the adsorption takes place in its surface, outside the solid structure. This general phenomenon occurs whenever an adsorbable gas (the adsorptive) is brought into contact with the surface of a solid (the adsorbent) and adsorbs in its surface (becoming the adsorbate). The adsorption space is the area occupied by the adsorbate. Adsorption can be physical (physisorption) or chemical (chemisorption) (Thommes et al., 2015). Physisorption is a physical adsorption attraction of an adsorbate to a surface, the outer surface, and the inner pore surface of an adsorbent by physical forces (Van der Waals forces) (CEN, 2014). Differently, in chemisorption, the adsorbate is trapped on the adsorbent surface due to the intermolecular forces involved in formatting chemical bonds (CEN, 2014; Thommes et al., 2015).

In the context of physisorption, the pores are defined according to their size as follows (Porada et al., 2013; Thommes et al., 2015):

- (i) *Macropores* are the ones with widths greater than about 50 nm;
- (ii) *Mesopores* are the ones with widths between 2 nm and 50 nm;
- (iii) *Micropores* are the ones with widths less than about 2 nm;

A carbonaceous adsorbent is represented in Figure 2, showing its amorphous form, the porous structure with the adsorbate on it, and its aromatic clusters.

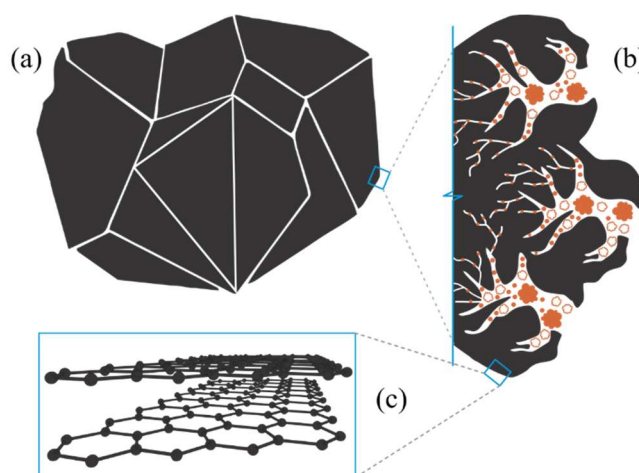


Figure 2. Representation of a carbonaceous adsorbent: (a) amorphous form; (b) porous structure with adsorbate; (c) aromatic clusters.  
Based on Celzard et al. (2007).

Adsorbents can be prepared by thermal decomposition of the material, eliminating non-carbon species and producing a fixed carbon mass with a rudimentary pore structure composed of fine and closed pores. The adsorbent can be activated via chemical or physical means to enlarge the pores' diameters and create new pores (Hu et al., 2001).

#### 2.2.2.1 Bioadsorbents

Nearly all biological materials (*e.g.*, microbial cells, plant and animal biomass, organic waste sludge) have the capacity of pollutant removal/recovery (Safarik et al., 2018). When dead biomass is used in the adsorption of pollutants, they are called bioadsorbents (Fomina et al., 2014). Biosorption is a physicochemical process in which low-cost raw biomass acts as adsorbent (Safarik et al., 2018). Functional groups located on the surface of bioadsorbents play an essential role in the biosorption of pollutants due to their interaction with target pollutants (Safarik et al., 2018). Among the proper handling of exhausted bioadsorbent after the adsorption process is its regeneration and re-use in subsequent biosorption cycles; also, use it as a precursor to producing pyrochars by pyrolysis (Baldikova et al., 2019).

#### 2.2.2.2 Pyrochars

Thermo-chemical processes, such as pyrolysis, are applied to produce char, oil, or gaseous product from biomass. Pyrolysis consists of the organic raw material's carbonization in an inert atmosphere (Yek et al., 2019). The thermal treatment dehydrates and devolatilizes the biomass during carbonization, resulting in a remaining solid char with high-carbon content, high porosity, large surface area, and high pore volumes, usually called pyrochar (Ioannidou et al., 2007; Lam et al., 2018; Lehmann et al., 2009; Mohamed et al., 2010).

The key parameters controlling the pyrochar properties during the pyrolysis process are temperature, followed by pyrolysis heating rate, nitrogen flow rate (used as the carbonizing agent), pyrolysis residence time, and feedstock type (Ahmad et al., 2014; Chen et al., 2017; Ioannidou et al., 2007; Mohamed et al., 2010).

Pyrolysis processing of biomass enlarges the crystallites and makes them more ordered, an effect that increases under high temperatures (Lehmann et al., 2009). As reported by Chen et al. (2017), the biomass is converted into a “3D network of benzene rings” with plenty of functional groups at temperatures below 500 °C during the pyrolysis process. At temperatures between 500 °C and 700 °C, it is transformed into a “2D structure of fused rings” with abundant porosity. At temperatures higher than 700 °C, it may transit into a “graphite microcrystalline structure”. The surface area of the biomass char dramatically increases from 400 to 900 °C. Figure 3 presents a schematic of pyrochar structure development under many temperature ranges.

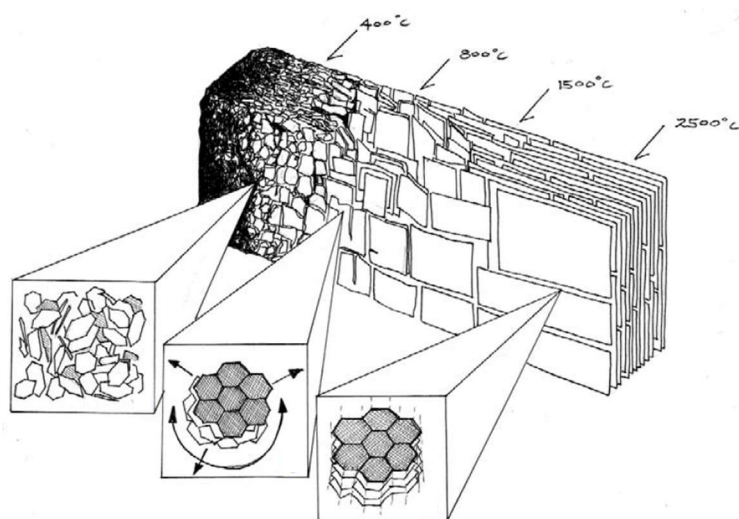


*Figure 3. Schematic of pyrochar structure development under many temperature ranges (Lehmann et al., 2009).*

Pyrochar has been used as a soil amendment (to increase soil health and productivity sustainably and a tool for atmospheric carbon dioxide sequestration in soils), biofuel, catalytic support, and adsorbent (Alhashimi & Aktas, 2017; Daramola et al., 2020; Lehmann et al., 2009). It has received recognition in diverse applications in recent years due to its adsorption properties (Alhashimi et al., 2017). Pyrochars obtained in relatively high pyrolysis temperatures usually present high surface area, good microporosity, and hydrophobicity, potentially useful in the sorption of organic contaminants. In contrast, pyrochars that are effective in the sorption of inorganic/polar organic contaminants are usually obtained in relatively low pyrolysis temperatures ( $\leq 500$  °C), presenting more oxygen-containing functional groups, electrostatic attraction, and precipitation (Ahmad et al., 2014).

As reported by Alhashimi & Aktas (2017), it is essential to investigate the environmental and economic impact perspective of pyrochar compared to alternative materials such as AC, presented in detail below. The same authors reported that pyrochars have lower environmental impacts than activated carbons. If engineered correctly for the specific application, they could be as efficient as activated carbon and less expensive. Nevertheless, significant gases are released during the pyrolysis process. In the case of pyrolysis of OS, Blanco López et al. (2002) mentioned CO, CO<sub>2</sub>, CH<sub>4</sub>, ethylene, ethane, and hydrogen as gases produced during this process, among which CO and CO<sub>2</sub> are the main ones.

### 2.2.2.3 Hydrochars

The hydrochar is a material obtained by HTC. It is another thermochemical process, which uses water, heat (range of 150 to 350 °C), and high pressure to convert biomass into carbonaceous materials through fractionation of the feedstock (Daramola et al., 2020; Jain et al., 2016; Lehmann et al., 2009; Ok et al., 2016). This process is considered a promising waste conversion technique by converting waste into value-added products. It presents the advantages to allow the use of high moisture-containing feedstock without requiring a pre-drying step and to do not generate any hazardous chemical waste or byproducts when performed only with water (Bruckman, 2016; Ok et al., 2016). HTC and pyrolysis are two of the most frequently used processes to prepare carbonaceous materials, with high adsorption capacity, from agriculture residues (Ok et al., 2016).

In HTC, due to temperature, steam is formed, and the pressure rises, leading to a thermo-chemical transformation of biomass (Daramola et al., 2020). Water acts as a solvent and a catalyst facilitating efficient hydrolysis and the partition of the lignocellulosic material (Jain et al., 2016). The hemicellulose content in biomass partly undergoes hydrolysis at lower temperatures and results in the formation of hydrochar through polymerization (water solubility homogenous reaction) (Jain et al., 2016).

HTC method has received growing attention due to its simplicity and ability to deliver hydrochar with many oxygenated functional groups (OFGs) (Jain et al., 2016; Ok et al., 2016). It is considered more environmentally sound because it usually does not generate hazardous outputs, as does dry pyrolysis. Besides, HTC requires less energy, implying economic benefits as well. Figure 4 illustrates the formation of OFGs by HTC.

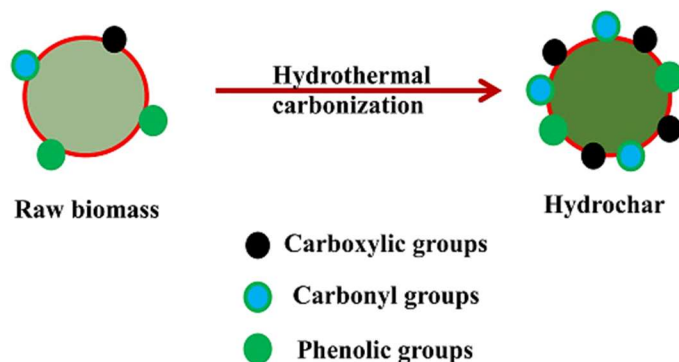


Figure 4. Hydrochar formation by hydrothermal carbonization (HTC) (Jain et al., 2016).

#### 2.2.2.4 Activated carbons

According to the IUPAC, AC is “a porous carbon material, a char which has been subjected to reaction with gases, sometimes with the addition of chemicals, before, during or after carbonization in order to increase its adsorptive properties” (IUPAC, 1997). The U.S Environmental Protection Agency describes AC as “a highly adsorbent form of carbon used to remove odors and toxic substances from liquid or gaseous emissions...” (US EPA, 2009b). AC consists of macrostructures formed by flat aromatic sheets, broken in places by slit-formed pores, and cross-linked amorphous carbon that defines cylindrical pores by its accidental orientation (Kurzweil, 2009; Shen et al., 2018). The main distinctions between pyrochar and AC are that activation is not performed during pyrochar production while it is crucial for AC production; also, the processes’ temperatures are usually different (Zhang et al., 2017).

AC is used to treat liquids and gases, and it generally has a large adsorption capacity, preferably for small molecules, because of its high pore volume and surface area. The adsorption of compounds by AC is a complex process that depends on a wide range of variables, including adsorbent properties, the nature of the adsorbate, operating conditions (relative humidity, temperature, pressure, and volumetric flow rate), and the presence of adsorption competition (Le-Minh et al., 2018).

An assortment of ACs having distinct porosity can be obtained by controlling activation and carbonization processes. This carbonaceous material is used generally in granular and powdered forms but can also be found in textile form prepared by controlled carbonization and activation of carbon fiber textiles (IUPAC, 1997).

According to Mohd Din et al. (2009), biomass can be converted into AC via chemical, physical, or physiochemical (a combination of the previous methods) activation.

The physical activation methods mostly involve carbonization of the biomass at temperatures below 700 °C, followed by controlled gasification of the char at higher temperatures in a stream of oxidizing with the activating agents steam (CO<sub>2</sub>, air, NH<sub>3</sub>, O<sub>2</sub>, or any mixture of these gases), without the presence of a chemical catalyst (Alslaibi et al., 2013; Chen et al., 2017; Hu et al., 2001). In this type of activation, the raw material is carbonized at first, then volatile compounds are removed, and oxidation sites are created.

The process results in increased aromatic cross-linked sheets, and carbon layers are removed by controlled oxidation. The activation process progress depends on the oxygen added to the steam. High temperatures, long residence times, and favorable oxidizing conditions result in larger micropores and small mesopores (Kurzweil, 2009).

The chemical activation is performed by the chemical treatment of the lignocellulosic material, in which the cellulose structures are destroyed, followed by carbonization and aromatization of the carbon skeleton (Kurzweil, 2009). At the beginning of the process, a chemical agent is added, followed by heat treatment, generally in the 450-900 °C range, of the impregnated material under an inert atmosphere to form the final porous structure known as AC (Mohamed et al., 2010; Sevilla & Mokaya, 2014). The activating agents of chemical activation consist of acids (mostly phosphoric acid,  $\text{H}_2\text{SO}_4$ , and nitric acid); alkalis (mainly potassium hydroxide (KOH), sodium hydroxide); and salts (mostly zinc chloride ( $\text{ZnCl}_2$ ), magnesium chloride, potassium carbonate) (Chen et al., 2017; Mohamed et al., 2010; Sevilla et al., 2014). Finally, the product is washed to remove and recover the excess of the activation agent (Kurzweil, 2009). Chemical activation may retain an abundant distribution of surface functional groups originated from a precursor, which could be effective for polar pollutants, such as  $\text{NH}_3$  (Zheng et al., 2016).

The main advantages of chemical activation over physical activation are: (i) relatively low energy cost due to lower pyrolysis temperatures; (ii) much higher carbon yield is obtained; (iii) adsorbents with a very high surface area can be produced, and (iv) the microporosity can be well developed, controlled and tailored to be narrowly distributed (Hu et al., 2001; Sevilla et al., 2014).

Hydrochars are frequently used as precursors of ACs, as shown the Figure 5. As described in the previous topic, HTC results in efficient hydrolysis and dehydration of biomass and bestows the hydrochar with high OFGs content, making it a suitable precursor to produce chemically activated carbon.



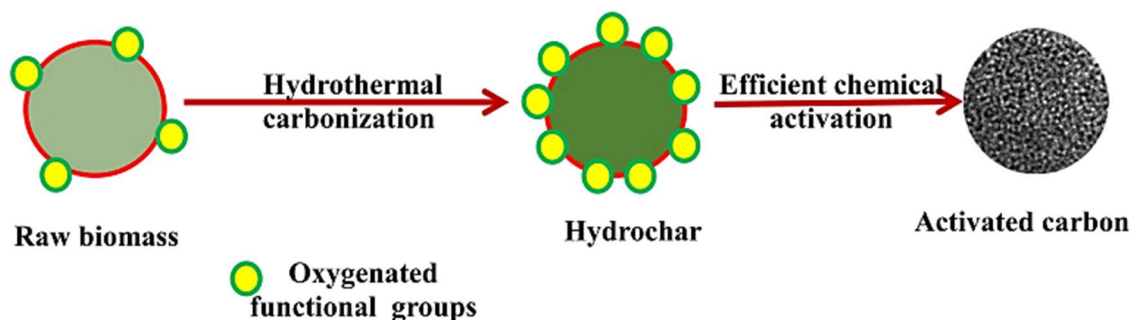


Figure 5. Preparation of AC by HTC, followed by chemical activation (Jain et al., 2016).

As reported by Yang & Lua (2003), activated carbons' chemical nature influences its adsorptive, electrochemical, catalytic, and other properties. Predominantly, activated carbons with acidic surface chemical properties are favorable for alkaline gas adsorption, while activated carbons with basic surface chemical properties are suitable for acidic gas adsorption.

Physiochemical activation mainly happened at high temperatures in the presence of dehydrating agents (*e.g.*, KOH, ZnCl<sub>2</sub>, H<sub>2</sub>SO<sub>4</sub>) and of oxidizing agents such as CO<sub>2</sub>/steam to provide further gasification effect (Alslaibi et al., 2013; Din et al., 2009).

### 2.2.3 Adsorbents derived from biomass

The solid biomass is available in different forms, with variable moisture contents and chemical elements, including agricultural and forestry residues, biological materials byproducts, wood, organic parts of municipal, and sludge waste (Sansaniwal et al., 2017). The various agricultural biomass wastes are among the most abundant, accessible, and renewable resources used to produce carbonaceous adsorbents, such as bioadsorbents, pyrochars, hydrochars, and ACs (Javidi Alsadi & Esfandiari, 2019).

The production of adsorbents using lignocellulosic materials as precursors has attracted much attention due to the high cost of producing adsorbents from coal, not to mention it is a non-renewable resource. Practically all lignocellulosic materials can be used as feedstock to produce applicable adsorbents. The use of a suitable precursor is mainly conditioned by its availability and cost, although it also depends on the manufactured carbon's particular applications and the type of installation available. The

big challenge in this field of study is to find cheap and efficient feedstock to produce adsorbents (Uçar et al., 2009).

According to recent scientific literature, many agricultural biomass wastes are being used as precursors to produce adsorbent materials; most of them are ACs. Many feedstocks are being physically and chemically activated using different activation agents, as reported by González-García (2018) in his scientific literature review. Table 3 and Table 4 present plenty of AC prepared from lignocellulosic precursors and their respective surface areas after the physical or chemical activations.

*Table 3.* Surface area values ( $\text{m}^2\cdot\text{g}^{-1}$ ) for physically activated carbons (ACs) obtained from different lignocellulosic precursors. Adapted from González-García (2018).

<b>Precursor</b>	<b>Activation agent</b>	<b>BET Surface area</b>	<b>Precursor</b>	<b>Activation agent</b>	<b>BET Surface area</b>
Cellulose	thermal	2,602	Palm kernel shells	CO <sub>2</sub>	912
Bamboo	thermal	2,169	Hemp	steam	877
Chicken droppings	thermal	1,618	Abaca	steam	860
Kapok	CO <sub>2</sub>	1,474	Almond shell	CO <sub>2</sub>	851
Date pits	steam	1,467	Jute	steam	840
Olive Stone	CO <sub>2</sub>	1,355	Coir	steam	822
Kenaf	CO <sub>2</sub>	1,352	Olive stone	steam	813
Oil cake/walnut	CO <sub>2</sub>	1,207	Olive stones	steam	807
Guava seeds	80% CO <sub>2</sub> , 20% H <sub>2</sub> O	1,201	Walnut shell	steam	792
Oil-palm shells	thermal	1,182	Fax	steam	776
Vine shoots	CO <sub>2</sub>	1,173	Peanut shells	steam	757
Agave Sisalana	CO <sub>2</sub>	1,140	Cornstarch	thermal	686
Almond shell	CO <sub>2</sub>	1,138	Almond shell	steam	601
Rice	steam	1,122	Finish wood	CO <sub>2</sub>	590
Rice	steam	1,111	Cocoa shell	CO <sub>2</sub>	558
Almond tree pruning	steam	1,080	Nutshells	CO <sub>2</sub>	485

(continued)

Table 3. Surface area values ( $\text{m}^2\cdot\text{g}^{-1}$ ) for physically activated carbons (ACs) obtained from different lignocellulosic precursors. Adapted from González-García (2018).

Precursor	Activation agent	BET Surface area	Precursor	Activation agent	BET Surface area
Dinde stones	80% CO <sub>2</sub> , 20% H <sub>2</sub> O	1,074	Sunflower stem	CO <sub>2</sub>	438
Rapeseed	CO <sub>2</sub>	1,036	Olive stone	CO <sub>2</sub>	438
Crofton weed	CO <sub>2</sub>	1,036	Walnut shells	CO <sub>2</sub>	379
Tropical almond shells	80% CO <sub>2</sub> , 20% H <sub>2</sub> O	1,029	Grape stalks	steam	300
pistachio-nut shells	CO <sub>2</sub>	1,014	Eucalyptus sawdust	CO <sub>2</sub>	298
Oil-palm shells	thermal	988	Grape pomace	steam	266
Olive Stone	steam	950	Sugar cane bagasse	CO <sub>2</sub>	260
<i>Moringa oleífera</i>	steam	932	Palm kernel	CO <sub>2</sub>	167

Table 4. Surface area values ( $\text{m}^2\cdot\text{g}^{-1}$ ) for chemically activated carbons (ACs) obtained from different lignocellulosic precursors.  
Adapted from González-García (2018).

Precursor	Activation agent	BET Surface area	Precursor	Activation agent	BET Surface area	Precursor	Activation agent	BET Surface area
Enteromorpha prolifera	KOH	3,332	Chinese fir	$\text{H}_3\text{PO}_4$	1,589	Licorice residue and pistachio-nut shell mixture	$\text{H}_3\text{PO}_4$	1,017
Rice	KOH	3,263	Willow catkins	KOH	1,586			
Eucalyptus wood	NaOH	3,167	Pomelo	KOH	1,533			
Corncob	KOH	3,054	Pine	$\text{K}_2\text{CO}_3$	1,509	Olive stones	$\text{H}_3\text{PO}_4$	1,014
Beechwood	NaOH	2,835				Apple pulp	$\text{H}_3\text{PO}_4$	1,004
Chinese fir	$\text{H}_3\text{PO}_4$	2,518	Licorice residue and pistachio-nut shell mixture	$\text{ZnCl}_2$	1,492	Choerospondias axillaris	NaOH	1,002
Carrageenan	KOH	2,502				Olive stones	$\text{H}_3\text{PO}_4$	990
Flamboyant pods	NaOH	2,463	Paulownia flower	KOH	1,471	Wheat straw	NaOH	970
Beechwood	KOH	2,460	Barley	$\text{ZnCl}_2$	1,445	Corncoobs	$\text{H}_3\text{PO}_4$	960
Flax	$\text{ZnCl}_2$	2,450	Peach stones	$\text{ZnCl}_2$	1,425	Stem of date palm	KOH	947
Coconut shells	$\text{ZnCl}_2$	2,450	Pine nutshell	$\text{CaHPO}_5$	1,418	Posidonia oceánica	$\text{H}_3\text{PO}_4$	946
Eucalyptus Wood	NaOH	2,415	Waste tea	$\text{H}_3\text{PO}_4$	1,398	Oil palm empty fruit bunch	$\text{H}_2\text{SO}_4$	928
Hemp	$\text{ZnCl}_2$	2,250	<i>Enteromorpha prolifera</i>	$\text{NaAlO}_2$	1,374	Pineapple	$\text{ZnCl}_2$	915
Pine nutshell	KOH	2,207	Soybean oil cake	$\text{K}_2\text{CO}_3$	1,353	Coir pith	$\text{ZnCl}_2$	910
Rye straw	KOH	2,200	Orange	$\text{ZnCl}_2$	1,353	Coffee endocarp	KOH	893
Cannabis sativa	KOH	2,192	Cotton stalks	KOH	1,311	Coffee	$\text{ZnCl}_2$	890

(continued)

Table 4. Surface area values ( $\text{m}^2\cdot\text{g}^{-1}$ ) for chemically activated carbons (ACs) obtained from different lignocellulosic precursors.  
Adapted from González-García (2018).

Precursor	Activation agent	BET Surface area	Precursor	Activation agent	BET Surface area	Precursor	Activation agent	BET Surface area
Peach stone	FePO <sub>4</sub>	2,160	Jatropha wood	KOH	1,305	Chestnut	H <sub>3</sub> PO <sub>4</sub>	783
Eucalyptus Wood	KOH	2,120	Vetch	ZnCl <sub>2</sub>	1,287	Date pits	FeCl <sub>3</sub>	780
Agar	KOH	2,118	Agave bagasse	ZnCl <sub>2</sub>	1,281	Corncob	ZnCl <sub>2</sub>	767
Banana	KOH	2,086	Hemp	HNO <sub>3</sub>	1,250	Posidonia oceánica	KOH	762
Starch-rich banana	H <sub>3</sub> PO <sub>4</sub>	2,068	Peanut Shell	K <sub>2</sub> CO <sub>3</sub> /Fe <sub>3</sub> O <sub>4</sub>	1,236	Peanut shells	H <sub>3</sub> PO <sub>4</sub>	751
Coconut shells	H <sub>2</sub> O <sub>2</sub> /ZnCl <sub>2</sub>	2,050	Peach stones	H <sub>3</sub> PO <sub>4</sub>	1,225	Palm kernel shell	KOH	727
Eucalyptus wood	KOH	2,000	Phoenix dactylifera L	H <sub>3</sub> PO <sub>4</sub>	1,225	Starch	KOH	714
Gelatin	KOH	1,957	Orange	K <sub>2</sub> CO <sub>3</sub>	1,215	Elaeagnus angustifolia seed	ZnCl <sub>2</sub>	697
Pistachio shell	FePO <sub>4</sub>	1,919	Sky fruit husk	H <sub>3</sub> PO <sub>4</sub>	1,211	Coffee	H <sub>3</sub> PO <sub>4</sub>	696
Chinese fir	H <sub>3</sub> PO <sub>4</sub>	1,910	Flax	H <sub>3</sub> PO <sub>4</sub>	1,200	Sisal	ZnCl <sub>2</sub>	616
Wood apple shell	H <sub>2</sub> SO <sub>4</sub>	1,898	Tabacco	HNO <sub>3</sub>	1,104	Olive stones	KOH	587
Olives stones	ZnCl <sub>2</sub>	1,860	Stem of date palm	H <sub>3</sub> PO <sub>4</sub>	1,100	Coir fiber	ZnCl <sub>2</sub>	540
Grape seeds	KOH	1,860	Date stones	H <sub>3</sub> PO <sub>4</sub>	1,100	Coconut pith	KOH	505
Albizia lebbeck	KOH	1,824	<i>Pinus sylvestris</i>	H <sub>3</sub> PO <sub>4</sub>	1,093	Posidonia oceánica	ZnCl <sub>2</sub>	503
Agave Sisalana	ZnCl <sub>2</sub>	1,765	Agave Sisalana	H <sub>3</sub> PO <sub>4</sub>	1,086	Leaves of Carnauba palm	CaCl <sub>2</sub>	431

(continued)

Table 4. Surface area values ( $\text{m}^2\cdot\text{g}^{-1}$ ) for chemically activated carbons (ACs) obtained from different lignocellulosic precursors.  
Adapted from González-García (2018).

Precursor	Activation agent	BET Surface area	Precursor	Activation agent	BET Surface area	Precursor	Activation agent	BET Surface area
Apricot and Peach stones	$\text{H}_3\text{PO}_4$	1,740	<i>Euphorbia rigida</i>	$\text{K}_2\text{CO}_3$	1,079	Plum kernel	$\text{H}_3\text{PO}_4$	417
Waste tea	$\text{K}_2\text{CO}_3$	1,722	<i>Arundo donax</i> Linn	KOH	1,065	Jacaranda	$\text{H}_3\text{PO}_4$	326
Hazelnut shells	KOH	1,700	Corkboard	KOH	1,065	<i>Posidonia oceánica</i>	$\text{H}_2\text{O}_2$	60
<i>Prosopis ruscifolia</i>	$\text{H}_3\text{PO}_4$	1,638	Orange	$\text{H}_3\text{PO}_4$	1,056	Palm flower	$\text{H}_2\text{SO}_4$	10
Oil palm shell	KOH	1,630	Potato waste	$\text{ZnCl}_2$	1,052	<i>Opuntia ficus indica</i>	$\text{HNO}_3$	5

#### 2.2.4 Regeneration of adsorbents

Once the carbonaceous adsorbent is saturated, it is generally discarded (*e.g.*, disposal in landfills/incineration) (Gamal et al., 2018). Regeneration of saturated adsorbents plays an essential role in environmental and economic spheres, as it may increase the adsorbent's lifespan, maximizing its re-use (Han et al., 2014; Sun et al., 2017).

Various methods have been used to regenerate adsorbents, including chemical, electrochemical, microwave, advanced oxidation treatments, and thermal, being the last one the most used in industry (Do et al., 2011; Ro et al., 2015). The thermal regeneration process requires high capital and energy consumption (Ro et al., 2015). A convenient regeneration process should be adopted considering the adsorbate's nature and process's cost and conditions (Gamal et al., 2018). The regeneration by itself is beneficial to the environment; however, environmentally sound regeneration techniques should be developed/improved (Sun et al., 2017).

Ro et al. (2015) proposed an environmentally sound method to regenerate pyrochar saturated with  $\text{NH}_3$  only using water. This method was justified by the high solubility of  $\text{NH}_3$  in water. It was found that the adsorption capacities of first-generation and regenerated pyrochars were very similar, suggesting the potential of regenerating saturated pyrochar only by using water. Another potential advantage of the process mentioned above, from environmental and economic perspectives, is that the nitrogen adsorbed in carbonaceous materials may be desorbed in an aqueous solution and be used as raw material for fertilizers (Amaral et al., 2016; Melenová et al., 2003).

### 2.3 Odorous air emissions

#### 2.3.1 Pollutants and sources of pollution

Air pollution is defined by the U.S. Environmental Protection Agency as "the presence of contaminants or pollutant substances in the air that interfere with human health or welfare, or produce other harmful environmental effects" (US EPA, 2009b). According to the World Health Organization, air pollution — both ambient (outdoor) and household (indoor) — represents the leading environmental risk to human health,

accounting for about one in every nine human deaths annually (WHO, 2016). In 2016, seven million deaths worldwide were attributed to the effects of ambient and indoor air pollution (WHO, 2018). The negative impacts of air pollution bring significant effects under social and economic perspectives. Among the more significant are: greater vulnerability of the disadvantaged population, increase in the cost of the health system due to the hospital admission, and decline in agriculture productivity (IEMA, 2014).

Air pollutants consist of gaseous and particle contaminants present in the atmosphere responsible for deteriorating air quality (Saxena & Naik, 2019; US EPA, 2019). Gaseous pollutants include  $\text{NO}_x$ ,  $\text{SO}_2$ ,  $\text{CO}$ ,  $\text{NH}_3$ ,  $\text{H}_2\text{S}$ , VOCs — organic compounds with vapor pressure high enough to be vaporized into the atmosphere under normal conditions —, ozone ( $\text{O}_3$ ), other toxic air pollutants, and some gaseous forms of metals (Saxena et al., 2019; US EPA, 2019). Particulate pollutants are frequently divided into particulate matter  $\text{PM}_{2.5}$  and  $\text{PM}_{10}$ , which represent airborne particles of equivalent aerodynamic diameter less than 2.5 and 10  $\mu\text{m}$ , respectively, and includes a mixture of compounds that can be grouped into five main categories: sulfate, nitrate, elemental (black) carbon, organic carbon and crustal material (US EPA, 2019). There are also the bioaerosols, which are microorganisms and other biological substances (Vallero, 2019b).

Some of the air pollutants are odorous. Environmental odors are usually complex mixtures of pollutants whose components are challenging to identify and quantify and vary between sources (Artiola et al., 2019; Le-Minh et al., 2018). The odor threshold is the minimum odor of an air sample detected by human olfaction (US EPA, 2009b). The concentrations of the odorous compounds are usually very low, but their olfactory thresholds are, in some cases, lower (Fang et al., 2012). The human nose is a sensitive detector of odorous compounds able to detect odor concentrations below the detection limit of some measuring equipment (Fang et al., 2012).

Odors can cause various undesirable reactions in humans, from annoyance to documented health consequences (Nicell, 2009). For example, VOCs can be absorbed through the airways, skin, and digestive tract, causing respiratory tract irritation and damage to the central nervous system and liver (Gil et al., 2014). Although there may be no immediately apparent disease or infirmity in communities exposed to odor emissions, there is undoubtedly no atmosphere of complete mental, social or physical well-being in these places (Nicell, 2009).



In 2005, odor pollution was identified as the second motive of environmental complaints in Europe, after noise (ADEME, 2005). According to Balestrini et al. (2018), based on community complaints reported from 2011 to 2019, industrial and agricultural activities and waste and wastewater treatment facilities account for 78% of odor sources across European countries. In Portugal, 100% of the odor sources are related to the activities/facilities presented above.

The proportions presented above point to the need to give attention to prevent and control the occurrence of odor problems in communities surrounded by those activities. The occurrence of odor problems in communities may threaten the health and the well-being of the population and impair the regular use of their properties. To safeguard the people's well-being, it is essential that industries and other operations that verge on odor emissions, being required to comply with an appropriate assessment and regulation of odor impacts with the implementation of technologies for the prevention and control of odorous gas emissions (Nicell, 2009).

Despite contributing to proper waste management, landfill facilities and organic waste treatment plants typically are sources of odor pollution, as shown above (Rincón et al., 2019). Generally, leachate contains high concentrations of ammoniacal nitrogen in both states, ionic state ( $\text{NH}_4^+$ ) and free gaseous ammonia ( $\text{NH}_3$ ) (Amaral et al., 2016). A study carried out by Cheng et al. (2019) showed that  $\text{H}_2\text{S}$ , benzene, and  $\text{NH}_3$  were the critical priority odorants for landfill facilities, while for organic waste treatment plants were  $\text{NH}_3$ , ethyl acetate, and benzene. Both waste treatment facilities have  $\text{NH}_3$  as one of the most critical offensive odorants, which should be considered on health risk assessment.

$\text{NH}_3$  is considered the most abundant alkaline gas in the atmosphere and a relevant air pollutant responsible for negative environmental impacts (Behera & Sharma, 2012; Wang et al., 2015). It not only contributes to eutrophication and acidification of ecosystems but also plays a fundamental role in fine particulate matter ( $\text{PM}_{2.5}$ ) formation by reacting with acidic species to form ammonium-containing aerosols (ammonium sulfate ( $(\text{NH}_4)_2\text{SO}_4$ ), ammonium bisulfate, ammonium nitrate, and ammonium chloride), which compose a substantial fraction of  $\text{PM}_{2.5}$  (Behera et al., 2012; Wang et al., 2015; Wu et al., 2016). In human space flights,  $\text{NH}_3$  could be emitted from urine or refrigeration system leaks, presenting a health risk to astronauts, such as eye irritation and headache,

so NASA gave the following maximum allowable concentrations for this pollutant: 20 ppm for a 24 h exposure and 3 ppm for a 7 days exposure (NASA, 2020).

The following table (Table 5) shows some of the main odorous compounds and their odor characteristics and detection thresholds.

Table 5. Characteristics and detection thresholds of the main odoriferous compounds.  
Adapted from Le Cloirec & Perrin (1994) and Van Gemert (2011).

Compound Type	IUPAC Name	Molar Mass (g mol <sup>-1</sup> )	Chemical Formula	Odor Characteristics	Odor threshold (mg Nm <sup>-3</sup> )
Sulfurous	Hydrogen sulfide	34.08	H <sub>2</sub> S	Rotten egg	0.0001-0.03
	Methanethiol	48.11	CH <sub>4</sub> S	Cabbage, garlic	0.0005–0.08
	Ethanethiol	62.10	C <sub>2</sub> H <sub>6</sub> S	Rotten cabbage	0.0001–0.03
	(Methylsulfanyl)methane	62.13	C <sub>2</sub> H <sub>6</sub> S	Rotten vegetables	0.0025–0.65
	1,1-Thiobisethane	90.19	C <sub>4</sub> H <sub>10</sub> S	Ethereal	0.0045–0.31
	(Methyldisulfanyl)methane	94.19	C <sub>2</sub> H <sub>6</sub> S <sub>2</sub>	Putrid	0.003–0.014
Nitrogenous	Ammonia	17.03	NH <sub>3</sub>	Very poignant, annoying	0.04–37
	Methanamine	31.06	CH <sub>5</sub> N	Rotten fish	0.02
	Ethanamine	45.09	C <sub>2</sub> H <sub>7</sub> N	Poignant, ammoniacal	0.05–0.83
	N-Methylmethanamine	45.09	(CH <sub>3</sub> ) <sub>2</sub> NH	Rotten fish	0.047–0.16
	3-Methyl-1H-indole	131.18	C <sub>9</sub> H <sub>9</sub> N	Faecal, nauseating	0.0008–0.10
Acids	Acetic acid	60.05	C <sub>2</sub> H <sub>4</sub> O <sub>2</sub>	Vinegar	0.025–6.5
	Butanoic acid	88.11	C <sub>3</sub> H <sub>7</sub> COOH	Rancid butter	0.0004–3
	Pentanoic acid	102.13	C <sub>4</sub> H <sub>10</sub> O <sub>2</sub>	Sweet	0.0008–1.3
Aldehydes & Ketones	Formaldehyde	30.03	CH <sub>2</sub> O	Acrid, suffocating	0.033–12
	Acetaldehyde	44.05	C <sub>2</sub> H <sub>4</sub> O	Fruity, apple	0.04–1.8
	Butanal	72.11	C <sub>4</sub> H <sub>8</sub> O	Rancid	0.013–15
	3-methylbutyraldehyde	86.13	C <sub>5</sub> H <sub>10</sub> O	Fruity, apple	0.07
	Propan-2-one	58.08	C <sub>3</sub> H <sub>6</sub> O	Sweet, fruity	1.1–240

### 2.3.2 Measuring, prevention, and control

Public health has been the principal driver for assessing and controlling air contaminants. Air pollution abatement laws and programs worldwide have also recognized the importance of welfare protection on air pollution prevention and control. According to Vallero (2019a), the central goal has been to decrease health harm, and the metric for harm is the risk. The health risk from an air pollutant is proportional to the exposure, which is the amount of pollutant reaching a person. The activities that are undertaken in different locations and the time spent are essential determinants of air pollution exposure.

Air quality monitoring is performed to estimate air pollutants' ambient concentrations at various locations. However, most people spend most of their time indoors, with distinctions among ambient, indoor, and personal-scale exposures (Vallero, 2019a). Therefore, due to the long period that humans spend indoors, it is indispensable to care about indoor air quality. So, air cleaning, which, by definition, is an indoor-air quality-control strategy to remove various air particulates and gases from the air, is a crucial tool to be applied (US EPA, 2009b).

Odor assessment can be performed by objective chemical analytical measurement and subjective olfactory analysis (human perception). The two types of evaluations are complementary and should be undertaken jointly for a complete assessment of negative odor impacts (Jiang et al., 2017). The objective assessment is critical for the quantitative characterization of odor composition (Jiang et al., 2017). In contrast, the subjective evaluation is an essential tool to assess the odor abatement efficiency of a gas cleaning system according to its ability to reduce the intensity and improve the hedonic odor tone of a gaseous effluent (VDI, 1992b).

The olfactory analysis can be done by dynamic olfactometry, which uses a panel of human assessors being the sensor (CEN, 2003). In 2003 the European Committee for Standardization released a final odor testing standard entitled EN 13725: “Air Quality-Determination of Odor Concentration by Dynamic Olfactometry” (CEN, 2003), which follows ISO quality assurance and scientific testing protocols. This standard unified the olfactometry standards of 18 countries: Austria, Belgium, Denmark, Finland, France, Greece, Germany, Iceland, Ireland, Italy, Luxembourg, Netherlands, Norway, Portugal,

Spain, Sweden, Switzerland, and the United Kingdom). It is worth mentioning that EN 13725:2003 only refers to dynamic olfactometry to measure odor concentration (Capelli et al., 2019). Nonetheless, dynamic olfactometry can also be applied for the determination of odor intensity and odor pleasantness/unpleasantness (hedonic tone), which are subjective parameters, as described in German guidelines VDI 3882 Part 1 and VDI 3882 Part 2 (Capelli et al., 2019; VDI, 1992a, 1992b).

For this reason, subjective assessment is fundamental as human odor perception is the ultimate criterion of the effectiveness of a mitigation measure for odor emissions. Both objective and subjective methods can help design, operate, and optimize different odor abatement systems (Jiang et al., 2017).

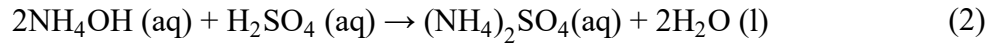
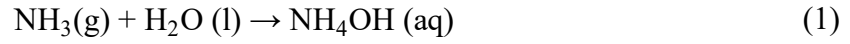
Air pollution managers and engineers are increasingly applying systems thinking and looking for more sustainable approaches (Vallero, 2019a). The technologies for odorous gas treatment can be classified into physical/chemical and biological methods. Adsorption and chemical scrubbers are among the physical/chemical processes, while biofilters, biotrickling filters, bioscrubbers, and activated sludge diffusion reactors are biological techniques for odor control (Ren et al., 2019).

Adsorbents are generally considered useful for small, decentralized applications, typical in environmental odor emissions, where robust technology with low routine maintenance and operating staff intervention is required (Le-Minh et al., 2018).

### 2.3.3 Adsorption of gaseous odorous pollutants

Carbonaceous materials with good porosity and numerous functional groups can work well as sorbents of gas pollutants. Concerning removing  $\text{NH}_3$ , the presence of an acidic oxygenated surface could be the decisive factor of the adsorption capacity of  $\text{NH}_3$  and regeneration efficiency of the adsorbent (Gonçalves et al., 2011; Zheng et al., 2016). On the other hand, surface area and pore volume do not directly control gaseous  $\text{NH}_3$  adsorption (C. Huang et al., 2008; Ro et al., 2015); however, a regular and interlinked pore system is also a crucial factor to  $\text{NH}_3$  adsorption (Yeom & Kim, 2017). The correlation between the amount of  $\text{NH}_3$  adsorbed and the total amount of acidic groups on the adsorbent surface is approximately linear (Gonçalves et al., 2011; C. Huang et al., 2008; Zheng et al., 2016). It was found that water has a fundamental role in the formation

of  $\text{NH}_4^+$  ions, essential for the adsorption through interaction with the Brønsted acid groups of the surface of the adsorbent (Gonçalves et al., 2011). As presented by Chou et al. (2006), reactive adsorption of gaseous  $\text{NH}_3$  in carbonaceous materials impregnated with  $\text{H}_2\text{SO}_4$  occurs according to Equations 1 and 2 and is explained below:



$\text{NH}_3$  is transported from the gas stream to the surface of the adsorbent.  $\text{NH}_3$  reacts with water and subsequently with  $\text{H}_2\text{SO}_4$  to form  $(\text{NH}_4)_2\text{SO}_4$ , which remains on the adsorbent (Amaral et al., 2016). Generally, in typical physical adsorptions, moisture competes with  $\text{NH}_3$ , resulting in the reduction of adsorption capacity of the adsorbent, but in the reactive adsorption of  $\text{NH}_3$  by using adsorbents impregnated with  $\text{H}_2\text{SO}_4$ , moisture is a crucial component in the reaction (Chou et al., 2006; Le Leuch & Bandosz, 2007), as shown in Equation 1.

The adsorption of gaseous pollutants occurs as explained below when it runs in continuous mode in a fixed-bed column. The polluted gas is injected at the adsorption column entrance packed with a fixed bed of adsorbent particles and passes through the column. As the pollutants are adsorbed in the bed, cleaned gas is produced at the column exit. The removal of contaminants decreases over time because of the adsorbent's limited adsorption capacity (Tan & Hameed, 2017). Many parameters influence adsorption, being the key ones: initial concentration of adsorbate ( $C_0$ ), flow rate, bed height, pH, the particle size of adsorbent, and temperature (Patel, 2019). An outstanding adsorption system design involves investigating the breakthrough curve (effluent' pollutant concentration vs. time of adsorption), which indicates the pollutant mass balance in the system (Ang et al., 2020).

Figure 6 shows a typical ideal fixed bed dynamic behavior in which gas is injected at a constant concentration of a particular pollutant at the column entrance. According to Tan & Hameed (2017), the gray-colored zone is the mass transfer zone (MTZ) where adsorption occurs, and concentration varies axially. The MTZ moves along the fixed bed. The breakthrough occurs when the leading front of MTZ, called mass transfer front,

reaches the column exit so that the concentration of pollutants is greater than zero at the column exit ( $C/C_o > 0$ ), in such a manner that the effluent presents a specified concentration of the adsorbate of interest. It is worth mentioning that a bed whose depth is less than the height of MTZ will show the immediate appearance of pollutants, and a short height MTZ confers more efficiency to the adsorbent utilized (ASTM, 2019). The stoichiometric time is reached when the ratio between the effluent concentration (concentration of the pollutant at the column exit) and the feed concentration (concentration of the pollutant at the column entrance) is equal to 0.5 ( $C/C_o = 0.5$ ). The adsorption column's complete saturation occurs when  $C/C_o$  is equal to 1, which means that the pollutant concentration at the column exit is approximately the same as the pollutant concentration at the column entrance. When the saturation is reached the column is no longer able to adsorb any pollutants. The curve plotted, which shows the concentration of pollutants at the column exit versus the time of the adsorption process, is named the breakthrough curve. The green area above the breakthrough curve represents the amount of pollutant adsorbed (Figure 6).

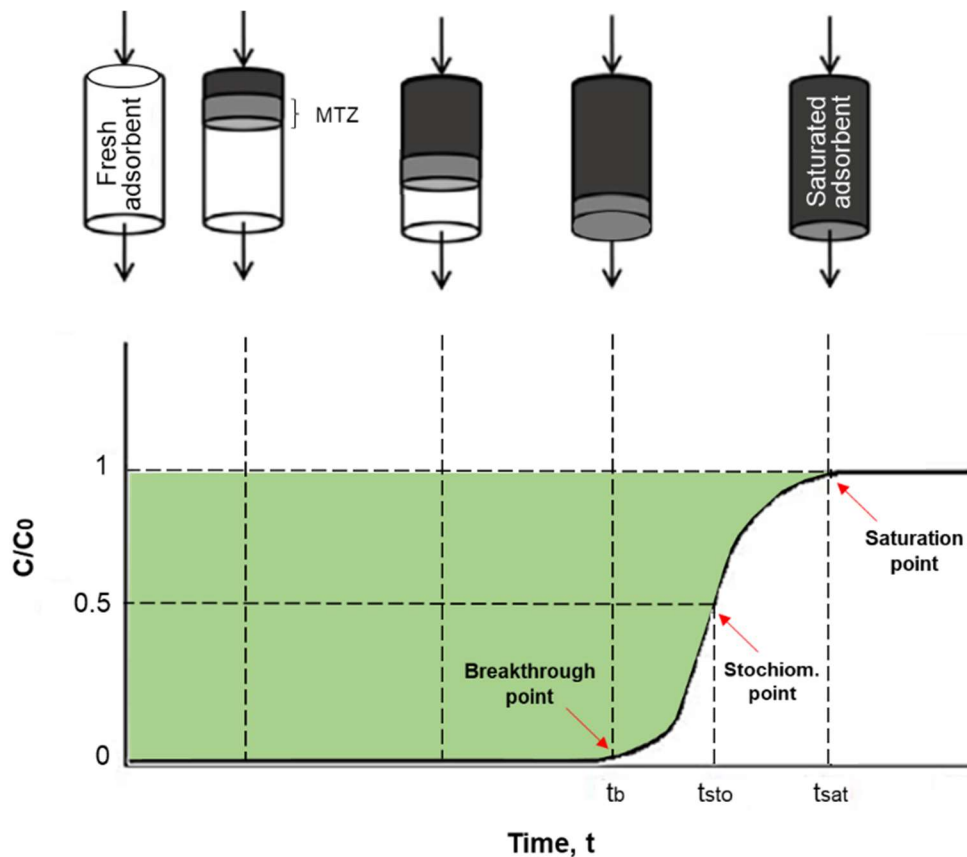


Figure 6. Ideal breakthrough curve: fixed-bed dynamic behavior in which gas is injected at a constant concentration of a particular pollutant at the column entrance.

Adapted from Ang et al. (2020) and Tan et al. (2017).

One of the most used and effective methods of controlling the emission of trace compounds in waste treatment plants' off-gases is using the adsorption process, having AC as the primary adsorbent material used (Shin et al., 2002). AC is also extensively used as an adsorbent for odor control in wastewater treatment plants (Ren et al., 2019). Special attention has been given to the simultaneous removal of multi-component pollutant gases due to the efficiency and economic advantage (Chen et al., 2017).

Most researches developed on odor adsorption only use isotherm models to estimate several odor compounds' adsorption capacities. It may not be sufficient to assess whether the adsorbents could effectively treat the odor problem due to the large gap among various odor compounds' thresholds (X. Huang et al., 2019).

#### 2.3.4 Legal framework on odorous air emissions

##### 2.3.4.1 Brazilian approach

The concern with the air quality was first mentioned in the Brazilian legislation back in 1981 through the *Política Nacional do Meio Ambiente* (National Policy Law for the Environment) established by the Law nº 6.938 (Brasil, 1981), of 31 August 1981, by including the rationalization of the use of air as one of its principle. Later the *Programa de Controle de Poluição do Ar por Veículos Automotores* (Motor Vehicle Air Pollution Control Program) – PROCONVE was established by Resolution CONAMA nº 18/1986 (Brasil, 1986), of 6 May 1986.

The *Programa Nacional de Controle da Poluição do Ar* – PRONAR was established by Resolution CONAMA nº 5/1989 (Brasil, 1989), of 15 June 1989. In the next year, Resolution CONAMA nº 3/1990 (Brasil, 1990), of 28 June 1990, was established, instituting the air quality standards in the PRONAR. The National Environment Council (CONAMA) recently published Resolution CONAMA nº. 491/2018 (Brasil, 2018), of 19 November 2018, an update on the air quality standards, which repealed and replaced the CONAMA Resolution nº. 3/1990, and the items 2.2.1 and 2.3 of the CONAMA Resolution nº 5/1989.



In 2009 Brazil instituted *the Política Nacional Sobre Mudança do Clima* (National Policy on Climate Change) through Law nº 12.187 (Brasil, 2009), of 29 December 2009, which made Brazil the first developing country to prepare a legal document on this matter.

Odorous pollutants are not regulated in Brazil yet, so no federal legislation establishes acceptable odor emissions limits until now. However, local (state and municipal) environmental laws are useful for the environmental regulatory agencies in mediating conflicts between the population and those responsible for the odor sources (Vieira & Lisboa, 2013). There are state and municipal laws regarding the odor emissions in all Brazilian regions (north, northeast, central-west, southeast, south).

The State of Paraná, through Resolution SEMA nº 041/2002 (repealed by the more recent Resolution SEMA nº 054/2006), was the pioneer in Brazil in regulating the odor emissions (Vieira et al., 2013). Resolution SEMA nº 054/2006 (Paraná, 2006), of 22 December 2006, required that facilities with a high potential of odor emissions must have treatment systems with a minimum efficiency of 85% odor removal using olfactometry as a measurement method (based on American and European standards and recommendations).

In the State of Minas Gerais, Regulatory Deliberation COPAM nº 187 (Minas Gerais, 2013), of 19 September 2013, established conditions and maximum emission levels of atmospheric pollutants of stationary sources. The Deliberation mentioned above presents that odorous gases derived from some specific activities/facilities that are potential sources (*e.g.*, grains roasting, source of H<sub>2</sub>S and mercaptans, among others) must be incinerated at a minimum temperature of 800°C or treated by another pollutant control system, with equal or higher efficiency. Despite those mentioned above, the regulation covers only a portion of activities/facilities that are a potential source of odors, not mention that known sources of odor are not specified (*e.g.*, landfills, organic waste treatment plants, and wastewater treatment plants).

In Minas Gerais, the city of Uberlândia stands out in terms of odor regulation to introduce concepts and definitions related to olfactometry and establish emission limits for some odoriferous compounds (Vieira et al., 2013). Decree nº 10.847 (Uberlândia, 2007), of 10 September 2007, regulating the Article 126 of Complementary Law nº 017/91, amended by Complementary Law nº 447/2007, establishes the policy of protection, control, and conservation of the environment and makes other provisions. The

Decree mentioned above establishes the obligation of activities that generate air pollution to present a *Programa de Automonitoramento de Emissões Atmosféricas* (Atmospheric Emissions Self-Monitoring Program). The Program must include the sources of odor emissions, characteristics of the odorous gases, control parameters, sampling methodologies, emission analysis, and schedules of actions and implementation of mechanisms that avoid, minimize, control, and monitor such emissions. Article 9 sets out that sampling and analysis of odorous emissions must be carried out following appropriate analytical methods (which includes the olfactometry) previously accepted by the competent municipal environmental agency. Article 10 sets out emission limits of sulfurous gases  $\text{H}_2\text{S}$  and  $\text{C}_2\text{H}_6\text{S}$  ( $4.7 \times 10^{-4}$  and  $3.0 \times 10^{-3}$  ppm, respectively), but do not present limits for other known odorous gases (*e.g.*,  $\text{NH}_3$ ). According to the decree mentioned above, for those odorous gases that do not cover Article 10, emission standards must comply with internationally recommended or accepted standards, not specified in the document.

#### 2.3.4.2 European and Portuguese approach

The EU set pollutant concentrations thresholds that shall not be exceeded in a given period through air quality Directives 2008/50/EC (European Union, 2008a), of 21 May 2008 (on Ambient Air Quality and Cleaner Air for Europe), and 2004/107/EC (European Union, 2004), of 15 December 2004 (on heavy metals and polycyclic aromatic hydrocarbons in ambient air). The first Portuguese legal document on air pollution emission control was Ordinance n° 286/1993 (Portugal, 1993), of 12 March 1993, which instituted the air quality standards to establish the emission limit values for  $\text{SO}_2$ , PM,  $\text{NO}_2$ , CO, Pb, and  $\text{O}_3$ . Later, Decree-Law n° 78 (Portugal, 2004), of 03 April 2004, presented principles, objectives, and instruments to prevent and control air emissions.

The global increase of environmental regulations in the 1970s created the need to standardize odor measurement methods. Consequently, European countries, Australia, and the United States began to develop odor regulations. (McGinley & McGinley, 2001). Some EU countries have already adopted specific legislation on odor emissions, such as Germany and the United Kingdom. Countries such as Canada inspired the EU countries (Ferreira et al., 2017).

Directive 2010/75/EU (European Union, 2010), of 24 November 2010, on industrial emissions (the Industrial Emissions Directive), is the main EU's instrument regulating pollutant emissions from industrial installations by establishing a framework for determining emission limits (including odorous pollutants') for industries.

Currently, there are no specific regulations for limiting emissions or managing odor pollution in Portugal. The Decree-Law n° 39 (Portugal, 2018a), of 11 June 2018 that regulates diffuse pollutants' emission, present in Article 9 that is an obligation of operators to minimize those emissions, which includes prevention and control of pollutants' emissions, but not expressly the odorous ones (Diaz et al., 2019). However, as EU's Member State, Industrial Emission Directive is applied in a manner such that industries that may cause odorous negative impact may comply with specific odor limits determined by olfactometric studies and modeling or other studies (Diaz et al., 2019).

The Portuguese Decree-Law n°127 (Portugal, 2013b), of 30 August 2013, rectified by Declaration of Rectification n° 45-A (Portugal, 2013a), of 29 October 2013, which transposed EU's Industrial Emission Directive, aims at preventing and reducing emissions to air, water and soil and the production of waste, by establishing the industrial emissions regime applicable to integrated pollution prevention and control. Article 5 of the decree mentioned above presents that environmental licensing is mandatory for industries. This environmental licensing system translates into a procedure for emitting a *Título Único Ambiental* (TUA) (Single Environmental Title). It is a single title of all the licensing acts in the environmental field, containing all the information related to the facility's or activity's applicable requirements. So that, the activities that generate odorous pollution shall include in the scope of its TUA the actions that will be taken to monitor, prevent and control odoriferous emissions, including an odor's management plan, when necessary.

Although there are no specific regulations for limiting emissions or managing odor pollution in Portugal, a legal document aims to reduce NH<sub>3</sub> emissions. Decree-Law n° 84 (Portugal, 2018b), of 23 October 2018 that transposes Directive (EU) 2016/2284 sets national commitments to reduce emissions of the acidifying, eutrophication, and ozone air pollution, that includes the pollutants NH<sub>3</sub>, sulfur dioxide, NO<sub>x</sub>, non-methane volatile organic compounds, and PM<sub>2.5</sub>. It establishes the obligation to elaborate, adopt, and execute the *Programa Nacional de Controlo da Poluição Atmosférica* (PNCPA)

(National Air Pollution Control Program), which is still being elaborated. Annex III presents the commitment to reducing NH<sub>3</sub> emission by 7% for any year from 2020 to 2029 and 15% for any year starting from 2030, having 2015 as the reference year.

### 3 MATERIALS AND METHODS

This chapter covers this work's detailed methodology, including the materials and equipment and the methods used. Firstly, it presents the methods of preparation of four types of adsorbents. Then the preparations processes' carbon and mass balance and the adsorbents' elemental analysis are explained. The adsorbents' characterization methods, including surface chemistry, ashes determination, textural properties, and void fraction characteristics, are presented. The setting-up of the lab-scale system is shown. The methods for evaluating the  $\text{NH}_3$  concentration in zero-air and leachate and its adsorption on the carbonaceous materials are presented. Lastly, the methods of regeneration and re-use of adsorbents saturated with  $\text{NH}_3$  and the characteristics of this process's liquid effluent are described.

#### 3.1 General methodology

This work consists of seven main stages: (1) preparation of adsorbent materials from OS and MB; (2) carbon and mass balance and characterization of the adsorbents prepared; (3) setting up of a lab-scale experimental system for adsorption assessment; (4) evaluation of zero-air and gases derived from leachate; (5) evaluation of the adsorption of  $\text{NH}_3$  derived from leachate by chemical analytical measurement and olfactory analysis; (6) regeneration and re-use of the saturated adsorbents and (7) carbon and mass balance of the adsorbents regenerated, and analysis of the liquid effluent.

Figure 7 illustrates a schematic diagram of the abovementioned stages, including all inputs and outputs of each stage.

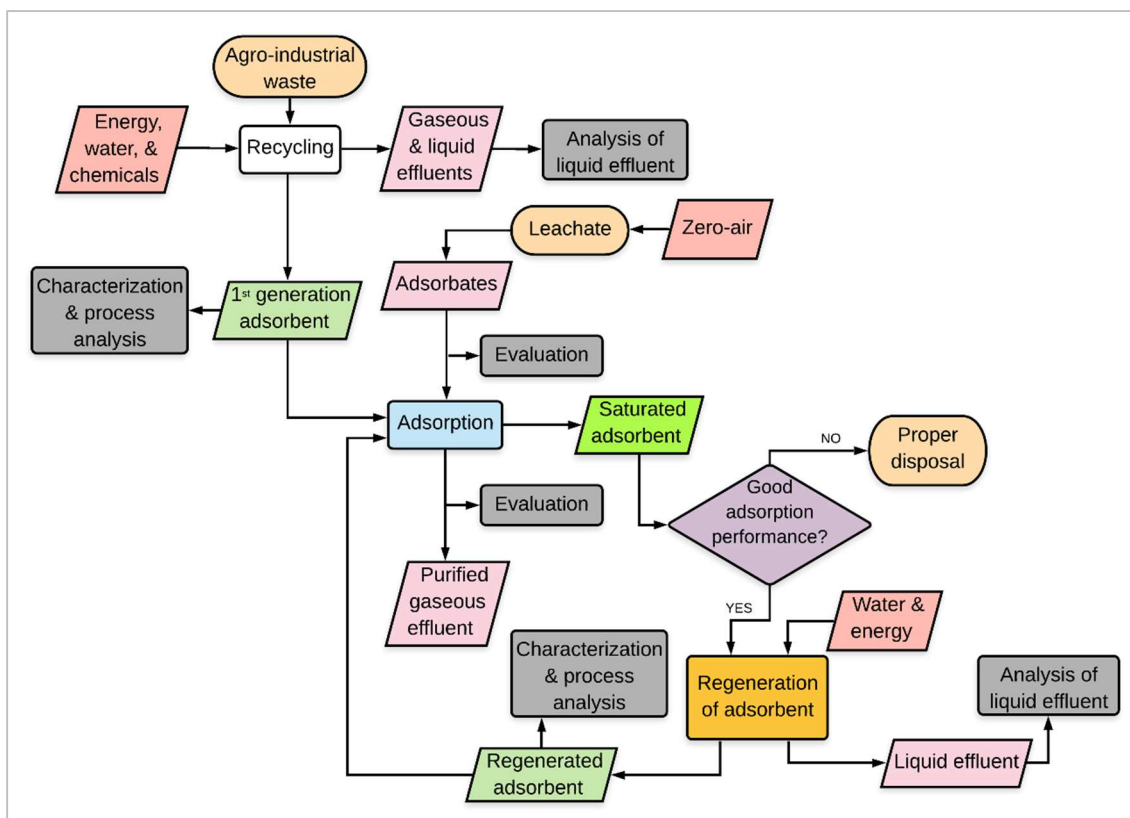


Figure 7. Schematic diagram of the stages of this work.

### 3.2 Materials and equipment

OS and MB were the feedstock used to prepare the adsorbent materials. The OS was obtained from black olives of brand DIA, S.A purchased in a local market. The MB was provided by the *Universidade Tecnológica Federal do Paraná* (UTFPR) (Federal Technological University of Paraná). Figure 8 shows the biomasses mentioned above.

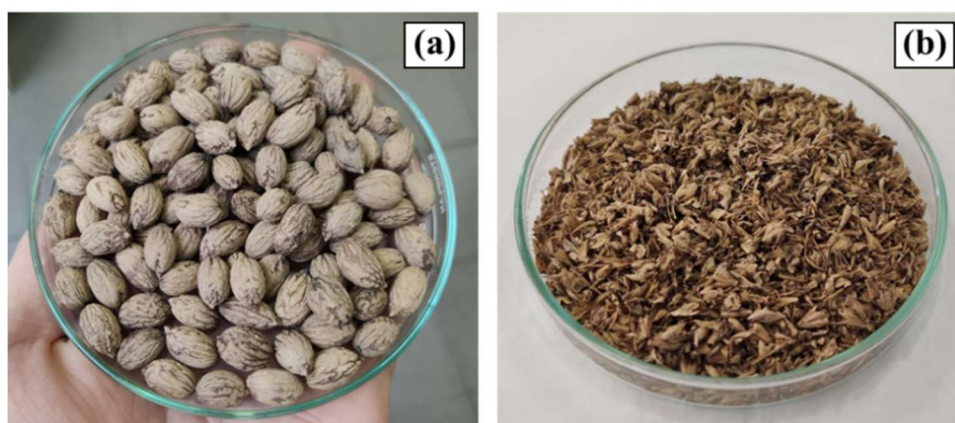


Figure 8. The feedstock (a) OS and (b) MB.

The leachate sample was obtained from the leachate storage tank of a composting line of a mechanical and biological treatment plant of organic wastes of the company *Resíduos do Nordeste*, EIM (Mirandela, Portugal). 95% sulfuric acid ( $\text{H}_2\text{SO}_4$ ), 99% sodium hydroxide ( $\text{NaOH}$ ), and 37% hydrochloric acid ( $\text{HCl}$ ) were obtained from VWR Chemicals. Nitrogen 99.995% was supplied from Praxair. Distilled water and ultrapure water were used throughout the research.

A heating chamber (model Binder FD 23) was used to dry all the samples and to prepare the hydrochars. A centrifugal mill and a ring sieve with trapezoid holes (model Retsch Ultra ZM 200) were used to mill the OS. Three high-pressure batch reactors (model 249M 4744-49, Parr Instrument Company) were used to perform the  $\text{H}_2\text{SO}_4$ -assisted HTC. A horizontal quartz tube furnace (model Thermconcept) was used to perform the pyrolysis. A Total Organic Carbon (TOC) analyzer (model Shimadzu TOC-L CSH/CSN) was used to determine the liquid phases' TOC. An elemental analyzer (model Carlo Erba Instrument EA 1108) was used to determine the adsorbents' elemental composition. An orbital shaker (model IKA KS 130 basic) was used in the adsorbents' surface chemistry analysis. A furnace (model Thermolyne 6000) was used to determine the ash content of the adsorbents. A gas adsorption analyzer (model Quantachrome NOVA TOUCH LX4) was used to obtain the adsorption-desorption isotherms used to determine the adsorbents' textural properties.

A zero-air generator (model SONIMIX 3012) was used to generate atmospheric air specially cleaned. A multi-gas analyzer (model GASERA ONE PULSE), which analyzes the infrared spectrum of the sample gases using a photoacoustic sensor based on the cantilever-enhanced optical microphone, was used to determine concentration rates of the gases  $\text{NH}_3$ ,  $\text{H}_2\text{O}$ ,  $\text{CH}_4$ ,  $\text{CO}_2$ , and  $\text{N}_2\text{O}$ . A mass flow controller and meter (model Brooks 4800 Series) was used in the gas evaluation and the adsorption tests. An air temperature and relative humidity sensor (model Campbell Scientific CS215) and a measurement and control data logger (model Campbell Scientific CR300), attached at a monitoring station, were used to measure and record air temperature data. Sample bags (model SKC Tedlar), with a storage capacity of 3 L, were used to collect the gas samples used in the olfactometric assessments.

A magnetic stirrer (model IKA C-MAG HS 7) and an electronic contact thermometer (model IKA ETS-D5) was used in the adsorbents' regeneration process.

### 3.3 Preparation of the adsorbents

Four types of adsorbents were prepared: (I) bioadsorbent; (II) pyrochar, (III) hydrochar, and (IV) activated carbon. Each sample was labeled following its respective feedstock (OS – olive stone; MB – malt bagasse) and preparation process (M for milling; P for pyrolysis; HTC for H<sub>2</sub>SO<sub>4</sub>-assisted HTC), as shown in Table 6. All samples were dried (at 60 °C for 24 h in a drying chamber) during preparation and before the adsorption tests to remove any remaining moisture.

*Table 6.* Types of adsorbent, process of preparation, feedstock, and sample label of the adsorbents prepared.

Type	Process of preparation	Feedstock	Sample
bioadsorbent	milling, drying	OS	OS-M
	drying	MB	MB
pyrochar	milling, drying, pyrolysis	OS	OS-M-P
	drying, pyrolysis	MB	MB-P
hydrochar	milling, drying, H <sub>2</sub> SO <sub>4</sub> -assisted HTC	OS	OS-M-HTC
	drying, H <sub>2</sub> SO <sub>4</sub> -assisted HTC	MB	MB-HTC
activated carbon	drying, H <sub>2</sub> SO <sub>4</sub> -assisted HTC, pyrolysis	MB	MB-HTC-P

Bioadsorbents consisted of raw biomass. Pyrochars were prepared by pyrolysis, hydrochars by H<sub>2</sub>SO<sub>4</sub>-assisted HTC, and activated carbon by sequential H<sub>2</sub>SO<sub>4</sub>-assisted HTC followed by pyrolysis.

#### 3.3.1 Bioadsorbents

The preparation of the samples derived from OS was preceded by carefully cleaning each stone with water and a sponge, removing remaining olive on the stones, and subsequently drying. Therefore, the pretreated stones were placed into a centrifugal mill and milled using a ring sieve with trapezoid holes of 0.25 mm, as shown in Figure 9.



The milled OS was dried again after milling. The milled and dried OS was used as adsorbent (sample OS-M) and as the precursor of samples OS-M-P, and OS-M-HTC.



Figure 9. The centrifugal mill and ring sieve with trapezoid holes used to mill the olive stones.

Differently, MB was not milled but only dried at 60 °C for 24 h to reduce its moisture. The dried MB was used as adsorbent (sample MB) and as the precursor of samples, MB-P, MB-HTC, and MB-HTC-P. Figure 10 shows the bioadsorbents OS-M and MB.

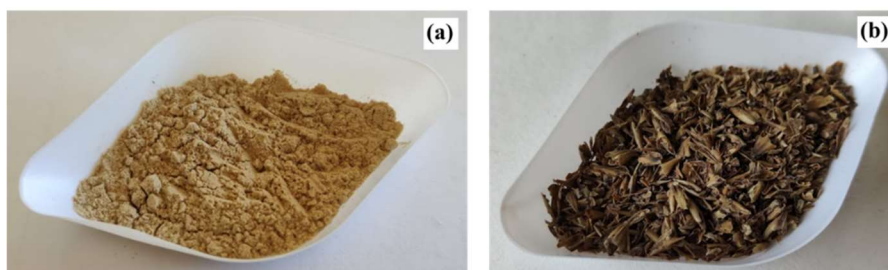


Figure 10. The bioadsorbents (a) OS-M and (b) MB prepared in this work.

### 3.3.2 Pyrochars

A mass of 5 g of the precursor (milled and dried OS or dried MB) was weighed in an analytical balance and put into a horizontal quartz tube furnace (Figure 11) to run pyrolysis, as elsewhere (Diaz de Tuesta et al., 2018). Briefly, the carbonization occurred under an N<sub>2</sub> continuous flow rate of 100 Ncm<sup>3</sup> min<sup>-1</sup>. The furnace was programmed to heat up at a rate of 10 °C min<sup>-1</sup> and keep isothermal phases of 1 h at 120 °C, 400 °C, and

600 °C. Subsequently, an isothermal phase of 4 h at 800 °C was performed, resulting in the pyrochars OS- M-P and MB-P, shown in Figure 12.



*Figure 11.* The horizontal tube furnace used to perform the pyrolysis.

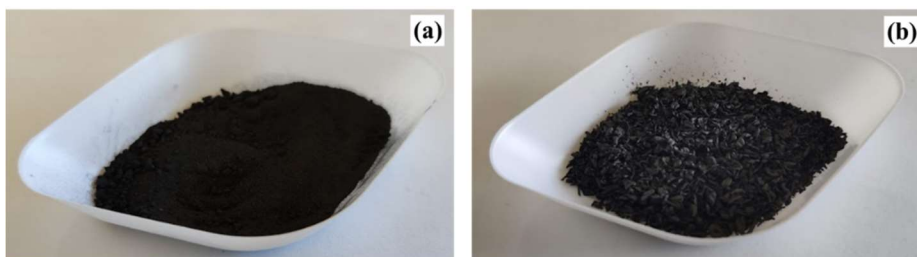


*Figure 12.* The pyrochars (a) OS-M-P and (b) MB-P prepared in this work.

### 3.3.3 Hydrochars

OS-M-HTC and MB-HTC were prepared by HTC assisted by  $\text{H}_2\text{SO}_4$ . A mass of 2.5 g of the precursor (milled and dried OS or dried MB) was immersed in 25 mL of 2.5 mol  $\text{L}^{-1}$   $\text{H}_2\text{SO}_4$  solution and kept in a high-pressure batch reactor, which has a 125 mL removable PTFE cup and stainless-steel body, under autogenous pressure at 200 °C for 3 h in a heating chamber. Figure 13 shows the three reactors that were used to prepare three samples at once.



Figure 13. The high-pressure batch reactors used to perform the  $\text{H}_2\text{SO}_4$ -assisted HTC.

After cooling, the solids were recovered by filtration and washed with distilled water until the rinsing waters reached the distilled water's pH and became translucent. The solid material was dried in a drying chamber at 100 °C for 24 h, resulting in the samples OS-M-HTC and MB-HTC (Figure 14). The liquid effluent of washing was collected for characterization. Figure 15 illustrates the filtration and washing explained above.

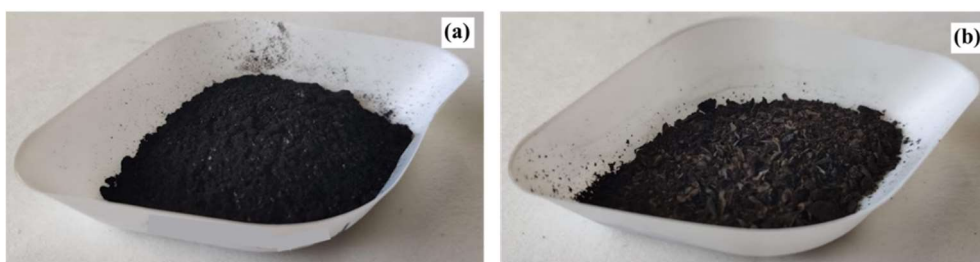


Figure 14. The hydrochars (a) OS-M-HTC, and (b) MB-HTC prepared in this work.



Figure 15. Filtration and washing of the HTC's solid product.

### 3.3.4 Activated carbon

Sample MB-HTC-P was prepared by using the hydrochar MB-HTC as a precursor. The precursor was subjected to pyrolysis at the same operating conditions explained in topic 3.3.2, as described elsewhere (Diaz de Tuesta et al., 2018).

## 3.4 Carbon and mass balance

### 3.4.1 Biomass loss

Biomass loss (B.L) represents the percentage of loss of biomass after passing the preparation processes. B.L was calculated by the difference between the initial biomass weight (before treatment process) and the final biomass weight (after treatment process), both weights on a dry basis. It was estimated for both prepared and regenerated samples.

### 3.4.2 TOC of the liquid effluent obtained by HTC

The degradation of the biomass through diverse reactions (*e.g.*, hydrolysis and dehydration) during the HTC results in finding organic matter in the liquid phase of the process (Kruse et al., 2013).

The liquid phase resulting from the preparation of OS-M-HTC and MB-HTC by H<sub>2</sub>SO<sub>4</sub>-assisted HTC was recovered to determine the TOC to assess the carbon release from raw biomass into the liquid phase. TOC quantification was determined using a TOC analyzer, shown in Figure 16.



Figure 16. TOC analyzer used to assess the carbon released in the liquid phase.

### 3.4.3 Elemental analysis

Elemental analysis was performed to determine the %wt of C, H, N, and S, of the adsorbents using an elemental analyzer. The %wt of O was estimated, given that the remaining of the CHNS-elemental analysis was considered ashes and O.

## 3.5 Characterization of the adsorbents

### 3.5.1 Surface chemistry characteristics

The acidity and basicity of the adsorbents' surface were determined by titration. The analysis started weighing 0.2 g of adsorbent and putting it in contact with 25 mL of sodium hydroxide (NaOH) 0.02 mol L<sup>-1</sup> solution in a 100 mL Erlenmeyer flask. Subsequently, 0.2g of the same adsorbent was weighed and placed with 25 mL of hydrochloric acid (HCl) 0.02 mol L<sup>-1</sup> solution in another flask. All flasks containing the mixture of adsorbent and solution were placed in an orbital shaker for 48 h at 320 rpm, as shown in Figure 17.



*Figure 17.* The flasks containing the mixture of adsorbent and solution placed in the orbital shaker.

Afterward, the mixtures were filtered, and 20 mL of each sample's liquid fraction (NaOH/HCl solutions) was titrated. To determine the acidity, the NaOH solutions were titrated with HCl 0.02 mol L<sup>-1</sup>. To determine the basicity, the HCl solutions were titrated

with NaOH 0.02 mol L<sup>-1</sup>. Acidity and basicity of the surface of the adsorbents were estimated, according to Equation 3.

$$\text{Acidity/Basicity} = \left( \frac{0.025}{m} \right) \times \left( C_{ab} - \left( \frac{V_t \times C_{tab}}{0.02} \right) \right) \times 1000 \quad (3)$$

Where Acidity/Basicity is given in mmol g<sup>-1</sup>,  $m$  is the mass of adsorbent (g),  $C_{ab}$  is the concentration of NaOH or HCl in solution (mol L<sup>-1</sup>),  $V_t$  is the titrated volume of NaOH or HCl (L), and  $C_{tab}$  is the concentration of NaOH or HCl for titration (mol L<sup>-1</sup>).

### 3.5.2 Ashes determination

The %wt of ash analysis was performed using a furnace, shown in Figure 18. A crucible was calcined at 800°C to remove any moisture and weighed. Calcination lasted until the crucible achieved constant weight (+/- 0.0003 g of difference was considered acceptable), representing the crucible dry weight ( $W_c$ ). Afterward, 0.1 g of adsorbent material ( $W_m$ ) was placed on the crucible, taken to the muffle for 3-4 h at 800 °C, and subsequently weighed. The crucible containing adsorbent material was taken to the muffle for one more hour and weighed again. Calcination lasted until the crucible containing adsorbent material achieved constant weight (+/- 0.0003 g of difference was considered acceptable), which represents the  $W_c$  plus the inorganic weight of inorganic material ( $W_{ci}$ ). The %wt of ash was estimated according to Equation 4:

$$\text{Ash} = \frac{(W_{ci} - W_c)}{W_m} \times 100 \quad (4)$$





Figure 18. The furnace used in the ash analysis.

### 3.5.3 Textural properties

The adsorbents' textural properties were determined by analysis of nitrogen (at its boiling temperature of 77 K) adsorption-desorption isotherms obtained using a gas adsorption analyzer, following the same procedure as elsewhere (Diaz de Tuesta et al., 2018). Briefly, the degassing method was performed at 200 °C for a period of 16 h, according to IUPAC recommendation. The Brunauer–Emmett–Teller (BET) specific surface area ( $S_{BET}$ ) was determined using BET methods. The external surface area ( $S_{ext}$ ) and micropore volume ( $V_{mic}$ ) were obtained by the  $t$ -method in which the thickness is calculated by using the ASTM D-6556-01 - Standard Test Method for Carbon Black — Total and External Surface Area by Nitrogen (ASTM, 2001). The total pore volume ( $V_{total}$ ) was calculated in a  $p/p_0$  of 0.98. Calculations of those methods were all done by using TouchWin<sup>TM</sup> software v1.21. Micropore surface area ( $S_{mic}$ ) and average pore diameter ( $W_{mic}$ ) were estimated by the approximations shown in Equations 5 and 6.

$$S_{mic} = S_{BET} - S_{ext} \quad (5)$$

$$W_{mic} = 4 \times \frac{V_{mic}}{S_{mic}} \quad (6)$$

The carbonaceous adsorbents were classified according to the physisorption isotherms. The adsorption-desorption isotherms, obtained by the experimental analysis mentioned above, were compared to the eight physisorption isotherms curves classification, established by IUPAC (Figure 19). Each of these curves' types is related to the pore structure's particular features and the underlying adsorption mechanism (Thommes et al., 2015).

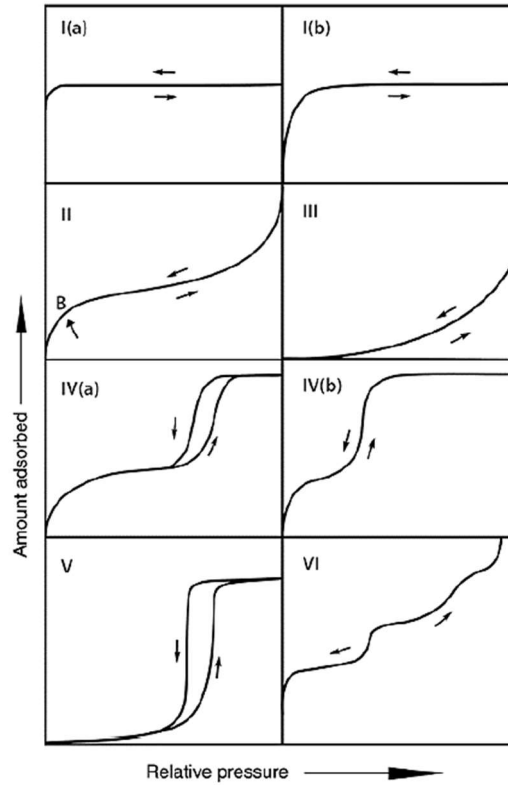


Figure 19. Main types of physisorption isotherms established by IUPAC. (Thommes et al., 2015).

#### 3.5.4 Void fraction characteristics

Interparticle void volume and external void fraction of the bed were estimated using a 10 mL graduated measuring cylinder and distilled water. Adsorbent material was placed into the cylinder until it reaches the 2 mL mark ( $V_m$ ). Subsequently, 2 mL of distilled water ( $V_w$ ) was added to the same cylinder containing the sample, and the total volume was registered ( $V_t$ ). The void volume ( $V_{void}$ ), in mL, was estimated according to Equation 7, and the void fraction ( $Void_f$ ), in %, was estimated according to Equation 8 (McCabe et al., 1993).



$$V_{void} = (V_m + V_w) - V_t \quad (7)$$

$$Void_f(\%) = \frac{V_{void}}{V_m} \times 100 \quad (8)$$

### 3.6 Set-up of the lab-scale system

A lab-scale system was assembled to run tests to evaluate the concentrations of  $\text{NH}_3$  in the zero-air (*za*) and the leachate and evaluate, objectively and subjectively, the  $\text{NH}_3$  adsorption capacity of the adsorbents. The *za* and the leachate were evaluated before the adsorption tests.

The system consisted of the following stages, connected by PTFE tubes and three valves (V1, V2, and V3), running continuously. Each sample collected by the multi-gas analyzer (MGA) takes about 3 minutes to be processed and registered by the equipment, and only after that period, the equipment collected the subsequent sample. Figure 20 represents a schematic of the lab-scale system assembled for evaluating zero-air, leachate off-gases, and the adsorbents' performance and effectiveness, which is explained in detail below.

- i. generation of *za* by a zero-air generator (ZAG);
- ii. flow control (FC) and flow meter (FM) monitoring;
- iii. odorous gas (*og*) emission from the source of the odor (SO);
- iv. upstream gas for subjective evaluation (*ugs*) taken upstream from the fixed-bed (FB) column;
- v. adsorption of pollutants on the adsorption column packed with FB of adsorbent;
- vi. gas sample is taken by the MGA (*za*, leachate off-gases, or downstream gas for objective evaluation (*dgo*)) taken downstream from the FB column.
- vii. downstream gas for subjective evaluation (*dgs*) taken downstream from the FB column;
- viii. effluent outlet (*eo*).

To evaluate the performance and effectiveness of the carbonaceous materials prepared from biomass in the adsorption of  $\text{NH}_3$ , atmospheric air was taken into a ZAG used to reduce significantly any main pollutant to generate *za* (i). The FC controlled the *za* flow to maintain a flow rate of  $0.8 \text{ L min}^{-1}$ , and the FM displayed the current flow rate (ii). Then, *za* was led to an empty gas washing bottle (placed to avoid leachate return into the FM) followed by another gas washing bottle in which 5 mL of leachate, the SO, was mixed with distilled water (1:10 dilution). The *za* was injected on top of the SO, enhancing the *og* emission (iii). The *og* flow was led toward upstream the adsorption FB. Switching V1 to position two, the *og* flow was led to a sample bag to collect the *ugs*, used on the procedure explained on topic 3.7.3 (iv). With V1 in position one, *og* was led to FB flowing downward through the adsorbent to avoid disturbing the bed (v), as recommended by ASTM International (2019). After passing through the adsorption column, with V2 in position two, the *dgo* was taken by the MGA (vi). With V2 to position one, the gas flow was led to V3. With V3 in position two, the cleaner gas flow was led to a sample bag to collect *dgs*, used on the procedure explained on topic 3.7.3 (vii). With V3 in position one, the cleaner gas reached the *eo* and was released into the atmosphere (viii).

In the evaluation of leachate off-gases, the same process explained in the previous paragraph was performed excluding the steps (iv), (v) and (vii); and in the evaluation of *za* steps (iii), (iv), (v) and (vii) were excluded (Figure 20).

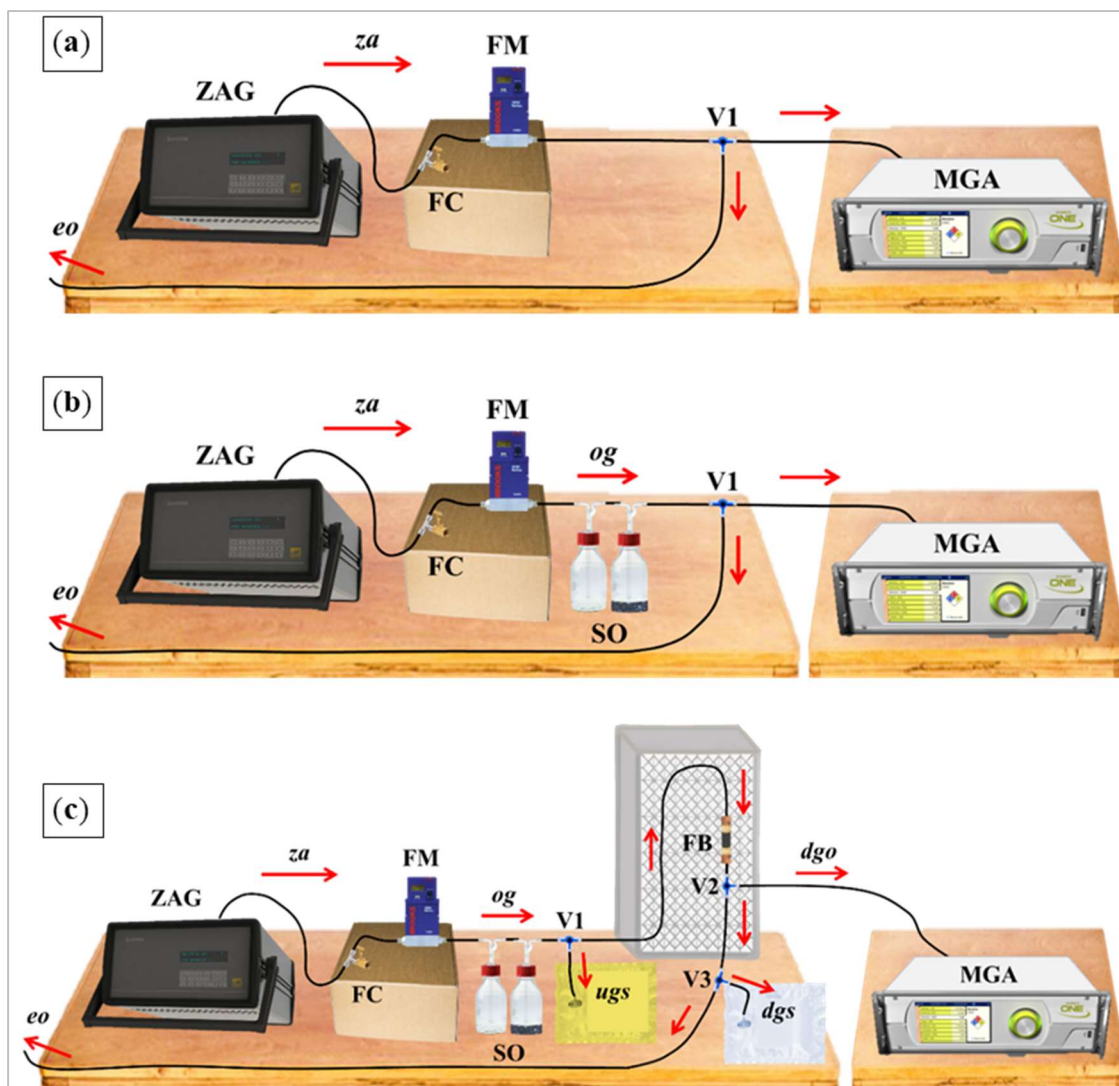


Figure 20. Schematic of the set-up of the lab-scale system for evaluating: (a) zero-air (za), (b) leachate off-gases, and (c) the performance and effectiveness of the adsorbents.

A photo of the lab-scale system is shown in Figure 21, in which the SO, the *ugs*, the FB column, the *dgo*, the *dgs*, and the MGA are detailed.

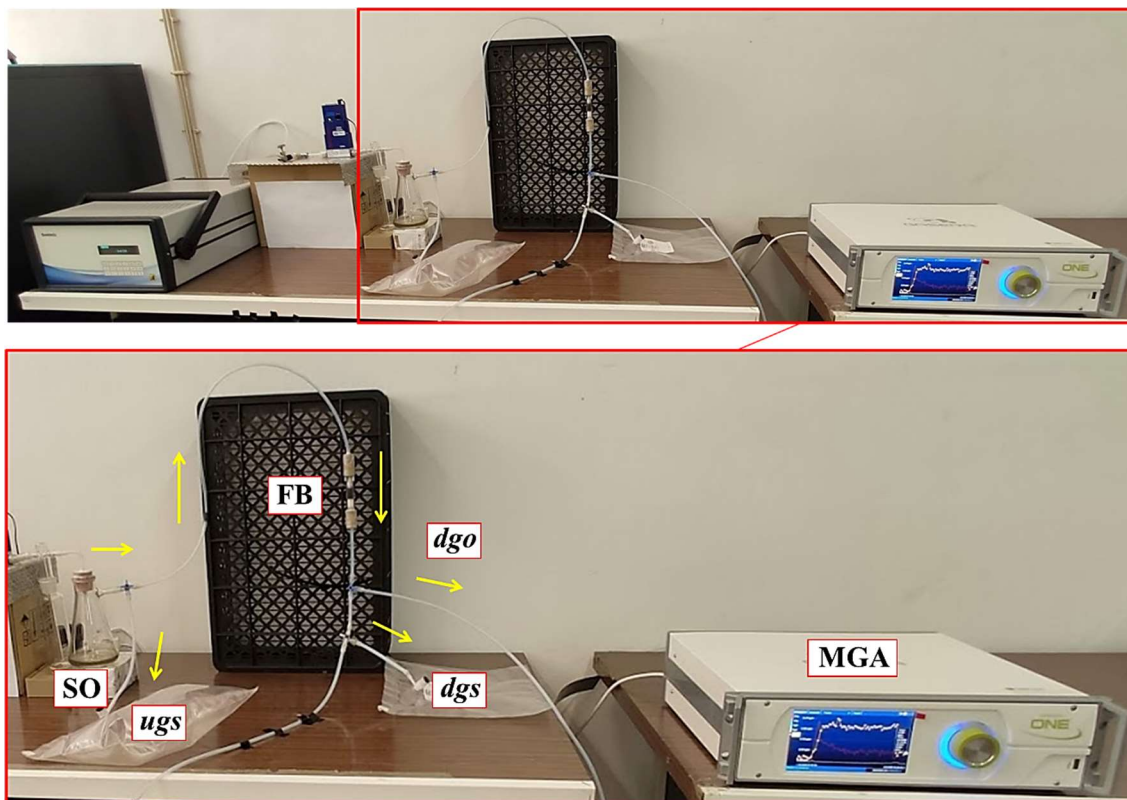


Figure 21. Photo of the lab-scale system assembled. In detail: source of odor (SO), upstream gas for subjective evaluation (*ugs*), fixed-bed (FB) column, downstream gas for objective evaluation (*dgo*), downstream gas for subjective evaluation (*dgs*), and multi-gas analyzer (MGA).

### 3.7 NH<sub>3</sub> concentration and adsorption

All tests were performed at a flow rate of 0.8 L min<sup>-1</sup>, room temperature, and atmospheric pressure (approximately 93.7 KPa). The temperature was measured and recorded during all tests since they were performed with the room door open to the outside area to prevent odors from being trapped inside the room. An air temperature sensor and a measurement and control datalogger attached at a monitoring station placed right next to the room door (Figure 22) were used for this purpose. The temperature was measured and recorded every 10 minutes.



Figure 22. Monitoring station containing the air temperature sensor and the data logger.

### 3.7.1 Evaluation of zero-air and gases derived from leachate

The *za* and leachate emissions were evaluated concerning  $\text{NH}_3$  concentrations. Three tests lasting 3h each were performed to evaluate the *za*. Differently, to evaluate leachate off-gases, four tests lasting 8 h each and two tests lasting 24 h each were performed.

The one-way analysis of variance (ANOVA) was used to determine whether any statistically significant differences between the *za* tests'  $\text{NH}_3$  means using the software Origin 2018, considering a significance level of 0.05. The same software was used to plot the  $\text{NH}_3$  emission curves of the leachate's tests. The curves mentioned before were plotted by smoothening data using the moving average method, considering the three adjacent ranges (back and forward).

### 3.7.2 Objective evaluation of $\text{NH}_3$ adsorption

Concentration rates of gases  $\text{NH}_3$ ,  $\text{H}_2\text{O}$ ,  $\text{CH}_4$ ,  $\text{CO}_2$ , and  $\text{N}_2\text{O}$  downstream from the FB were determined. Since the MGA can simultaneously measure  $\text{NH}_3$  and the gases  $\text{H}_2\text{O}$ ,  $\text{CH}_4$ ,  $\text{CO}_2$ , and  $\text{N}_2\text{O}$ , these non-odorous gases were also evaluated to verify any possible competitive adsorption.

Mean  $\text{NH}_3$  inlet concentration was determined before adsorption tests, ranging from 6 ppm to 10 ppm. Three tests were performed for samples OS-M, OS-M-HTC,

MB-HTC; two tests for samples OS-M-P, MB, MB-P, and one test for sample MB-HTC-P. The breakthrough curve of each sample was plotted as being the mean curve of its respective tests.

The FB column was designed based on ASTM D5160-95(19) – Standard Guide for Gas-phase Adsorption Testing of Activated Carbon (ASTM, 2019). It consisted of a vertically supported cylindrical acetate sample tube (inner diameter = 1.2 cm, height = 8.5 cm) filled with adsorbent and supported at its lower end by a fine flat mesh stainless steel screen in order to ensure fixed packing of the bed. Another mesh was placed at its upper end to ensure uniformity of flow profile across the adsorbent bed. Inert glass wool was used above and below the adsorbent to avoid slippage. A schematic of the FB column is shown in Figure 23.

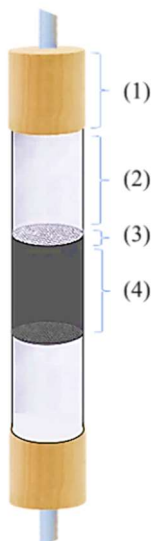


*Figure 23.* Schematic of the fixed-bed column: (1) cap, (2) glass wool, (3) mesh, and (4) adsorbent.

The height of the adsorption bed ( $Z$ ) has been established for each sample, and  $\text{NH}_3$  inlet concentration was estimated.  $\text{NH}_3$  concentration downstream from the adsorption column was measured every 3 minutes until the saturation of the bed. The software Origin 2018 was used to plot the breakthrough curves. The normalized breakthrough curves were plotted by smoothening data using the moving average method, considering the three adjacent ranges (back and forward). The curve of each sample represents the average values of all tests performed using that adsorbent. Various parameters were determined from the analysis of breakthrough curves:

breakthrough time ( $t_b$ ), stoichiometric time ( $t_{sto}$ ), saturation time ( $t_{sat}$ ), the height of mass transfer zone ( $H_{MTZ}$ ), and dynamic adsorption capacity ( $q_a$ ).

The  $t_b$  was defined as the time it takes the pollutant to break through the fixed bed of adsorbent; hence the time at the pollutant concentration increased. The  $t_{sto}$  was defined as the time in which the pollutant's concentration in the outlet stream reaches 50% of the inlet concentration ( $C/C_0 = 0.50$ ). The  $t_{sat}$  was defined as the time in which the pollutant's concentration in the outlet stream reaches 95% of the inlet concentration ( $C/C_0 = 0.95$ ).

The  $H_{MTZ}$  was determined by the  $t_b$  and  $t_{sat}$  values from the breakthrough curves and the  $Z$ . The  $H_{MTZ}$  was estimated by Equation 9 (Ang et al., 2020):

$$H_{MTZ} = Z \cdot \frac{t_{sat} - t_b}{t_{sat}} \quad (9)$$

with  $Z$  in cm,  $t_b$ , and  $t_{sat}$  in min.

The  $q_a$  (milligrams of adsorbate/grams of adsorbent) of the adsorbents were estimated by integration of the area under the breakthrough curve, also considering the system flow rate and the mass of adsorbent used (Ang et al., 2020; Balsamo et al., 2013; Gonçalves et al., 2011), as expressed in Equation 10:

$$q_a = \frac{Q}{m} \cdot \int_0^{t_{sat}} (C_0 - C_t) dt \quad (10)$$

where  $Q$  is the gas flow rate ( $L \min^{-1}$ ), and  $m$  is the mass of adsorbent (g), with  $t_{sat}$  ( $C_t = C_0$ ) in min.

The integration was calculated using the graphing and analysis software Origin 2018, by the Peak Analyzer tool. Peaks were found by the Fourier Self-Deconvolution method, with a predefined smoothing factor of 0.1 and 2 local points.  $C_0$  was converted from ppm to  $g \text{ cm}^{-3}$  using the ideal gas law, considering the temperature of 298.15 K (25 °C) and standard atmospheric pressure ( $\sim 1013.25$  mbar). Figure 24 graphically illustrates the method mentioned above, which, differently from the ideal breakthrough presented in Figure 6, shows a real breakthrough curve obtained in an adsorption test performed in this work.



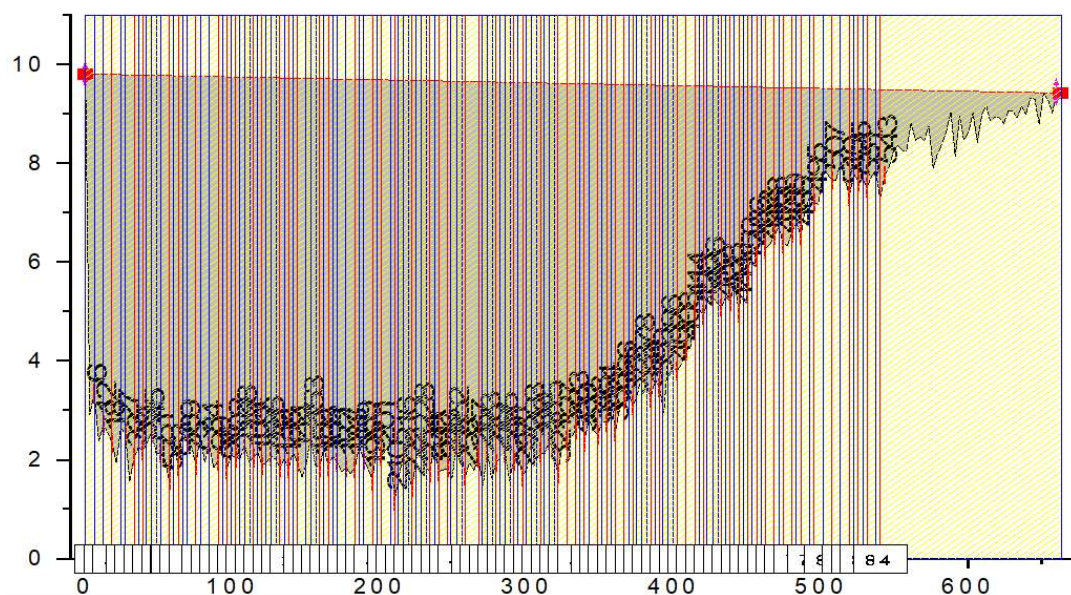


Figure 24. Illustration of the integration calculation using the Peak Analyzer tool in a real breakthrough curve obtained in an adsorption test performed in this work.

### 3.7.3 Subjective evaluation of $\text{NH}_3$ adsorption

Subjective evaluation of odorous pollutants' adsorption consisted of olfactory analysis, which uses odorants' effect on the human sense of smell. The experiments were based on the recommendations of the EU standard EN 13725, Air Quality- Determination of Odor Concentration by Dynamic Olfactometry (CEN, 2003) and the German standard VDI 3882, Part1: Olfactometry – Determination of Odor Intensity (VDI, 1992a); and Part 2: Olfactometry – Determination of Hedonic Odor Tone (VDI, 1992b), regard to materials and methods. The data record sheet used for odor intensity/hedonic odor tone assessment, shown in Appendix A, was adapted from the German standard VDI 3940, Part 3: Measurement of odor impact by field inspection - Determination of odor intensity and hedonic odor tone (VDI, 2010).

The gas samples were collected during the tests with selected adsorbents, as explained in section 3.6. A panel of twenty assessors was selected to judge samples. All members were at least 16 years old at the date of tests and were asked to meet the following conditions:

- do not be feeling hungry or thirsty or have eaten any strongly flavored foods on the day of the analysis;
- do not drink alcoholic beverages on the day of the analysis;



- do not smoke from at least 30 minutes before olfactometric measurements;
- preferably do not eat, drink (except water), use chewing gum or sweets from at least 30 minutes before olfactometric measurements;
- preferably do not use perfumes, deodorants, body lotions, or any other cosmetic or personal hygiene, which may interfere with their olfactive perception on the day of the analysis.
- do not be suffering from a cold or any other ailment affecting their perception of smell (*e.g.*, allergic fits, sinusitis, etc.) at the moment of the analysis.

The olfactometric assessments were performed using samples collected upstream and downstream of the FB column, as explained in topic 3.6, using 3 L sample bags. Before gas collection, the bags were tested for leakage and purged with clean air (*za*) several times to remove any remaining smell. The bags filled with samples were stored in a closed box to prevent direct sunlight, and the interval between the sampling and the analysis by delayed olfactometry did not exceed 30 h. Figure 25 shows pictures of an empty sample bag, the filling procedure, and the filled bag's storage.



Figure 25. Pictures of sampling and storing steps: (a) empty sample bag, (b) sample being taken from the adsorption test, and (c) bags filled with samples stored.

One sample was taken upstream of the FB column and labeled  $SE_{Feed}$ . Four samples were taken downstream of the FB column:  $SE_{Clean}$  - at maximum removal capacity;  $SE_{Break}$  - between breakthrough and stoichiometric times;  $SE_{Stoic}$  - between stoichiometric and saturation times; and  $SE_{Satur}$  - right after saturation. Figure 26 shows a schematic representation of the points of the breakthrough curve in which samples were collected.

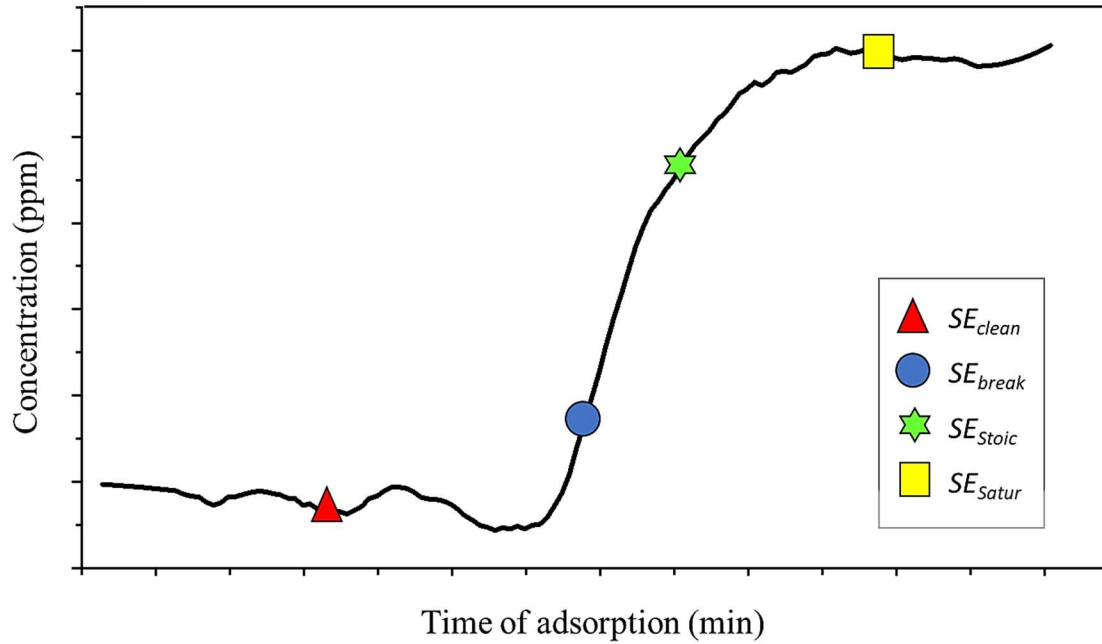


Figure 26. Schematic representation of downstream samples on the breakthrough curve.  $SE_{Clean}$  - at maximum removal capacity;  $SE_{Break}$  - between breakthrough and stoichiometric times;  $SE_{Stoic}$  - between stoichiometric and saturation times; and  $SE_{Satur}$  - right after saturation.

The odors were evaluated concerning its intensity and hedonic tone (pleasant/unpleasant quality), as shown in Figure 27. According to VDI (1992a), the intensity level is verbal (or written) descriptions of an odor sensation to which numerical values are assigned and shall be expressed on a scale ranging from 0 (not perceptible) to 6 (extremely strong). On the other hand, the hedonic tone is verbal (or written) descriptions of an odor sensation to which numerical values are assigned and shall be expressed on a scale ranging from 4 (extremely unpleasant) to +4 (extremely pleasant) (VDI, 1992a).

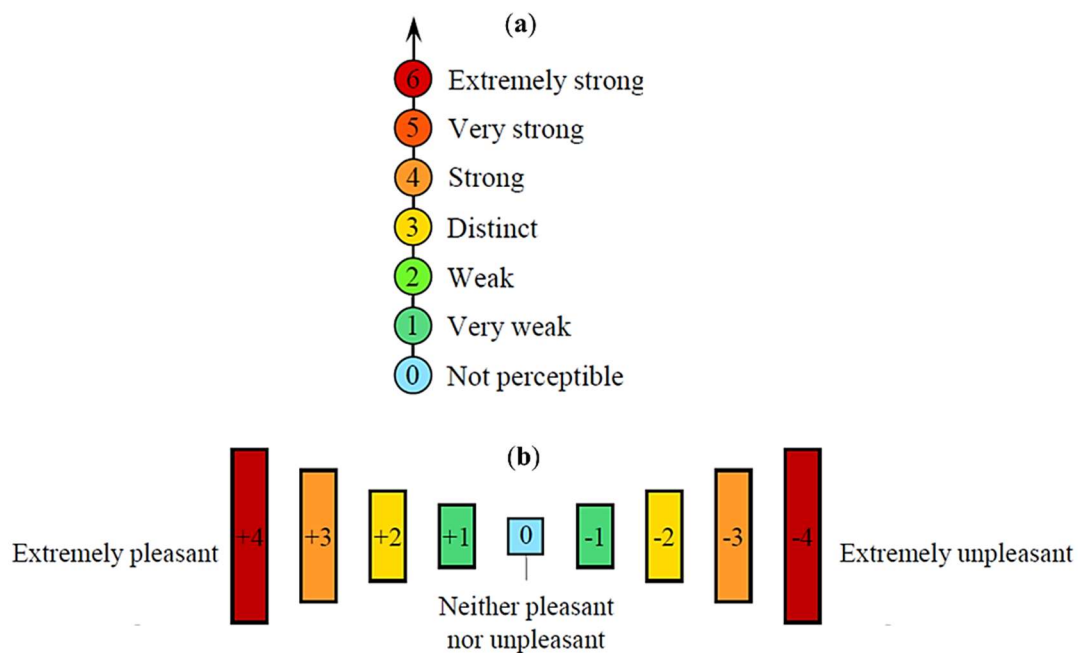


Figure 27. Odor (a) intensity and (b) hedonic tone scales. Based on (VDI, 1992a).

Figure 28 shows the olfactometric assessment set-up, in which an olfactometer was assembled and used to present the undiluted gas samples to panelists for inhalation. The olfactometer was composed of ZAG, FC, FM, two sniffing ports (SP<sub>1</sub> and SP<sub>2</sub>), the bag filled with sample, and PTFE tubing.

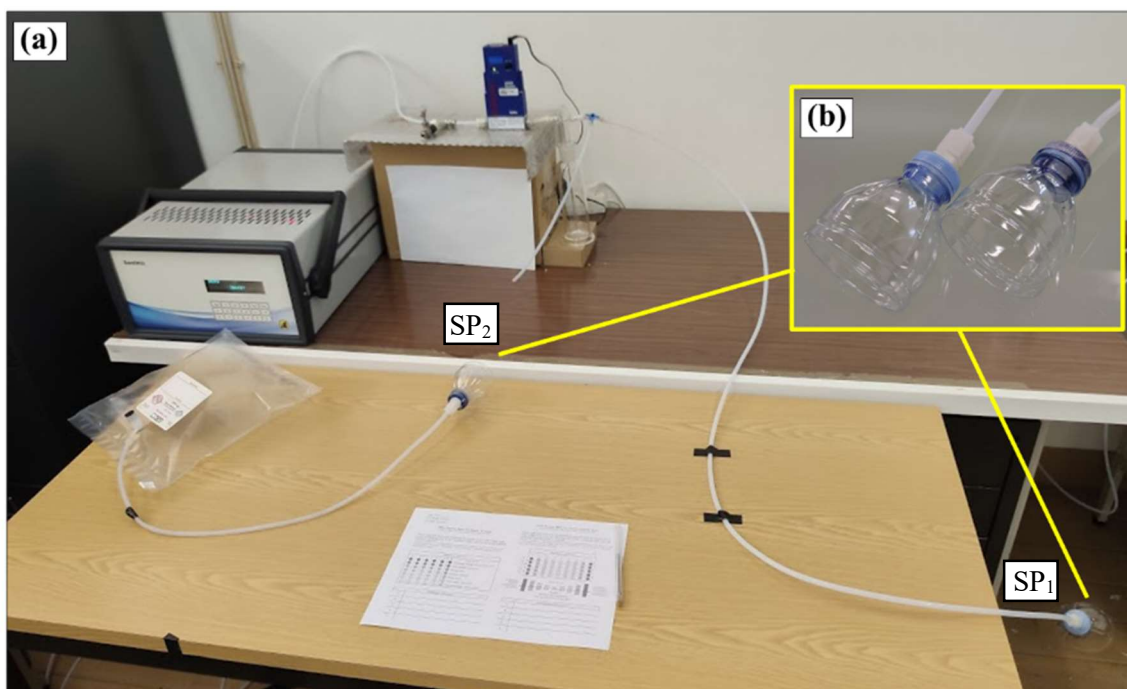


Figure 28. Set-up of the olfactometric analysis: (a) olfactometer and (b) the sniffing ports in detail.

Each of the undiluted samples (odor stimulus) was presented for 10 seconds, using the  $SP_2$ , with an additional decision time of 5 seconds. The odor stimuli followed the sequence:  $SE_{Clean}$ ,  $SE_{Break}$ ,  $SE_{Stoic}$ ,  $SE_{Feed}$ , and  $SE_{Satur}$ . The rounds of odor stimuli were interspersed with a break of 60 seconds between each stimulus, during which zero-air (neutral air) was presented as a sensory reference, using the  $SP_1$ , to reset the sense of smell, avoiding adaptation of the odors. The analysis series started with neutral air, followed by a sample. Before each odor stimulus, the tube connected to the  $SP_2$  was flushed with neutral air to remove any odor traces that might be retained inside of it, derived from the previous sample.

The series explained above was presented to each assessor twice, one time to intensity assessment and another time to hedonic tone assessment. The assessors did not know what samples they were evaluating in any case. Each assessor used a different pair of sniffing ports to avoid interferences and due to health issues.

Before each of the olfactometric analysis, the panel members were informed that there is no “right” or “wrong” answer so that what matters is their impression. The assessor was also instructed to:

- I. put the nose entirely in the nozzle and inhale from the nose and exhale from the mouth, two or three times;
- II. immediately decide, as spontaneously as possible without too much reflection, and evaluate the odors regarding their intensity or pleasantness/unpleasantness, following the scales presented.

### 3.8 Regeneration of saturated adsorbents

#### 3.8.1 Experimental procedure

Regeneration of selected samples (OS-M and OS-M-HTC) was performed based on the method presented by Ro et al. (2015), which aimed to regenerate adsorbents saturated with  $NH_3$  using water, based on the fact that gaseous  $NH_3$  can be dissolved in water (ATSDR, 2011). In this sense, the saturated sample was placed in a round-bottomed flask containing ultrapure water (UPw) and a stir magnetic. The flask containing the sample mixed with water was placed on a magnetic stirrer to stir. An electronic contact

thermometer was used to control the temperature. Figure 29 illustrates the regeneration process.



Figure 29. Set-up of the adsorbents' regeneration process.

All regeneration processes were conducted at 25-80 °C and lasted 24 h stirring at a 1220 rpm speed. The saturated material's concentration ranged from 2.4 to 16 g L<sup>-1</sup>. Subsequently, the flasks' content was filtered, and the regenerated material was placed into a drying chamber at 100 °C for 24 h. The conditions and the label of the regenerated samples, in which the letter R represents “regenerated”, are summarized in Table 7.

Table 7. Sample labeling and regeneration operating conditions.

Regenerated Sample	<i>m</i> (g)	<i>T</i> (°C)	<i>V</i> <sub>UPw</sub> (mL)	Agitation speed (rpm)	Duration of process (h)
R_I_OS-M	1.2	25	500	1220	24
R_II_OS-M	2.4	25	150		
R_III_OS-M	1.2	80	500		
R_OS-M-HTC	0.5	25	100		

One sorption cycle was performed, using each regenerated material, in the same experimental system explained in section 3.6. The same methodologies explained in section 3.7.2 were applied to evaluate the regenerated adsorbents' performance and effectiveness in removing gaseous  $\text{NH}_3$ .

### 3.8.2 TOC, conductivity, and pH of the liquid phase

The liquid phase resulting from the regeneration of OS-M and OS-M-HTC were recovered to determine the TOC in order to assess the carbon release from raw biomass into the liquid phase. TOC quantification was determined using a TOC analyzer, shown in Figure 16.

Before (ultrapure water) and after the regeneration process, the liquid phase's conductivity and pH were measured using a pH meter and a conductivity meter.

## 4 RESULTS AND DISCUSSION

This chapter presents the results obtained after developing the steps explained in Chapter 3 and its discussion based on literature. The results are presented in the following order: the preparation processes' carbon and mass balance and the adsorbents' elemental analysis; the  $\text{NH}_3$  concentration in zero-air and feed stream from leachate; the chemical and olfactometric analysis of  $\text{NH}_3$  adsorption; the surface chemistry, textural properties, and void fraction characterization; the regeneration and re-use of adsorbents saturated with  $\text{NH}_3$ ; and the characteristics of this regeneration's liquid effluent.

### 4.1 Carbon and mass balance

#### 4.1.1 Biomass loss

The B.L was determined by the difference between the initial biomass weight (before the treatment process) and the final biomass weight (after the treatment process), both on a dry basis. Table 8 shows the B.L of the samples prepared in this work.

*Table 8.* Biomass loss (B.L) of samples prepared in this work.

<b>Sample</b>	<b>B.L (%)</b>
OS-M-P	74.9
MB-P	75.8
OS-M-HTC	50.7
MB-HTC	59.7
MB-HTC-P	85.3

As presented in Table 8, the combination of  $\text{H}_2\text{SO}_4$ -assisted HTC, followed by pyrolysis (sample MB-HTC-P), led to the greatest B.L of 85.3%. The biomass pyrolysis also caused significant mass loss with samples OS-M-P and MB-P presenting B.L of 74.9 and 75.8%, respectively. On the other hand, biomass prepared by  $\text{H}_2\text{SO}_4$ -assisted HTC losses more than half of the initial mass, with samples OS-M-HTC and MB-HTC presenting B.L of 50.67 and 59.66%, respectively.

B.L is mainly due to removal of moisture, volatilization of organic matter, attack of chemical agents, the solubility of the components in the chemical solutions, and loss in washing and filtration process (Ioannidou et al., 2007; Martín-Lara et al., 2013).

#### 4.1.2 TOC of the liquid effluent obtained by HTC

The liquid phases resulting from the preparation of OS-M-HTC and MB-HTC by H<sub>2</sub>SO<sub>4</sub>-assisted HTC were recovered to determine the TOC. Table 9 shows the values obtained by TOC analysis.

*Table 9.* Total Organic Carbon (TOC) of the liquid phase resulting from the H<sub>2</sub>SO<sub>4</sub>-assisted HTC processes.

<b>Sample</b>	<b>TOC (g L<sup>-1</sup>)</b>
OS-M-HTC	9.42
MB-HTC	11.76

The liquid phase of the HTC presents organic matter due to the degradation of the biomass through diverse reactions (*e.g.*, hydrolysis and dehydration) (Kruse et al., 2013), which is evidenced by the carbon results presented in Table 9.

Both samples presented similar carbon loss, with the MB-HTC slightly higher (11.76 g L<sup>-1</sup>). According to Ronda et al. (2015), a decrease of TOC content of samples subject to chemical treatments is one of the main changes produced during chemical treatments. The TOC found in the liquid phases analyzed shows a decrease in the solid carbonaceous materials' TOC content. Leng & Zhou (2018) presented in a literature review that TOC values of the aqueous phase of the HTC of various biomass feedstock ranged from 2.38 to 104.2 g L<sup>-1</sup>, with most ranging from 9 to 23 g L<sup>-1</sup>. The TOC of samples presented in Table 9 may be considered low, comparing to the values presented above, which is positive since recent studies are focused on decreasing the load of organic matter dissolved in the liquid effluent in the HTC (Kruse et al., 2013).



## 4.1.3 Elemental analyses and ashes determination

Table 10 presents the results of the elemental analyses of the adsorbents prepared, performed to determine the composition weight percentages (%wt) of carbon (C), hydrogen (H), nitrogen (N), sulfur (S), estimated oxygen (O) and ash.

Table 10. Elemental composition of the adsorbents.

	(%wt)						C/H
	C	H	N	S	O*	Ash	
<b>OS-M</b>	49.30	6.27	0.15	0.06	43.58	0.64	7.86
<b>OS-M-P</b>	87.98	1.04	1.10	0.08	5.82	3.99	85.32
<b>OS-M-HTC</b>	-	-	-	-	-	0.16	-
<b>MB</b>	44.90	6.60	2.40	0.20	42.72	3.18	6.80
<b>MB-P</b>	72.50	1.30	3.30	0.00	11.50	11.40	55.77
<b>MB-HTC</b>	68.10	6.20	0.70	0.80	23.10	1.10	10.98
<b>MB-HTC-P</b>	81.80	1.20	1.10	0.20	9.40	6.30	68.17

\* Estimated by difference ( $O = 100 \text{ wt\%} - C - H - N - S - \text{ash}$ ) (Yek et al., 2019)

Based on the results shown in Table 10, the pyrolyzed samples (OS-M-P, MB-P, and MB-HTC-P) showed higher C content and lower H and O content, hence higher C/H ratios. Sample OS-M-P presented the highest C content (87.98%) and C/H ratio (85.32%), which is almost 12 times greater than that of OS-M. Sample MB-HTC-P, prepared from MB by H<sub>2</sub>SO<sub>4</sub>-assisted HTC followed by pyrolysis, showed a higher C/H ratio (68.17%) than those prepared by the same feedstock only by pyrolysis (55.77%) and H<sub>2</sub>SO<sub>4</sub>-assisted HTC (10.98%). The results presented above may be related to the decomposition and carbonization reactions, in which organic fractions of the feedstocks may have either being decomposed into volatile matter (*e.g.*, CO, CO<sub>2</sub>, and CH<sub>4</sub>) and released as gases, or carbonized forming the pyrochars with improved aromaticity (Chen et al., 2017; Lam et al., 2017; Yek et al., 2019).

Table 10 also showed that the HTC of biomass, producing the sample MB-HTC, also increased C and decreased H and O contents (hence increasing C/H), compared to the raw feedstock (MB). However, the decrease in H and O content was slighter than those observed for the pyrochars. It may be explained by the fact that a small fraction of

gases (CO, CO<sub>2</sub>, H<sub>2</sub>, and CH<sub>4</sub>) are generated during the hydrothermal process, especially when performed in temperatures below 260°C (Basso et al., 2015).

Compared to the precursors' content, the H<sub>2</sub>SO<sub>4</sub>-assisted HTC also decreased ash content from 3 to 4 times (Table 10). It means that the process mentioned above reduces the amount of inorganic matter in the composition of the adsorbents after H<sub>2</sub>SO<sub>4</sub> treatment of OS, which was also observed by Cagnon et al. (2009). The reduction in ashes may be ascribed to the metals' leaching from the raw biomass into the liquid phase by the acid attack during the HTC process.

The values of composition weight percentages (%wt) founded for OS-M correspond with those presented by Ghouma et al. (2015), Martín-Lara et al. (2013), Cagnon et al. (2009), and González et al. (2009), which are within the ranges: 43.1 – 52.34 for C; 5.9 – 7.11 for H; 0.03 – 1.0 for N; 0.01 – 0.8 for S; 40.47 – 49.1 for O and 0.37 – 4.4 for ash. On the other hand, the values of composition weight percentages (%wt) founded for BM are similar to those presented by Franciski et al. (2018) and Mello et al. (2014) 46.84 for C; 8.18 for H; 3.86 for N; 0.38 for S; 40.74 for O and 2.78 for ash.

The high carbon content of samples suggests that expectable carbon-rich materials have been prepared in this work.

## 4.2 NH<sub>3</sub> concentration and adsorption

### 4.2.1 NH<sub>3</sub> concentration in zero-air

The concentration of NH<sub>3</sub> in the *za* was evaluated. Three tests lasting 3 h each were performed. Figure 30 shows a box chart of NH<sub>3</sub> concentrations in the zero-air stream generated by ZAG, used in the adsorption runs.

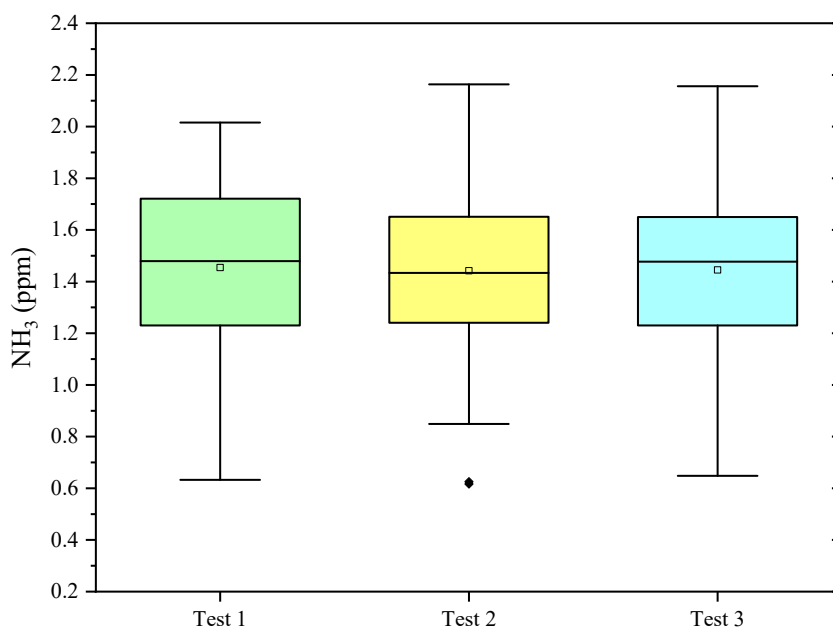


Figure 30. Concentrations of  $\text{NH}_3$  in the zero-air (za).

All tests were performed at a flow rate of  $0.8 \text{ L min}^{-1}$ . Temperatures ranged between  $20.6 - 25.5$ ,  $20.5 - 28.2$ , and  $17.3 - 24.2^\circ\text{C}$  during Tests 1, 2, and 3, respectively. The means of  $\text{NH}_3$  concentration in Tests 1, 2, and 3 were, respectively,  $1.454 \pm 0.316$ ,  $1.442 \pm 0.332$ , and  $1.445 \pm 0.333 \text{ ppm}$ , which are graphically represented in Figure 30. Using the method Analysis of Variance (ANOVA), it was found that there was no significant difference in the means of  $\text{NH}_3$  concentration, with a  $p > 0.05$  (equals to 0.97414).

#### 4.2.2 $\text{NH}_3$ concentration in feed stream from leachate

The concentration of  $\text{NH}_3$  in the inlet stream of the adsorption process (leachate off-gases) was evaluated. Four tests lasting 8 h and two tests lasting 24 h were performed at a flow rate of  $0.8 \text{ L min}^{-1}$ .

Figure 31 shows the results of tests that lasted 8 h and the temperatures registered during each one. Temperatures ranged between  $26.4 - 36.9$ ,  $20.6 - 27.3$ ,  $20.7 - 27$ , and  $22 - 33.4^\circ\text{C}$  during Tests 1, 2, 3, and 4, respectively.

It was observed that the considerable variations of temperatures (increasing during Tests 1 and 4 and decreasing during Tests 2 and 3) did not contribute to a significant variation of  $\text{NH}_3$  emission. It was also noticed that about 2 h were necessary until

stabilization of emissions (Figure 31). Starting from hour 2, the  $\text{NH}_3$  concentration of all tests decreased slowly upon the time of contact. Decay ranged from 1 – 1.8 ppm within 8 h of emission, which means a decay rate of  $0.2 - 0.3 \text{ ppm h}^{-1}$ .

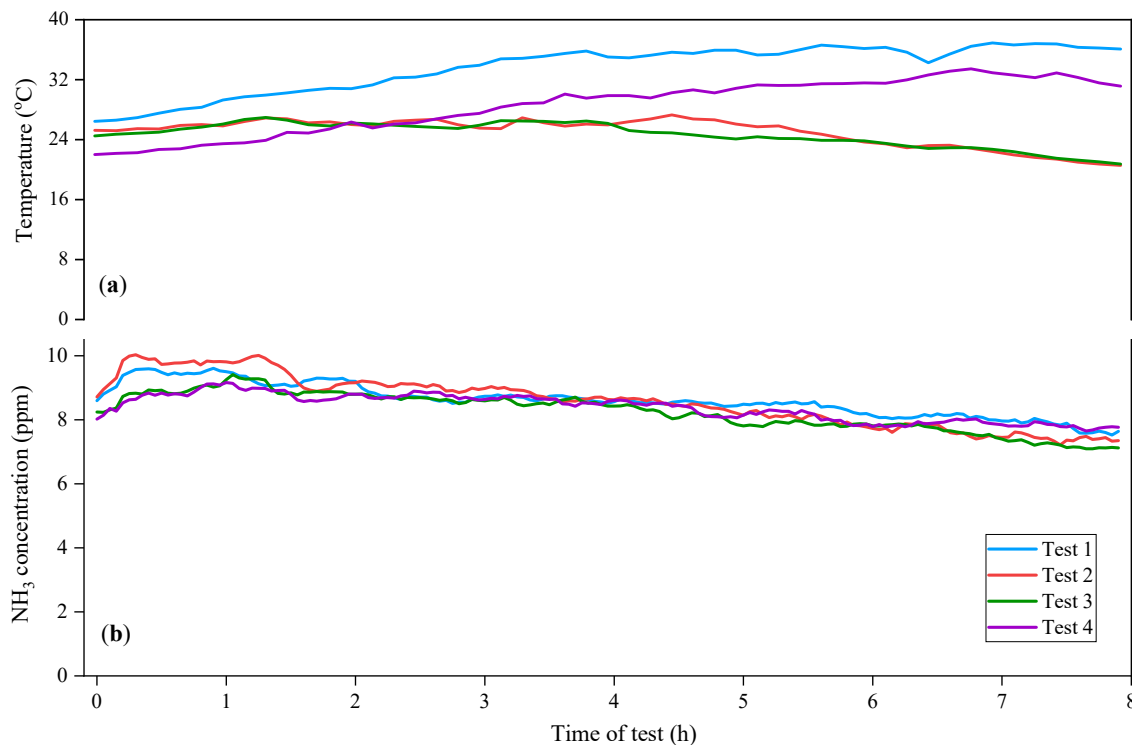


Figure 31. Tests that lasted 8 h: (a) temperature during the tests and (b) concentration of  $\text{NH}_3$  emitted from leachate.

Figure 32 shows the results of the tests that lasted 24 h. Tests were considered after the stabilization of the emissions, noticed in the previous tests. It was noticed that the  $\text{NH}_3$  concentration of all tests decreased almost linearly until approximately 16 h. The  $\text{NH}_3$  concentration decayed by  $4.6 - 4.7 \text{ ppm}$  after 16 h of experiment, which means a slight decay rate of  $0.29 \text{ ppm h}^{-1}$ . It was observed that a slight increase of  $\text{NH}_3$  concentration starting at 14 – 16 h of experiment matches with the considerable increase of temperature (Figure 32), which may be ascribed to the fact of  $\text{NH}_3$  volatilization from leachate is increased by increasing the temperature (IPNI, n.d.).

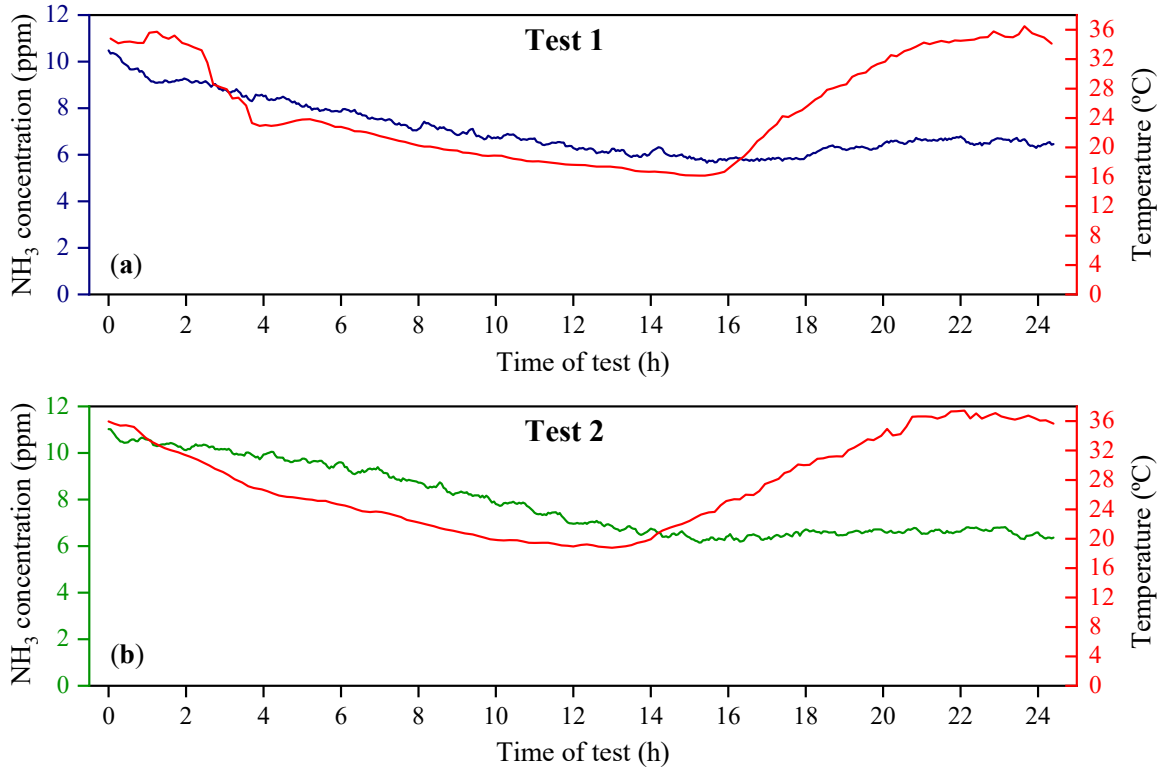


Figure 32. Tests that lasted 24 h: temperature during the tests and concentration of NH<sub>3</sub> emitted from leachate. (a) Test 1, and (b) Test 2.

#### 4.2.3 Chemical analysis of NH<sub>3</sub> adsorption

The concentration of NH<sub>3</sub> downstream from the adsorption column was measured every 3 minutes until the bed's saturation. Normalized breakthrough curves are presented in Figure 33, in which the blue lines represent the materials prepared from OS, and the red represents the ones prepared from MB. Table 11 presents the values of  $m$ ,  $Z$ , and the results of  $C_0$ ,  $t_b$ ,  $t_{sto}$ ,  $t_{sat}$ ,  $H_{MTZ}$ , and  $q_a$ .

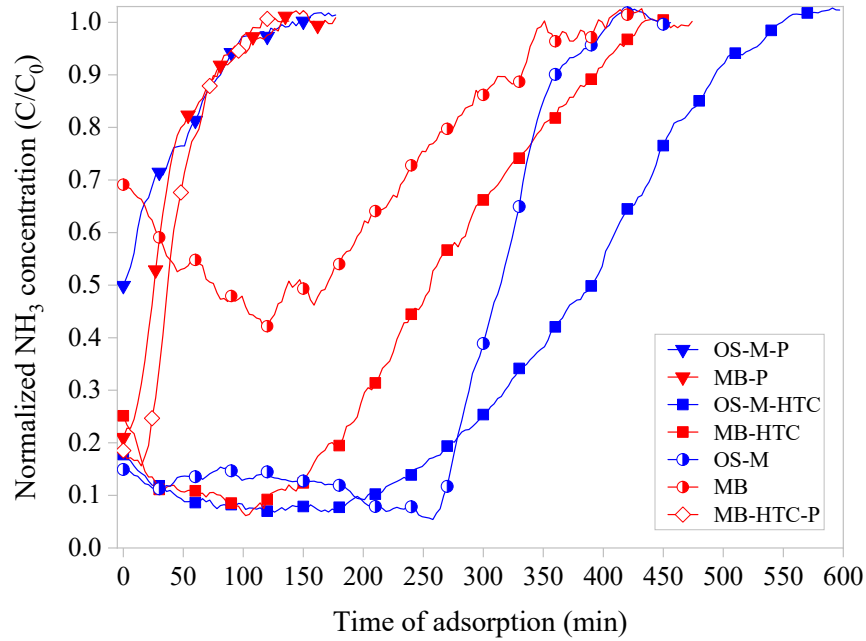


Figure 33. Normalized breakthrough curves of the adsorption tests performed in this work.

Table 11. Values of the mass of adsorbent ( $m$ ) and height of the adsorption bed ( $Z$ ), and the results of  $\text{NH}_3$  inlet concentration ( $C_0$ ), breakthrough time ( $t_b$ ), stoichiometric time ( $t_{sto}$ ), saturation time ( $t_{sat}$ ), height of mass transfer zone ( $H_{MTZ}$ ), and dynamic adsorption capacity ( $q_a$ ).

Sample	$m$ (g)	$Z$ (cm)	$C_0$ estimated (ppm)	$t_b$ (min)	$t_{sto}$ (min)	$t_{sat}$ (min)	$H_{MTZ}$ (cm)	$q_a$ (mg g <sup>-1</sup> )
OS-M	1.2	2.8	8.9 - 11.5	279 - 330	288 - 342	345 - 399	0.484 - 0.565	0.975 - 1.455
MB	1.2	4.5	5.5 - 7.4	—	—	—	—	0.442 - 0.424
OS-M-P	1.2	3.3	8.10	0	3 - 9	93 - 99	3.194 - 3.200	0.067 - 0.075
MB-P	0.5	2.5	6.5 - 6.7	15 - 24	21 - 27	81 - 90	1.759 - 2.083	0.198 - 0.216
OS-M-HTC	0.2	1	8.8 - 10.6	219 - 378	294 - 414	456 - 552	0.315 - 0.520	9.445 - 11.421
MB-HTC	0.2	2	7.6 - 8.5	168 - 231	198 - 267	384 - 411	0.876 - 1.125	6.237 - 8.145
MB-HTC-P	0.5	4.5	8.61	30	36	81	2.833	0.378

Based on the results shown in Table 11, it was noticed that the samples OS-M-P and MB-P presented the lowest  $t_b$  and  $t_{sat}$ , which means that their mass transfer front reaches the column exit rapidly due to the high  $H_{MTZ}$  values of these samples, that were very close to their  $Z$  values. On the other hand, samples OS-M-HTC and OS-M showed the highest  $t_b$  and  $t_{sat}$ , which means that their mass transfer front takes longer to reach the column exit due to the low  $H_{MTZ}$  values of these samples. The samples OS-M-HTC and

OS-M also showed the highest  $t_{sto}$ , which means that it took longer until the  $\text{NH}_3$  concentration at the column was equal to 50% of the  $\text{NH}_3$  concentration at the column entrance. The sample MB-HTC-P showed low values of  $t_b$ ,  $t_{sto}$ , and  $t_{sat}$  and a high value of  $H_{MTZ}$ . It was not possible to observe the breakthrough curve rightly for the MB sample at the tested operating conditions, so  $t_b$ ,  $t_{sto}$ , and  $t_{sat}$  were not determined.

Table 11 also presents that the bioadsorbents OS-M and MB showed a greater  $q_a$  than the pyrochars OS-M-P and MB-P. The  $q_a$  of OS-M ( $0.975 - 1.455 \text{ mg g}^{-1}$ ) is within the range of non-activated pyrochars prepared by Ro et al. (2015), which is  $0.15 - 5.09 \text{ mg g}^{-1}$ . Pyrolysis of OS-M, producing sample OS-M-P, resulted in 14 to 19 times the decrease in  $\text{NH}_3$  adsorption capacity. Hydrochars OS-M-HTC and MB-HTC showed a greater  $q_a$ , ranging from  $9.445 - 11.421$  and  $6.2437 - 8.145 \text{ mg g}^{-1}$ , respectively. The  $q_a$  of OS-M-HTC was 8 to 10 times greater than the value obtained for OS-M. Similar values were found by C. Huang et al. (2008) using a treated commercial coconut shell AC with  $\text{H}_2\text{SO}_4$  ( $5.691 - 11.245 \text{ mg g}^{-1}$ ). It is worth mentioning that OS-M-HTC and MB-HTC showed a  $q_a$  greater than the commercial ACs derived from biomass presented by Rodrigues et al. (2007) ( $0.6$  to  $1.8 \text{ mg g}^{-1}$ ), Gonçalves et al. (2011) ( $4.7 - 5.3 \text{ mg g}^{-1}$ ) and C. Huang et al. (2008) ( $2.3 \text{ mg g}^{-1}$ ). On the other hand, the pyrolysis of MB-HTC, producing MB-HTC-P, resulted in 14 to 19 times the decrease of the  $q_a$ .

Steep breakthrough curves were observed for samples OS-M, OS-M-P, MB-P, and MB-HTC-P (Figure 33), suggesting that the adsorption process does not have a significant mass transfer barrier for those samples (Chou et al., 2006). On the other hand, a relatively gradual slope on the breakthrough curves was observed for samples OS-M-HTC, MB, and MB-HTC, which indicates that transportation of  $\text{NH}_3$  from the gas stream to the adsorbents may present a significant mass transfer resistance. In the samples OS-M-HTC and MB-HTC, the mass transfer is enhanced by the feasible chemical adsorption of  $\text{NH}_3$  with  $\text{H}_2\text{SO}_4$ , which compensates the resistance observed by the slope of its breakthrough curves (Chou et al., 2006).

According to ASTM International (2019), the best adsorbent for most applications should have a high  $q_a$  coupled with a short  $H_{MTZ}$ . Therefore, OS-M-HTC was the best adsorbent for  $\text{NH}_3$  removal produced in this work since it has shown the lowest  $H_{MTZ}$  and the highest  $q_a$ .

The evaluation showed that adsorption of CH<sub>4</sub>, CO<sub>2</sub>, and N<sub>2</sub>O was not perceptible, which demonstrates non-competitive adsorption of NH<sub>3</sub> with those gases. Differently, a perceptible amount of gaseous H<sub>2</sub>O was adsorbed.

#### 4.2.4 Olfactometric analysis of NH<sub>3</sub> adsorption

The samples used in the subjective evaluation of odorous pollutants' adsorption were collected during tests (presented in section 3.6) using the material with the highest uptake capacity (OS-M-HTC) and its precursor (OS-M) as adsorbents to compare each other. Five samples were collected in order to perform the subject evaluation:  $SE_{Feed}$ ,  $SE_{Clean}$ ,  $SE_{Break}$ ,  $SE_{Stoic}$ , and  $SE_{Satur}$ .

Odor's hedonic tone was expressed on a scale ranging from -4 (extremely unpleasant) to +4 (extremely pleasant), while intensity was expressed on a scale ranging from 0 (not perceptible) to 6 (extremely strong). Appendix B shows the results of the odor's hedonic tone and odor intensity assessments, respectively.

To better interpret the subject evaluation, responses were grouped according to the following: odor hedonic tone – pleasant, neutral, and unpleasant; odor intensity – not perceptible, very weak/weak, distinct/strong, very strong/extremely strong.

The odor hedonic tone's results of the tests using the samples derived from adsorption tests are represented in Figure 34. As observed, sample  $SE_{Feed}$  was unpleasant for the assessors (90% and 100% for OS-M and OS-M-HTC, respectively), been considered the most unpleasant sample. On the other hand, samples  $SE_{Clean}$  and  $SE_{Satur}$  were neutral or pleasant for 40 and 30% of the assessors, respectively, for both OS-M and OS-M-HTC, whereas sample  $SE_{Break}$  33 and 60%, sample  $SE_{Stoic}$  20 and 50%, for OS-M and OS-M-HTC, respectively. Samples  $SE_{Clean}$ ,  $SE_{Break}$ , and  $SE_{Stoic}$  were the only considered pleasant for both materials. The results presented above showed that the adsorption using materials OS-M and OS-M-HTC reduced the effluent's unpleasantness.



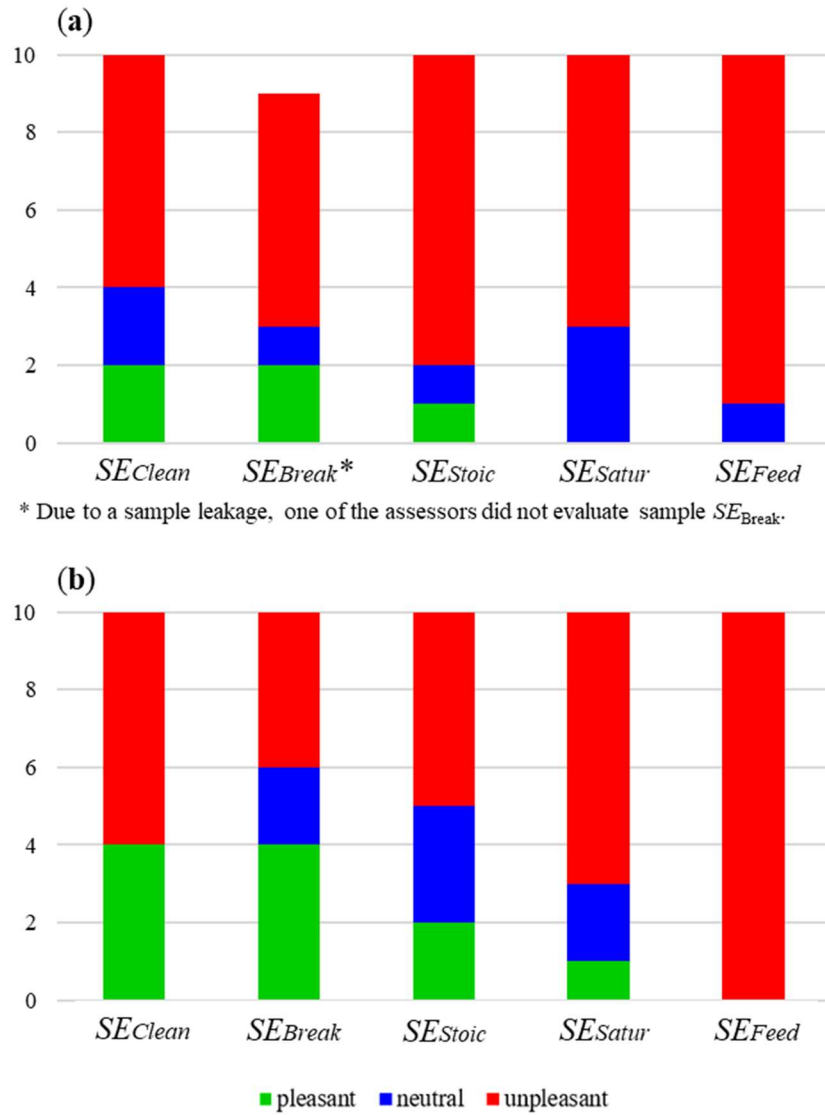


Figure 34. Evaluation of odor hedonic tone of samples derived from adsorption tests using (a) OS-M and (b) OS-M-HTC.

The intensity's results of the tests using the samples derived from adsorption tests are represented in Figure 35. As observed, the evaluation of samples derived from tests using OS-M showed that sample  $SE_{Feed}$  was very strong or extremely strong for 20% of the assessors and distinct or strong for 40%. Differently, sample  $SE_{Clean}$  was very strong or extremely strong for 10% of the assessors, and distinct or strong for 60%. On the other hand, samples  $SE_{Stoic}$  and  $SE_{Satur}$  were very weak or weak for most assessors (50% and 60%, respectively). None of the samples was considered not perceptible regard to odor intensity.

The evaluation of samples derived from adsorption tests using OS-M-HTC has shown that samples  $SE_{Clean}$  and  $SE_{Feed}$  was considered very strong or extremely strong for

20% of the assessors. On the other hand, samples  $SE_{Clean}$  was very weak or weak for 50% of the assessors. Differently, sample  $SE_{Feed}$  was distinct or strong for 80% of the assessors, so that none of the assessors considered this sample's intensity very weak or weak. None of the samples was considered not perceptible regarding odor intensity. The results showed that the adsorption might have slightly reduced the intensity of the odorous gases.

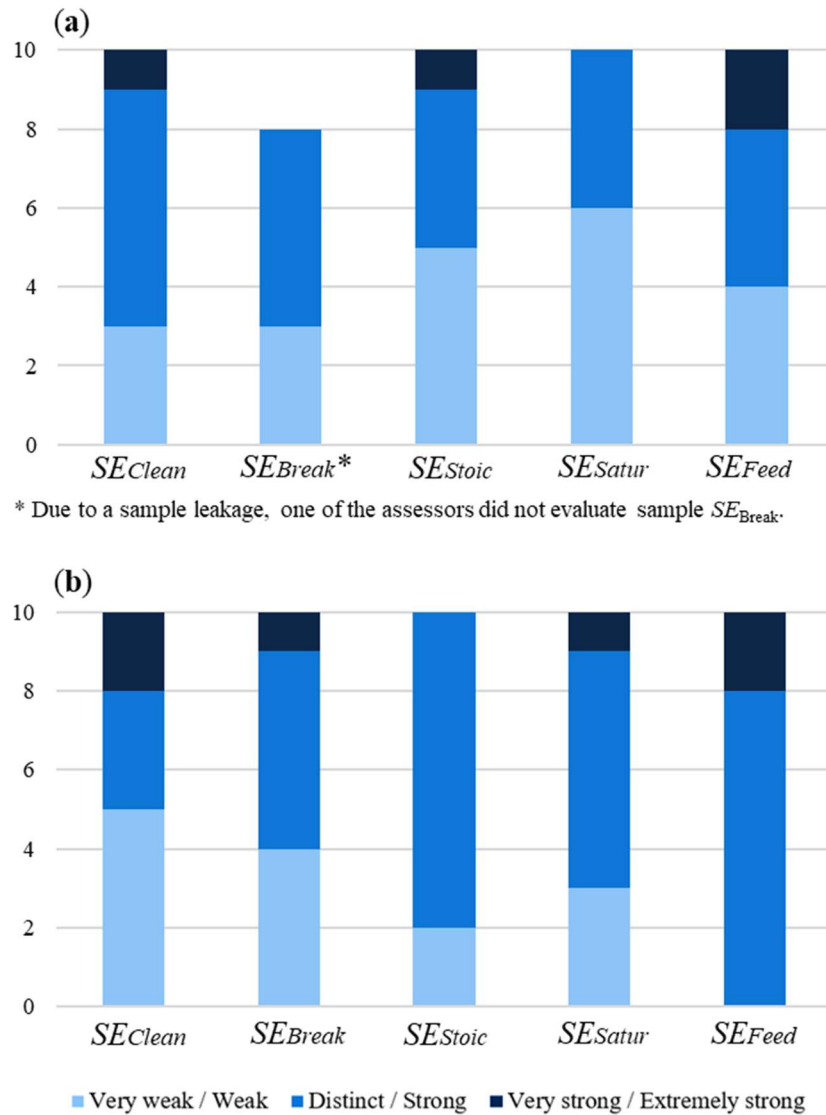


Figure 35. Evaluation of odor intensity of samples derived from adsorption tests using (a) OS-M and (b) OS-M-HTC.

Complementarily to odor intensity and hedonic odor tone assessments, comments were written by the assessors. Appendix C shows the comments and their respective periodicity.

Comments regarding odor hedonic tone, concerning samples derived from adsorption tests using OS-M-HTC, indicated similarity between samples  $SE_{Clean}$ ,  $SE_{Break}$ ,  $SE_{Stoic}$ , and  $SE_{Satur}$ ; some comments considered some more/less unpleasant than others. The samples mentioned above also presented the smell of chemical products (chemical product or poison, acid, cleaning product, dentist's office, brand new-sneakers, and polystyrene), which may be related to the preparation process of the sample OS-M-HTC by  $H_2SO_4$ -assisted HTC. One comment regarding sample  $SE_{Clean}$  showed that it presented smell of exhaust fumes of a car with malfunctioning catalyst, which may be related to the presence of  $H_2S$ , as it is the main responsible for odor from the exhaust of vehicles in which the catalytic converter is not functioning properly (Windawi & Truex, 1988). Comments on sample  $SE_{Feed}$  showed its unpleasantness, as it presented the smell of something rotten, sewage, wood in decomposition, and stable. Comments regarding odor intensity concerning samples derived from adsorption tests using OS-M-HTC showed that the odor of sample  $SE_{Feed}$  is different from the odors of samples  $SE_{Clean}$ ,  $SE_{Break}$ , and  $SE_{Stoic}$ , but with similar or little more intensity. Sample  $SE_{Satur}$  was considered a little less intense than sample  $SE_{Feed}$  in one comment.

Comments regarding odor hedonic tone, concerning samples derived from adsorption tests using OS-M, indicate similarity between samples  $SE_{Clean}$ ,  $SE_{Break}$ , and  $SE_{Stoic}$ , and between samples  $SE_{Feed}$  and  $SE_{Satur}$ . A comment specifying the unpleasantness regard to sample  $SE_{Feed}$  was made. No comments were made on odor intensity concerning the samples derived from adsorption tests using OS-M.

### 4.3 Characterization of the adsorbents

#### 4.3.1 Surface chemistry characteristics

Acidity and basicity of the surface of fresh and saturated first-generated adsorbents were determined. Table 12 presents the values of basicity and acidity in  $mmol\ g^{-1}$ .

Table 12. Acidity and basicity of the surface of fresh and saturated first-generation adsorbents.

Sample	Basicity (mmol g <sup>-1</sup> )	Acidity (mmol g <sup>-1</sup> )
OS-M	0.41	1.47
OS-M (saturated)	0.31	1.43
MB	0.44	1.42
MB (saturated)	0.47	1.32
OS-M-P	1.10	0.32
MB-P	0.59	0.34
OS-M-HTC	0.11	2.34
OS-M-HTC (saturated)	0.45	1.95
MB-HTC	0.14	2.37
MB-HTC (saturated)	0.40	2.28

As presented in Table 12, samples OS-M-HTC and MB-HTC showed similar acidity results, 2.34 and 2.37 mmol g<sup>-1</sup>, respectively. Content of acid groups in the bioadsorbents OS-M and MB was also significant, 1.47 and 1.42 mmol g<sup>-1</sup>, respectively. Besides increasing the adsorbents' surface acidity due to the assistance of H<sub>2</sub>SO<sub>4</sub>, the HTC process is expected to produce a material with high concentrations of OFGs, including the acid ones (Jain et al., 2016; Ok et al., 2016). The presence of acidic groups gives a polar character to the adsorbent's surface, affecting the preferential adsorption of polar alkaline adsorbates, being such groups considered the key factor on the NH<sub>3</sub>  $q_a$  (Foo et al., 2013; Gonçalves et al., 2011). The correlation between the amount of NH<sub>3</sub> adsorbed and the total amount of acidic groups on the surface of the adsorbent is approximately linear (Gonçalves et al., 2011; C. Huang et al., 2008; Mochizuki et al., 2016; J. Wang et al., 2016; Zheng et al., 2016). The greater NH<sub>3</sub>  $q_a$  of samples OS-M-HTC and MB-HTC, which also present greater surface acidity, confirm the statement above.

The pyrochars OS-M-P and MB-P, on the other hand, presented greater content of basic groups, 1.10 and 0.59 mmol g<sup>-1</sup>, respectively, and lower content of acidic groups, 0.32 and 0.34 mmol g<sup>-1</sup>, respectively (Table 12). The samples mentioned above were also the ones that presented a very low NH<sub>3</sub>  $q_a$ , as shown in topic 4.2.3. Pyrochars that are effective in the sorption of inorganic or polar organic contaminants, such as NH<sub>3</sub>, are

usually obtained in relatively low pyrolysis temperatures ( $\leq 500$  °C), presenting more oxygen-containing functional groups, electrostatic attraction, and precipitation (Ahmad et al., 2014). Nonetheless, the pyrochars produced in this work were obtained by pyrolysis in high temperatures (up to 800 °C), which caused a decrease of acidic functional groups (especially carboxylic functional groups), and the appearance of basic functional groups (Tomczyk et al., 2020).

Based on the results presented in Table 12, it was noticed that all samples saturated with  $\text{NH}_3$  showed a slight decrease in the content of acid groups. Samples prepared by  $\text{H}_2\text{SO}_4$ -assisted HTC saturated with  $\text{NH}_3$  showed a significant increase in the content of basic groups, with the saturated OS-M-HTC increasing the basicity four times and saturated MB-HTC almost three times. The significant increase of basic groups on the surface of those saturated adsorbents may be ascribed to the higher amount of  $\text{NH}_3$  adsorbed.

#### 4.3.2 Textural properties

Figure 36 shows  $\text{N}_2$  isotherms adsorption of the materials OS-M-P, MB-P, OS-M-HTC, MB-HTC, and MB-HTC-P. The samples subject to pyrolysis (OS-M-P, MB-P, and MB-HTC-P) showed isotherms type I (b), given by microporous materials with relatively small external surfaces, with pore size distributions including wider micropores and possibly narrow mesopores ( $W_{\text{mic}} < \sim 2.5$  nm). The samples subject only to  $\text{H}_2\text{SO}_4$ -assisted HTC (OS-M-HTC and MB-HTC) showed isotherms type III, given by nonporous or macroporous materials.

The textural properties  $S_{\text{BET}}$ ,  $S_{\text{ext}}$ ,  $S_{\text{mic}}$ ,  $V_{\text{mic}}$ ,  $V_{\text{total}}$ , and  $W_{\text{mic}}$  of the adsorbents are summarized in Table 13.

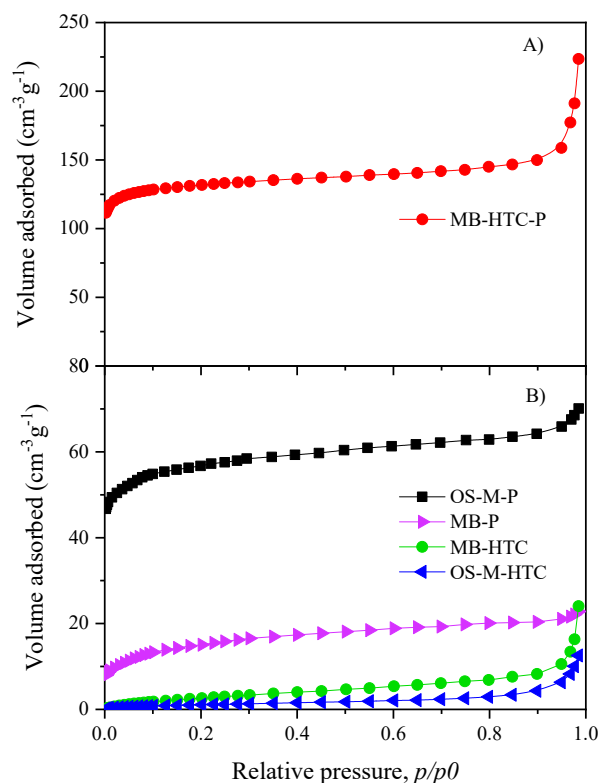


Figure 36. N<sub>2</sub> adsorption-desorption isotherms of the adsorbents at 77 K.

Table 13. Textural properties of the adsorbents: specific surface area ( $S_{BET}$ ), external surface area ( $S_{ext}$ ), micropore surface area ( $S_{mic}$ ), micropore volume ( $V_{mic}$ ), total pore volume ( $V_{total}$ ), and average pore diameter ( $W_{mic}$ ).

Sample	$S_{BET}$ (m <sup>2</sup> g <sup>-1</sup> )	$S_{ext}$ (m <sup>2</sup> g <sup>-1</sup> )	$S_{mic}$ (m <sup>2</sup> g <sup>-1</sup> )	$V_{mic}$ (mm <sup>3</sup> g <sup>-1</sup> )	$V_{total}$ (mm <sup>3</sup> g <sup>-1</sup> )	$V_{mic}/V_{total}$ (%)	$W_{mic}$ (nm)
OS-M-P	172	14	158	83	109	76	2.1
MB-P	50	11	39	20	34	59	2.1
OS-M-HTC	4	4	0	0	16	0	-
MB-HTC	12	11	1	0	25	0	-
MB-HTC-P	391	32	359	193	297	65	2.1

Table 13 shows that the combination of H<sub>2</sub>SO<sub>4</sub> assisted-HTC followed by pyrolysis resulted in the adsorbent (MB-HTC-P) with the highest values of  $S_{BET}$ ,  $S_{ext}$ ,  $S_{mic}$ ,  $V_{mic}$ , and  $V_{total}$ . These results were expected since, when used as precursors, hydrochars play an essential role in forming porosity and higher surface areas of ACs (Jain et al., 2016).

The samples subjected to pyrolysis showed the greatest  $S_{BET}$ ,  $S_{mic}$ ,  $V_{mic}$ ,  $V_{total}$ , and  $W_{mic}$  (Table 13), likely due that the removal of volatile matter through this process

enriched the carbon composition, as seen in Table 10, forming the porosity on these adsorbents (Yek et al., 2019). Those samples are predominately microporous, as shown in the  $V_{mic}/V_{total}$  proportion.

It was also noticed that the sample OS-M-P showed  $S_{BET}$  3 times greater and  $S_{mic}$  4 times greater than the sample's MB-P same properties. Even though the same pyrolysis process prepared both samples, the MB-P precursor was not subjected to milling before preparation to reduce the precursors' particle size. Since particle size affected the pyrochar structure (Asadullah et al., 2010), the smaller particle size of biomass OS led to a greater available surface area subjected to pyrolysis, which may explain greater  $S_{BET}$  and  $S_{mic}$  of sample OS-M-P.

The samples OS-M-HTC and MB-HTC, which presented greater  $NH_3$  adsorption capacity, shown in topic 4.2.3, showed very low values for all textural parameters, some of them even zero (Table 13). That may be explained by the fact that the specific surface area and pore volume do not directly influence the adsorbing amount of  $NH_3$  (C. Huang et al., 2008).

#### 4.3.3 Void fraction characteristics

Table 14 shows the parameters and results of the determination of the void fraction characteristics of the adsorbents.

Table 14. Void fraction characteristics determination: volume of adsorbent material ( $V_m$ ), volume of distilled water ( $V_w$ ), total volume ( $V_t$ ), volume of voids in the bed ( $V_{void}$ ), and void fraction ( $Void_f$ ).

Sample	$V_m$ (mL)	$V_w$ (mL)	$V_t$ (mL)	$V_{void}$ (mL)	Void <sub>f</sub> (%)
OS-M	2	2	3	1	50
OS-M-P			3.8	0.2	10
OS-M-HTC			3.6	0.4	20
MB			2.5	1.5	75
MB-P			3.4	0.6	30
MB-HTC			3.8	0.2	10

Table 14 presents that the bioadsorbent MB showed the greatest  $\text{Void}_f$  (75%), likely due to its greater particle size and irregular shape, which was not measured in this work but was visibly perceived, as shown in Figure 10. The reduction of the  $\text{Void}_f$  of the raw materials MB and OS-M after being subjected to pyrolysis (resulting in OS-M-P and MB-P) and  $\text{H}_2\text{SO}_4$ -assisted HTC (resulting in OS-M-HTC and MB-HTC) may be ascribed to the reduction of the particles sizes after these processes, resulting in less interparticle voids.

Reducing the  $\text{Void}_f$  is beneficial to the adsorption process since fewer void spaces mean greater available surface area to retain the adsorptive gaseous pollutant.

#### 4.4 Regeneration of saturated adsorbents

##### 4.4.1 $\text{NH}_3$ adsorption with regenerated samples

Normalized breakthrough curves obtained with OS-M and OS-M-HTC regenerated materials are presented in Figure 37. The parameters and results of adsorption tests using regenerated adsorbents (R\_X\_OS-M and R\_X\_OS-M-HTC) are presented in Table 15. The breakthrough curves, the parameters, and the results related to first-generation samples OS-M and OS-M-HTC, presented in section 4.2.3, are also shown in the following figure and table for comparison purposes.

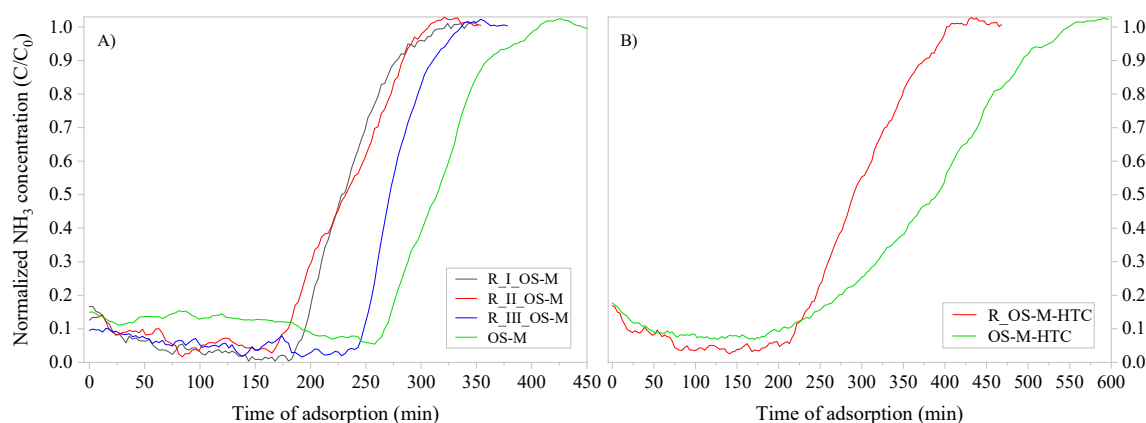


Figure 37. Normalized breakthrough curves of adsorption tests using regenerated (R\_X\_OS-M and R\_X\_OS-M-HTC) and first-generation (OS-M and OS-M-HTC) samples.  
(A) bioadsorbents and (B) hydrochars.



Based on the curves presented in Figure 37, it was noticed that all the regenerated samples showed  $t_b$  and  $t_{sat}$ , lower than the mean values of the same parameters of the first-generation samples. The figure also showed that all the regenerated samples have also shown steeper breakthrough curves (being the R\_III\_OS-M the steepest one) than those of its respective first-generation samples, suggesting that the adsorption process on the water-washed samples does not show a significant mass transfer barrier (Chou et al., 2006). It was also noticed that all the regenerated samples had shown more efficiency in  $\text{NH}_3$  removal before its respective  $t_b$ . Both statements presented above may be explained by the fact that washing the samples might have increased the access to their pore sites that could be blocked before washing (Ro et al., 2015).

Based on the results presented in Table 15, after the first  $\text{NH}_3$  desorption-sorption cycle, samples R\_I\_OS-M, R\_II\_OS-M, and R\_III\_OS-M showed 94, 76, and 107% of the mean  $q_a$  of the first-generation OS-M. Differently, after the first  $\text{NH}_3$  desorption-sorption cycle, sample R\_OS-M-HTC has shown 68% of the mean  $q_a$  of the first-generation OS-M-HTC.

Table 15 also showed that the samples R\_I\_OS-M and R\_III\_OS-M, with 1.2 g of material washed with 500 mL of ultrapure water in temperatures of 25 and 80 °C, respectively, presented approximately the same  $H_{MTZ}$  as the one of the first-generation OS-M, and a  $q_a$  very close to or better than the mean  $q_a$  of the first-generation OS-M. Differently, the sample R\_II\_OS-M, with 2.4 g of material washed with 150 mL of ultrapure water in temperatures of 25 °C, presented a higher  $H_{MTZ}$  and a lower  $q_a$  than the same parameters of the first-generation OS-M. On the other hand, the sample R\_OS-M-HTC, with 0.5 g of material washed with 100 mL of ultrapure water in temperatures of 25 °C, presented an  $H_{MTZ}$  close to and a  $q_a$  lower than those of the first-generation OS-M-HTC.

The results indicate that the use of greater  $V_{UPw}$  (500mL) and regeneration process performed in higher  $T$  (80°C) may produce a regenerated adsorbent with greater adsorption capacity since the parameters pointed above resulted in the sample R\_III\_OS-M, which showed  $H_{MTZ}$  very similar to and a  $q_a$  higher than the ones of the first-generation OS-M (Table 15), and the steepest breakthrough curve (Figure 37).

Table 15. Values of the mass of adsorbent regenerated ( $m$ ), regeneration temperature ( $T$ ), volume of ultrapure water ( $V_{UPw}$ ), mass of regenerated adsorbent in the fixed-bed column ( $FB_m$ ), height of the adsorption bed ( $Z$ ), and the results of  $\text{NH}_3$  inlet concentration ( $C_0$ ), breakthrough time ( $t_b$ ), stoichiometric time ( $t_{sto}$ ), saturation time ( $t_{sat}$ ), height of mass transfer zone ( $H_{MTZ}$ ), and dynamic adsorption capacity ( $q_a$ ).

Sample	$m$ (g)	$T$ (°C)	$V_{UPw}$ (mL)	$FB_m$ (g)	$Z$ (cm)	$C_0$ estimated (ppm)	$t_b$ (min)	$t_{sto}$ (min)	$t_{sat}$ (min)	$H_{MTZ}$ (cm)	$q_a$ (mg g <sup>-1</sup> )
OS-M	-	-	-	1.2	2.8	8.9 - 11.5	279 - 330	288 - 342	345 - 399	0.484 - 0.565	0.975 - 1.455
R_I_OS-M	0.93	25	500	0.93	2.2	8.3	207	222	276	0.550	1.147
R_II_OS-M	2.12	25	150	1.2	2.8	8.3	198	216	288	0.875	0.926
R_III_OS-M	1	80	500	1	2.5	9.0	261	270	330	0.523	1.304
OS-M-HTC	-	-	-	0.2	1	8.8 - 10.6	219 - 378	294 - 414	456 - 552	0.315 - 0.520	9.445 - 11.421
R_OS-M-HTC	0.45	25	100	0.2	1	10	252	288	387	0.349	7.082

#### 4.4.2 Biomass loss

The B.L. was determined by the difference between the initial biomass weight (before the regeneration process) and the final biomass weight (after the regeneration process), both on a dry basis. Table 16 shows the parameters of the regeneration processes and the B.L. of each sample.

*Table 16.* Parameters of the regeneration processes and biomass loss: regeneration temperature ( $T$ ), volume of ultrapure water ( $V_{UPw}$ ), initial and final mass of adsorbent, and biomass loss (B.L).

Sample	$T$ (°C)	$V_{UPw}$ (mL)	Initial $m$ (g)	Final $m$ (g)	B.L (%)
R_I_OS-M	25	500	1.2	0.93	22.5
R_II_OS-M	25	150	2.4	2.12	11.7
R_III_OS-M	80	500	1.2	1	16.7
R_OS-M-HTC	25	100	0.5	0.45	10.1

As shown in Table 16, the sample R\_OS-M-HTC, which had the lowest initial mass and was washed with the lowest ultrapure water volume, showed lower B.L. On the other hand, the samples R\_I\_OS-M and R\_III\_OS-M, washed with a greater  $V_{UPw}$ , showed greater B.L. resulted from the filtration process.

#### 4.4.3 TOC, conductivity, and pH of the liquid phase

Table 17 presents the regeneration processes' parameters and the values of TOC, conductivity, and pH of liquid phases of each regenerated sample, before and after the regeneration. Conductivity and pH values were corrected to the reference temperature of 25 °C.

The results presented in Table 17 showed that the samples R\_I\_OS-M and R\_III\_OS-M, with 1.2 g of material washed with 500 mL of ultrapure water in temperatures of 25 and 80 °C, respectively, as well as sample R\_OS-M-HTC, with 0.5 g

of material washed with 100 mL of ultrapure water in temperatures of 25 °C, presented the same TOC values. Differently, sample R\_II\_OS-M, with 2.4 g of material washed with 150 mL of ultrapure water in temperatures of 25 °C, presented a higher TOC value, which can be explained by the fact that the carbonaceous mass washed was double that the mass of samples R\_I\_OS-M and R\_III\_OS-M.

As shown in Table 17, after the regeneration process, the pH of the liquid phase of all samples increased. The difference between the pH of ultrapure water (before regeneration) and the liquid phase (after regeneration) ranged from 1.4 and 2.3. The desorption of alkaline  $\text{NH}_3$  may explain the increase of pH in the liquid phase. The sample R\_OS-M-HTC, derived from saturated OS-M-HTC, the one with the highest  $q_a$ , shows the greatest pH increase. It was expected since a greater amount of  $\text{NH}_3$  should be desorbed during the regeneration of the adsorbent.

The conductivity of the liquid phase of all samples increased after regeneration. The rising of conductivity may be explained by the increasing of ions due to polar compounds' desorption, predominately  $\text{NH}_3$ , in this case. Samples R\_II\_OS-M and R\_OS-M-HTC show the highest conductivity, 266 and 76  $\mu\text{S cm}^{-1}$ , respectively (Table 17). They were the ones with a greater content of  $\text{NH}_3$  since the sample R\_II\_OS-M had the greater mass of saturated adsorbent (2.4 g), and the sample R\_OS-M-HTC is derived from the adsorbent with the highest  $\text{NH}_3$   $q_a$  (OS-M-HTC).

Besides the solubility of  $\text{NH}_3$  in water, washing the saturated samples may have increased the access to pores that might have been blocked by a mineral content, and/or washing with ultrapure water might have removed other ions from its surface (Ro et al., 2015). On the other hand, washing causes loss of carbon content, as shown by TOC results.

*Table 17.* Parameters of the regeneration processes and liquid phase characteristics: mass of adsorbent before regeneration ( $m$ ), temperature ( $T$ ), volume of ultrapure water ( $V_{UPw}$ ), TOC, and conductivity and pH of the liquid phase (before and after the regeneration).

Sample	$m$ (g)	$T$ (°C)	$V_{UPw}$ (mL)	$TOC$ (g L <sup>-1</sup> )	Before regeneration		After regeneration	
					$pH$	Conductivity ( $\mu\text{s cm}^{-1}$ )	$pH$	Conductivity ( $\mu\text{s cm}^{-1}$ )
R_I_OS-M	1.2	25	500	0.04	5.6	1	7.4	30
R_II_OS-M	2.4	25	150	0.15			7	266
R_III_OS-M	1.2	80	500	0.04			7.2	46
R_OS-M-HTC	0.5	25	100	0.04			7.9	76

## 5 CONCLUSIONS AND RECOMMENDATIONS FOR FUTURE WORK

### 5.1 Conclusions

Different adsorbents were prepared, using agro-industrial residues as precursors. They were tested for odor abatement in an experimental lab-scale adsorption system developed for this purpose, showing that biomass waste can be valorized into high-added-value products with environmental applications.

The concentration of the odorous pollutant  $\text{NH}_3$  in zero-air and composting leachate was evaluated using the experimental system. Even though an odor's actual source was used,  $\text{NH}_3$  emission rates were considerably stable over time, making it possible to use it as a source of gaseous pollutants in the adsorption tests performed using the adsorbents prepared from biomass. Despite using a mixture of gases instead of a standard  $\text{NH}_3$  gas, selective removal of  $\text{NH}_3$  was observed, as no competitive adsorption was noticed.

The samples prepared by  $\text{H}_2\text{SO}_4$ -assisted HTC showed greater content of acid groups and  $\text{NH}_3$  adsorption capacities. Although the good performance of the hydrochars mentioned above on  $\text{NH}_3$  adsorption, they lost more than half of weight during preparation. Samples subjected to pyrolyzation show significant biomass loss (75 to 85%), good textural properties, and minimal  $\text{NH}_3$  adsorption capacity. It confirms the crucial role of acidic functional groups in  $\text{NH}_3$  adsorption and the fact that surface area and pore volume, independently, do not directly influence the adsorption of  $\text{NH}_3$ . The bioadsorbent prepared only by milling OS was also capable of adsorbing  $\text{NH}_3$  and presented the advantage of being environmentally-sound since it requires low energy expenditure, and no chemicals are expended in its preparation. Additionally, the samples prepared from OS showed the lowest height of mass transfer zone, which confers more efficiency to the adsorbents (ASTM, 2019).

Additionally, the regeneration process using water delivered adsorbents capable of being used in one  $\text{NH}_3$  sorption-desorption cycle with satisfactory performance, leading to increasing the materials' resource-use efficiency. Keeping the adsorbents in use longer by reusing them makes the process more sustainable, promoting a circular economy (Baldikova et al., 2019).

A low-cost olfactometer was prepared and successfully used in the subjective evaluation of  $\text{NH}_3$  adsorption. Olfactometric evaluations confirmed that adsorbents prepared by OS are capable of reducing odor annoyance of leachate off-gases.

Finally, this work reinforced the importance of objective and subjective evaluation of odor abatement undertaken jointly for a complete assessment of odor control.

## 5.2 Recommendations for future work

Considering that the materials prepared in this work by pyrolysis presented greater surface area and pore volume, further research is recommended to investigate the preparation of adsorbents from these materials by functionalization with an acid, to provide more functional acid groups on its surface, which could result in a material with great  $\text{NH}_3$  adsorption capacity. The use of environmentally-sound acids is suggested in order to reduce the risk of negative environmental impacts. The solid acid catalyst prepared by Gong et al. (2014) showed to be an effective and stable alternative of  $\text{H}_2\text{SO}_4$  and could be a possible green acid to be used. As odor from leachate may be related both to  $\text{NH}_3$  and  $\text{H}_2\text{S}$  off-gases (Cheng et al., 2019) and by the fact that adsorption of  $\text{H}_2\text{S}$  may be correlated with pore structure, especially with micropore surface area ( $S_{mic}$ ) (Mochizuki et al., 2016), a material prepared by the process mentioned above could be capable of adsorbing both pollutants. The removal of multi-component pollutant gases is efficient and economically advantageous (Chen et al., 2017). According to Yeom et al. (2017), a regular and interlinked adsorbent pore system was found to be more crucial than larger surface areas in  $\text{NH}_3$  adsorption, so that it should also be considered for further studies.

It is also recommended as further studies improving techniques to allow the reuse of the adsorbents by its regeneration. The regeneration using water, presented in this work, could be improved by further investigations of the role of parameters  $m$ ,  $T$ , and  $V_{UPw}$  in the regenerated adsorbents' performance on  $\text{NH}_3$  adsorption. Additionally, the OS-M sample could be subject to various adsorption-desorption cycles until it loses the  $\text{NH}_3$  adsorption capacity and, then, be used as a precursor to prepared materials impregnated with eco-friendly acid, to be used in other adsorption-desorption cycles until its exhaustion. This action could considerably prolong the lifespan of the material.

Further studies could also evaluate the use of exhausted adsorbents and the liquid phase of regeneration, both nitrogen sources, as raw material for fertilizers (Amaral et al., 2016; Chou et al., 2006; Melenová et al., 2003). Figure 38 shows the possible improvement of this work's stages after further studies that are recommended above.

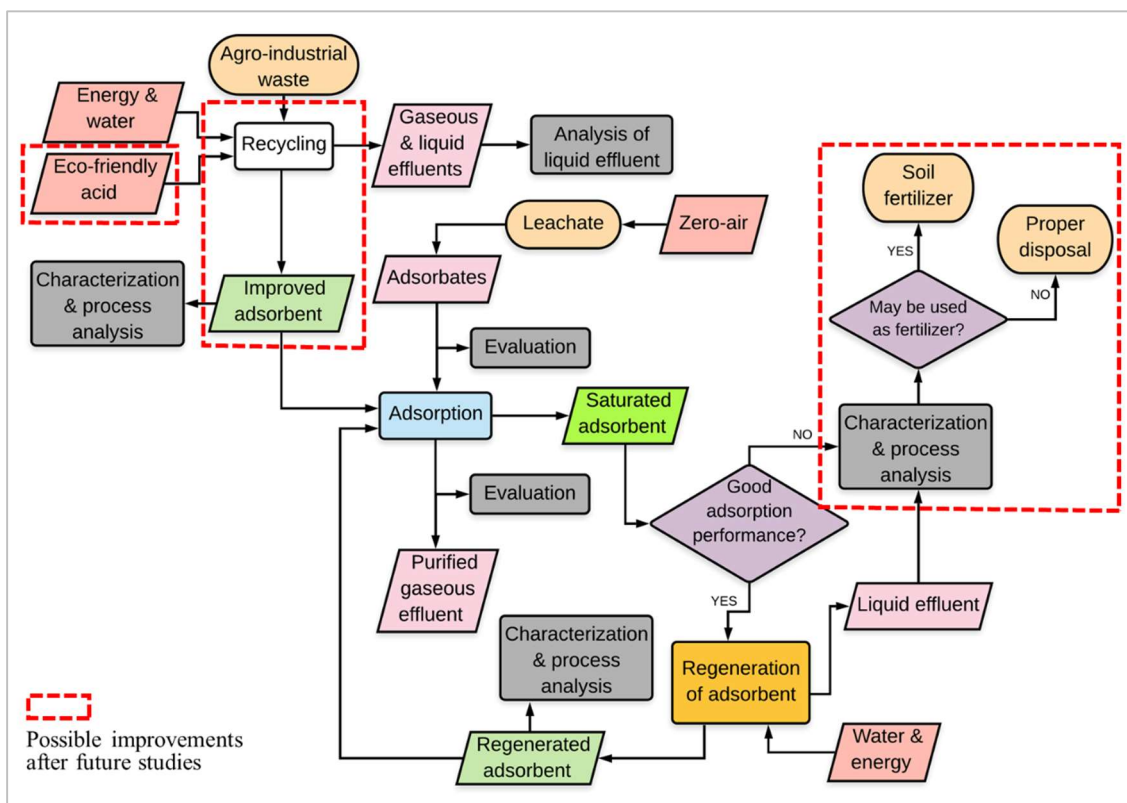


Figure 38. Possible improvement of the stages of this work after future studies.

Therefore, after being subjected to various adsorption-desorption cycles until its  $\text{NH}_3$  adsorption capacity being considerably reduced, exhausted adsorbents and liquid phase of the regeneration process could be reused as fertilizers instead of being disposed/incinerated.

In conclusion, the implementation of the improvements presented above could result in a process even more sustainable.



## LIST OF REFERENCES

- ABNT, N. (2004). *10004: Resíduos sólidos - Classificação* (2nd ed.). Rio de Janeiro: Associação Brasileira de Normas Técnicas.
- ADEME. (2005). *Pollutions olfactives: origine, législation, analyse, traitement*. Paris: Dunod.
- Ahmad, M., Rajapaksha, A. U., Lim, J. E., Zhang, M., Bolan, N., Mohan, D., ... Ok, Y. S. (2014). Biochar as a sorbent for contaminant management in soil and water: A review. *Chemosphere*, 99, 19–33. <https://doi.org/10.1016/j.chemosphere.2013.10.071>
- Al Bulushi, K., Attard, T. M., North, M., & Hunt, A. J. (2018). Optimisation and economic evaluation of the supercritical carbon dioxide extraction of waxes from waste date palm (*Phoenix dactylifera*) leaves. *Journal of Cleaner Production*, 186, 988–996. <https://doi.org/10.1016/j.jclepro.2018.03.117>
- Alhashimi, H. A., & Aktas, C. B. (2017). Life cycle environmental and economic performance of biochar compared with activated carbon: A meta-analysis. *Resources, Conservation and Recycling*, 118, 13–26. <https://doi.org/10.1016/j.resconrec.2016.11.016>
- Alslaibi, T. M., Abustan, I., Ahmad, M. A., & Foul, A. A. (2013). A review: Production of activated carbon from agricultural byproducts via conventional and microwave heating. *Journal of Chemical Technology and Biotechnology*, 88(7), 1183–1190. <https://doi.org/10.1002/jctb.4028>
- Amaral, M. C. S., Magalhães, N. C., Moravia, W. G., & Ferreira, C. D. (2016). Ammonia recovery from landfill leachate using hydrophobic membrane contactors. *Water Science and Technology*, 74(9), 2177–2184. <https://doi.org/10.2166/wst.2016.375>
- Ang, T. N., Young, B. R., Taylor, M., Burrell, R., Aroua, M. K., & Baroutian, S. (2020). Breakthrough analysis of continuous fixed-bed adsorption of sevoflurane using activated carbons. *Chemosphere*, 239. <https://doi.org/10.1016/j.chemosphere.2019.124839>
- Artiola, J. F., Reynolds, K. A., & Brusseau, M. L. (2019). Chapter 18: Urban and Household Pollution. In *Environmental and Pollution Science* (3rd ed., pp. 311–326). <https://doi.org/10.1016/B978-0-12-814719-1.00018-5>
- Asadullah, M., Zhang, S., & Li, C. (2010). Evaluation of structural features of chars from pyrolysis of biomass of different particle sizes. *Fuel Processing Technology*, 91(8), 877–881. <https://doi.org/10.1016/j.fuproc.2009.08.008>
- ASTM. (2001). *D6556-01: Standard Test Method for Carbon Black - Total and External Surface Area by Nitrogen Adsorption*. ASTM International.
- ASTM. (2019). *D5160-95 (Reapproved 2019) - Standard Guide for Gas-Phase Adsorption Testing of Activated Carbon*. ASTM International.
- ATSDR. (2011). Toxic Substances: ammonia. Retrieved from Toxic Substance Portal. Agency for Toxic Substances and Disease Registry. website: <https://www.atsdr.cdc.gov/substances/toxsubstance.asp?toxid=2>
- Baldikova, E., Mullerova, S., Prochazkova, J., Rouskova, M., Solcova, O., Safarik, I., & Pospiskova, K. (2019). Use of waste *Japonochytrium* sp. biomass after lipid extraction as an efficient adsorbent for triphenylmethane dye applied in aquaculture. *Biomass Conversion and Biorefinery*, (9), 479–488. <https://doi.org/10.1007/s13399-018-0362-2>
- Balestrini, M., Creus, J., Errandonea, L., Arias, R., & Salas Seoane, N. (2018). *Map of odour issues and priorities. Multilevel engagement plan for stakeholders and communities*. D-NOSES, H2020-SwafS-23-2017-789315.

- Balsamo, M., Rodríguez-Reinoso, F., Montagnaro, F., Lancia, A., & Erto, A. (2013). Highlighting the role of activated carbon particle size on CO<sub>2</sub> capture from model flue gas. *Industrial and Engineering Chemistry Research*, 52(34), 12183–12191. <https://doi.org/10.1021/ie4018034>
- Basso, D., Weiss-Hortala, E., Patuzzi, F., Castello, D., Baratieri, M., & Fiori, L. (2015). Hydrothermal carbonization of off-specification compost: A byproduct of the organic municipal solid waste treatment. *Bioresource Technology*, 182, 217–224. <https://doi.org/10.1016/j.biortech.2015.01.118>
- Behera, S. N., & Sharma, M. (2012). Transformation of atmospheric ammonia and acid gases into components of PM<sub>2.5</sub>: an environmental chamber study. *Environmental Science and Pollution Research*, 19(4), 1187–1197. <https://doi.org/10.1007/s11356-011-0635-9>
- Bhatnagar, A., Kesari, K. K., & Shurpali, N. (2016). Multidisciplinary Approaches to Handling Wastes in Sugar Industries. *Water, Air, and Soil Pollution*, 227(1). <https://doi.org/10.1007/s11270-015-2705-y>
- Blanco López, M. C. ., Blanco, C. G., Martínez-Alonso, A., & Tascón, J. M. D. (2002). Composition of gases released during olive stones pyrolysis. *Journal of Analytical and Applied Pyrolysis*, 65(2), 313–322. [https://doi.org/10.1016/S0165-2370\(02\)00008-6](https://doi.org/10.1016/S0165-2370(02)00008-6)
- Bordonal, R. de O., Carvalho, J. L. N., Lal, R., de Figueiredo, E. B., de Oliveira, B. G., & La Scala, N. (2018). Sustainability of sugarcane production in Brazil. A review. *Agronomy for Sustainable Development*, 38(2), 13. <https://doi.org/10.1007/s13593-018-0490-x>
- Brasil. (1981). Lei nº 6.938, de 31 de agosto de 1981. Dispõe sobre a Política Nacional do Meio Ambiente, seus fins e mecanismos de formulação e aplicação, e dá outras providências. *Diário Oficial da União*. Retrieved from [http://www.planalto.gov.br/ccivil\\_03/leis/L6938.htm](http://www.planalto.gov.br/ccivil_03/leis/L6938.htm)
- Brasil. (1986). Resolução CONAMA nº 18, de 6 de maio de 1986. Dispõe sobre a criação do Programa de Controle de Poluição do Ar por veículos Automotores – PROCONVE. *Conselho Nacional do Meio Ambiente (CONAMA)*. Retrieved from <http://www2.mma.gov.br/port/conama/legiabre.cfm?codlegi=41>
- Brasil. (1989). Resolução CONAMA nº 5, de 15 de junho de 1989. Dispõe sobre o Programa Nacional de Controle da Poluição do Ar – PRONAR. *Conselho Nacional do Meio Ambiente (CONAMA)*. Retrieved from <http://www2.mma.gov.br/port/conama/legiabre.cfm?codlegi=81>
- Brasil. (1990). Resolução CONAMA nº 3, de 28 de junho de 1990. Intitui os padrões de qualidade do ar do Programa Nacional de Controle da Qualidade do ar (PRONAR). *Conselho Nacional do Meio Ambiente (CONAMA)*. Retrieved from <http://www2.mma.gov.br/port/conama/res/res90/res0390.html>
- Brasil. (2009). Lei nº 12.187, de 29 de dezembro de 2009. Intitui a Política Nacional sobre Mudança do Clima - PNMC e dá outras providências. *Diário Oficial da União*. Retrieved from [http://www.planalto.gov.br/ccivil\\_03/\\_ato2007-2010/2009/lei/112187.htm](http://www.planalto.gov.br/ccivil_03/_ato2007-2010/2009/lei/112187.htm)
- Brasil. (2010). Lei nº 12.305, de 2 de agosto de 2010. Institui a Política Nacional de Resíduos Sólidos; altera a Lei nº 9.605, de 12 de fevereiro de 1998; e dá outras providências. *Diário Oficial da União*. Retrieved from [https://www.planalto.gov.br/ccivil\\_03/\\_ato2007-2010/2010/lei/112305.htm](https://www.planalto.gov.br/ccivil_03/_ato2007-2010/2010/lei/112305.htm)
- Brasil. (2018). Resolução CONAMA nº 491, de 19 de novembro de 2018. Dispõe sobre padrões de qualidade do ar. *Conselho Nacional do Meio Ambiente (CONAMA)*. Retrieved from [https://www.in.gov.br/materia/-/asset\\_publisher/Kujrw0TZC2Mb/content/id/51058895](https://www.in.gov.br/materia/-/asset_publisher/Kujrw0TZC2Mb/content/id/51058895)
- Bruckman, V. J. (2016). *Biochar: A Regional Supply Chain Approach in View of Climate Change Mitigation* (V. J. Bruckman, E. A. Varol, B. B. Uzun, & J. Liu, Eds.). New York: Cambridge University Press.

- Cagnon, B., Py, X., Guillot, A., Stoeckli, F., & Chambat, G. (2009). Contributions of hemicellulose, cellulose and lignin to the mass and the porous properties of chars and steam activated carbons from various lignocellulosic precursors. *Bioresource Technology*, 100(1), 292–298. <https://doi.org/10.1016/j.biortech.2008.06.009>
- Calero, M., Hernáinz, F., Blázquez, G., & Martín-Lara, M. Á. (2010). Potentiometric Titrations for the Characterization of Functional Groups on Solid Wastes of the Olive Oil Production. *Environmental Progress & Sustainable Energy*, 29(2), 249–258. <https://doi.org/10.1002/ep>
- Capelli, L., Bax, C., Diaz, C., Izquierdo, C., Arias, R., & Salas Seone, N. (2019). *Review on odour pollution, odour measurement, abatement techniques*. D-NOSES, H2020-SwafS-23-2017-789315.
- Celzard, A., Fierro, V., Marêché, J. F., & Furdin, G. (2007). Advanced preparative strategies for activated carbons designed for the adsorptive storage of hydrogen. *Adsorption Science and Technology*, 25(3–4), 129–142. <https://doi.org/10.1260/026361707782398254>
- CEN. (2003). *EN 13725:2003: Air quality - Determination of odour concentration by dynamic olfactometry*. London: British Standards.
- CEN. (2014). *EN ISO 10121-1:2014: Test methods for assessing the performance of gas-phase air cleaning media and devices for general ventilation*. London: British Standards.
- Chen, Y., Zhang, X., Chen, W., Yang, H., & Chen, H. (2017). The structure evolution of biochar from biomass pyrolysis and its correlation with gas pollutant adsorption performance. *Bioresource Technology*, 246, 101–109. <https://doi.org/10.1016/j.biortech.2017.08.138>
- Cheng, Z., Sun, Z., Zhu, S., Lou, Z., Zhu, N., & Feng, L. (2019). The identification and health risk assessment of odor emissions from waste landfilling and composting. *Science of the Total Environment*, 649, 1038–1044. <https://doi.org/10.1016/j.scitotenv.2018.08.230>
- Chou, L., Tsai, R., Chang, J., & Lee, M. (2006). Regenerable adsorbent for removing ammonia evolved from anaerobic reaction of animal urine. *Journal of Environmental Sciences*, 18(6), 1176–1181. [https://doi.org/10.1016/S1001-0742\(06\)60058-2](https://doi.org/10.1016/S1001-0742(06)60058-2)
- Dai, Y., Sun, Q., Wang, W., Lu, L., Liu, M., Li, J., ... Zhang, Y. (2018). Utilizations of agricultural waste as adsorbent for the removal of contaminants: A review. *Chemosphere*, 211, 235–253. <https://doi.org/10.1016/j.chemosphere.2018.06.179>
- Daramola, M. O., & Ayeni, A. O. (Eds.). (2020). *Valorization of Biomass to Value-Added Commodities: current trends, challenges and future prospects*. *Green Energy and Technology*. <https://doi.org/10.1007/978-3-030-38032-8>
- Diaz, C., Izquierdo, C., Capelli, L., Arias, R., & Salas Seone, N. (2019). *Analysis of existing regulations in odour pollution, odour impact criteria I*. D-NOSES, H2020-SwafS-23-2017-789315.
- Diaz de Tuesta, J. L., Silva, A. M. T., Faria, J. L., & Gomes, H. T. (2018). Removal of Sudan IV from a simulated biphasic oily wastewater by using lipophilic carbon adsorbents. *Chemical Engineering Journal*, 347, 963–971. <https://doi.org/10.1016/j.cej.2018.04.105>
- Din, A. T. M., Hameed, B. H., & Ahmad, A. L. (2009). Batch adsorption of phenol onto physiochemical-activated coconut shell. *Journal of Hazardous Materials*, 161(2–3), 1522–1529. <https://doi.org/10.1016/j.jhazmat.2008.05.009>
- Do, M. H., Phan, N. H., Nguyen, T. D., Pham, T. T. S., Nguyen, V. K., Vu, T. T. T., & Nguyen, T. K. P. (2011). Activated carbon/Fe<sub>3</sub>O<sub>4</sub> nanoparticle composite: Fabrication, methyl orange removal and regeneration by hydrogen peroxide. *Chemosphere*, 85(8), 1269–1276. <https://doi.org/10.1016/j.chemosphere.2011.07.023>

- Eslami, A., Borghei, S. M., Rashidi, A., & Takdastan, A. (2018). Preparation of activated carbon dots from sugarcane bagasse for naphthalene removal from aqueous solutions. *Separation Science and Technology*, 53(16), 2536–2549. <https://doi.org/10.1080/01496395.2018.1462832>
- European Union. (2004). Directive 2004/107/EC, of the European Parliament and of the Council, of 15 December 2004, relating to arsenic, cadmium, mercury, nickel and polycyclic aromatic hydrocarbons in ambient air. *Official Journal of the European Union*. Retrieved from <https://eur-lex.europa.eu/eli/dir/2004/107/oj>
- European Union. (2008a). Directive 2008/50/EC, of the European Parliament and of the Council, of 21 May 2008, on ambient air quality and cleaner air for Europe. *Official Journal of the European Union*. Retrieved from <https://eur-lex.europa.eu/legal-content/en/ALL/?uri=CELEX%3A32008L0050>
- European Union. (2008b). Directive 2008/98/EC, of the European Parliament and of the Council, of 19 November 2008, on waste and repealing certain Directives. *Official Journal of the European Union*. Retrieved from <http://eur-lex.europa.eu/legal-content/EN/TXT/PDF/?uri=CELEX:32008L0098&from=EN>
- European Union. (2010). Directive 2010/75/EU, of the European Parliament and of the Council, of 24 November 2010, on industrial emissions (integrated pollution prevention and control). *Official Journal of the European Union*. Retrieved from <https://eur-lex.europa.eu/legal-content/EN/TXT/PDF/?uri=CELEX:32010L0075&from=EN>
- European Union. (2014). Decision 2014/955/EU, of 18 December 2014, amending Decision 2000/ 532/EC on the list of waste pursuant to Directive 2008/98/EC of the European Parliament and of the Council. *Official Journal of the European Union*. Strasbourg.
- European Union. (2018). Directive (EU) 2018/851, of the European Parliament and of the Council, of 30 May 2018, amending Directive 2008/98/EC on waste. *Official Journal of the European Union*. Retrieved from <https://eur-lex.europa.eu/legal-content/EN/TXT/PDF/?uri=CELEX:32018L0851&from=EN>
- Eurostat. (2020). Eurostat’s crop statistics. Olive by production. Retrieved from <https://ec.europa.eu/eurostat/databrowser/view/tag00122/default/table?lang=en>
- Fang, J. J., Yang, N., Cen, D. Y., Shao, L. M., & He, P. J. (2012). Odor compounds from different sources of landfill: Characterization and source identification. *Waste Management*, 32(7), 1401–1410. <https://doi.org/10.1016/j.wasman.2012.02.013>
- Ferreira, F. F., Pereira, P., Teixeira, S., Monjardino, J., & Mendes, L. (2017). *Relatório Final – Programa de Monitorização de Odores no Ecoparque da Abrunheira*. Retrieved from Trato Lixo Gestão de Resíduos Urbanos website: <http://www.tratolixo.pt/assets/docs/Estudo de Odores Abrunheira Mafra - 2017.pdf>
- Fomina, M., & Gadd, G. M. (2014). Biosorption: current perspectives on concept, definition and application. *Bioresource Technology*, 160, 3–14. <https://doi.org/10.1016/j.biortech.2013.12.102>
- Foo, K. Y., Lee, L. K., & Hameed, B. H. (2013). Preparation of activated carbon from sugarcane bagasse by microwave assisted activation for the remediation of semi-aerobic landfill leachate. *Bioresource Technology*, 134, 166–172. <https://doi.org/10.1016/j.biortech.2013.01.139>
- Franciski, M. A., Peres, E. C., Godinho, M., Perondi, D., Foletto, E. L., Collazzo, G. C., & Dotto, G. L. (2018). Development of CO<sub>2</sub> activated biochar from solid wastes of a beer industry and its application for methylene blue adsorption. *Waste Management*, 78, 630–638. <https://doi.org/10.1016/j.wasman.2018.06.040>

- Gamal, M. El, Mousa, H. A., El-Naas, M. H., Zacharia, R., & Judd, S. (2018). Bio-regeneration of activated carbon: A comprehensive review. *Separation and Purification Technology*, 197, 345–359. <https://doi.org/10.1016/j.seppur.2018.01.015>
- Ghouma, I., Jeguirim, M., Dorge, S., Limousy, L., Ghimbeu, C. M., & Ouederni, A. (2015). Activated carbon prepared by physical activation of olive stones for the removal of NO<sub>2</sub> at ambient temperature. *Comptes Rendus Chimie*, 18(1), 63–74. <https://doi.org/10.1016/j.crci.2014.05.006>
- Gil, R. R., Ruiz, B., Lozano, M. S., Martín, M. J., & Fuente, E. (2014). VOCs removal by adsorption onto activated carbons from biocollagenic wastes of vegetable tanning. *Chemical Engineering Journal*, 245, 80–88. <https://doi.org/10.1016/j.cej.2014.02.012>
- Gonçalves, M., Sánchez-García, L., Jardim, E. de O., Silvestre-Albero, J., & Rodríguez-Reinoso, F. (2011). Ammonia removal using activated carbons: effect of the surface chemistry in dry and moist conditions. *Environmental Science & Technology*, 45(24), 10605–10610. <https://doi.org/10.1021/es203093v>
- Gong, S., Liu, L., Zhang, J., & Cui, Q. (2014). Stable and eco-friendly solid acids as alternative to sulfuric acid in the liquid phase nitration of toluene. *Process Safety and Environmental Protection*, 92(6), 577–582. <https://doi.org/10.1016/j.psep.2013.03.005>
- González-García, P. (2018). Activated carbon from lignocellulosics precursors: A review of the synthesis methods, characterization techniques and applications. *Renewable and Sustainable Energy Reviews*, 82(1), 1393–1414. <https://doi.org/10.1016/j.rser.2017.04.117>
- González, J. F., Román, S., Encinar, J. M., & Martínez, G. (2009). Pyrolysis of various biomass residues and char utilization for the production of activated carbons. *Journal of Analytical and Applied Pyrolysis*, 85(1–2), 134–141. <https://doi.org/10.1016/j.jaap.2008.11.035>
- Han, X., Lin, H., & Zheng, Y. (2014). Regeneration methods to restore carbon adsorptive capacity of dibenzothiophene and neutral nitrogen heteroaromatic compounds. *Chemical Engineering Journal*, 243, 315–325. <https://doi.org/10.1016/j.cej.2013.12.074>
- Hu, Z., Srinivasan, M. P., & Ni, Y. (2001). Novel activation process for preparing highly microporous and mesoporous activated carbons. *Carbon*, 39(6), 877–886. [https://doi.org/10.1016/S0008-6223\(00\)00198-6](https://doi.org/10.1016/S0008-6223(00)00198-6)
- Huang, C., Li, H., & Chen, C. (2008). Effect of surface acidic oxides of activated carbon on adsorption of ammonia. *Journal of Hazardous Materials*, 159(2–3), 523–527. <https://doi.org/10.1016/j.jhazmat.2008.02.051>
- Huang, X., Lu, Q., Hao, H., Wei, Q., Shi, B., Yu, J., ... Wang, Y. (2019). Evaluation of the treatability of various odor compounds by powdered activated carbon. *Water Research*, 156, 414–424. <https://doi.org/10.1016/j.watres.2019.03.043>
- Huang, Y. Y. (2017). Research progress of wastewater treatment by agricultural wastes as biological adsorbent. *Applied Chemical Industry*, 46(2), 368–372.
- IEMA. (2014). *1º Diagnóstico da rede de monitoramento da qualidade do ar no Brasil*. Retrieved from Instituto de Energia e Meio Ambiente do Brasil (IEMA) website: <http://www.energiaeambiente.org.br/wp-content/uploads/2015/08/1-diagnostico-da-rede-de-monitoramento-da-qualidade-do-ar-no-brasil.pdf>
- Ioannidou, O., & Zabaniotou, A. (2007). Agricultural residues as precursors for activated carbon production-A review. *Renewable and Sustainable Energy Reviews*, 11(9), 1966–2005. <https://doi.org/10.1016/j.rser.2006.03.013>
- IPNI. (n.d.). Nitrogen Notes. Ammonia Volatilization. Retrieved from International Plant Nutrition Institute website: [http://www.ipni.net/publication/nitrogen-en.nsf/0/B219184650778DB985257DD60005826A/\\$FILE/NitrogenNotes-EN-6.pdf](http://www.ipni.net/publication/nitrogen-en.nsf/0/B219184650778DB985257DD60005826A/$FILE/NitrogenNotes-EN-6.pdf)

- Islas, J., Manzini, F., Masera, O., & Vargas, V. (2019). Solid Biomass to Heat and Power. In C. Lago, N. Caldés, & Y. Lechón (Eds.), *The Role of Bioenergy in the Bioeconomy* (pp. 145–177). <https://doi.org/10.1016/B978-0-12-813056-8.00004-2>
- IUPAC. (1997). Compendium of Chemical Terminology. In A. D. McNaught & A. Wilkinson (Eds.), *IUPAC Compendium of Chemical Terminology* (2nd ed., Vol. 2). <https://doi.org/10.1351/goldbook.A00090>
- Jain, A., Balasubramanian, R., & Srinivasan, M. P. (2016). Hydrothermal conversion of biomass waste to activated carbon with high porosity: A review. *Chemical Engineering Journal*, 283, 789–805. <https://doi.org/10.1016/j.cej.2015.08.014>
- Javidi Alsadi, K., & Esfandiari, N. (2019). Synthesis of Activated Carbon from Sugarcane Bagasse and Application for Mercury Adsorption. *Pollution*, 5(3), 585–596. <https://doi.org/10.22059/poll.2019.269364.540>
- Jiang, G., Melder, D., Keller, J., & Yuan, Z. (2017). Odor emissions from domestic wastewater: A review. *Critical Reviews in Environmental Science and Technology*, 47(17), 1581–1611. <https://doi.org/10.1080/10643389.2017.1386952>
- Kastner, J. R., Miller, J., & Das, K. C. (2009). Pyrolysis conditions and ozone oxidation effects on ammonia adsorption in biomass generated chars. *Journal of Hazardous Materials*, 164(2–3), 1420–1427. <https://doi.org/10.1016/j.jhazmat.2008.09.051>
- Kruse, A., Funke, A., & Titirici, M. (2013). Hydrothermal conversion of biomass to fuels and energetic materials. *Current Opinion in Chemical Biology*, 17(3), 515–521. <https://doi.org/10.1016/j.cbpa.2013.05.004>
- Kurzweil, P. (2009). CAPACITORS | Electrochemical Double-Layer Capacitors: Carbon Materials. In *Encyclopedia of Electrochemical Power Sources* (pp. 634–648). <https://doi.org/10.1016/B978-044452745-5.00353-1>
- Lam, S. S., Liew, R. K., Cheng, C. K., Rasit, N., Ooi, C. K., Ma, N. L., ... Chase, H. A. (2018). Pyrolysis production of fruit peel biochar for potential use in treatment of palm oil mill effluent. *Journal of Environmental Management*, 213, 400–408. <https://doi.org/10.1016/j.jenvman.2018.02.092>
- Lam, S. S., Liew, R. K., Wong, Y. M., Yek, P. N. Y., Ma, N. L., Lee, C. L., & Chase, H. A. (2017). Microwave-assisted pyrolysis with chemical activation, an innovative method to convert orange peel into activated carbon with improved properties as dye adsorbent. *Journal of Cleaner Production*, 162, 1376–1387. <https://doi.org/10.1016/j.jclepro.2017.06.131>
- Le-Minh, N., Sivret, E. C., Shammay, A., & Stuetz, R. M. (2018). Factors affecting the adsorption of gaseous environmental odors by activated carbon: A critical review. *Critical Reviews in Environmental Science and Technology*, 48(4), 341–375. <https://doi.org/10.1080/10643389.2018.1460984>
- Le Cloirec, P., & Perrin, M. (1994). Metrology and Sampling. In G. Martin & P. Laffort (Eds.), *Odors and deodorization in the environment* (pp. 265–282). New York: VCH Publishers.
- Le Leuch, L. M., & Bandosz, T. J. (2007). The role of water and surface acidity on the reactive adsorption of ammonia on modified activated carbons. *Carbon*, 45(3), 568–578. <https://doi.org/10.1016/j.carbon.2006.10.016>
- Lehmann, J., & Joseph, S. (Eds.). (2009). *Biochar for Environmental Management: Science and Technology*. London: Earthscan Publishers.
- Leng, L., & Zhou, W. (2018). Chemical compositions and wastewater properties of aqueous phase (wastewater) produced from the hydrothermal treatment of wet biomass: A review. *Energy Sources, Part A: Recovery, Utilization, and Environmental Effects*, 40(22), 2648–2659. <https://doi.org/10.1080/15567036.2018.1495780>

- Mannan, M. A., & Ganapathy, C. (2004). Concrete from an agricultural waste-oil palm shell (OPS). *Building and Environment*, 39(4), 441–448. <https://doi.org/10.1016/j.buildenv.2003.10.007>
- Martín-Lara, M. A., Blázquez, G., Ronda, A., Pérez, A., & Calero, M. (2013). Development and characterization of biosorbents to remove heavy metals from aqueous solutions by chemical treatment of olive stone. *Industrial and Engineering Chemistry Research*, 52(31), 10809–10819. <https://doi.org/10.1021/ie401246c>
- McCabe, W. L., Smith, J. C., & Harriott, P. (1993). *Unit Operations of Chemical Engineering* (5th ed.). McGraw-Hill, Inc.
- McGinley, M. A., & McGinley, C. M. (2001). The new European olfactometry standard: implementation, experience and perspectives. *Air and Waste Management Association, 2001 Annual Conference Technical Program, Session No. EE-6b: Modelling, Analysis and Management of Odours*. Retrieved from [http://www.fivesenses.com/Documents/Library/35](http://www.fivesenses.com/Documents/Library/35%20New%20Euro%20Odor%20Standard.pdf) New Euro Odor Standard.pdf
- Melenová, L., Ciahotny, K., Jirglová, H., Kusá, H., & Ruzek, P. (2003). Removal of Ammonia from Waste Gases by Adsorption on Zeolites and Their Utilization in Agriculture. *Chemické Listy*, 97(7), 562–568.
- Mello, L. R. P. F., & Mali, S. (2014). Use of malt bagasse to produce biodegradable baked foams made from cassava starch. *Industrial Crops and Products*, 55, 187–193. <https://doi.org/10.1016/j.indcrop.2014.02.015>
- Minas Gerais. (2009). Lei nº 18.031, de 12 de janeiro de 2009. Dispõe sobre a Política Estadual Resíduos Sólidos. *Diário do Legislativo de Minas Gerais*. Retrieved from [https://www.almg.gov.br/consulte/legislacao/completa/completa.html?num=18031&ano=2009&tipo=LEI&aba=js\\_textoAtualizado](https://www.almg.gov.br/consulte/legislacao/completa/completa.html?num=18031&ano=2009&tipo=LEI&aba=js_textoAtualizado)
- Minas Gerais. (2013). Deliberação Normativa COPAM nº 187, de 19 de setembro de 2013. Estabelece condições e limites máximos de emissão de poluentes atmosféricos para fontes fixas e dá outras providências. *Diário do Executivo de Minas Gerais*. Retrieved from <https://www.jornalminasgerais.mg.gov.br/?dataJornal=2013-09-20>
- Minas Gerais. (2014). Lei nº 21.557, de 22 de dezembro de 2014. Acrescenta dispositivos à Lei nº 18.031, de 12 de janeiro de 2009, com o objetivo de proibir a utilização da tecnologia de incineração nos casos que especifica. *Diário do Legislativo de Minas Gerais*. Retrieved from <https://www.almg.gov.br/consulte/legislacao/completa/completa.html?num=21557&ano=2014&tipo=LEI>
- Mochizuki, T., Kubota, M., Matsuda, H., & Camacho, L. F. D. (2016). Adsorption behaviors of ammonia and hydrogen sulfide on activated carbon prepared from petroleum coke by KOH chemical activation. *Fuel Processing Technology*, 144, 164–169. <https://doi.org/10.1016/j.fuproc.2015.12.012>
- Mohamed, A. R., Mohammadi, M., & Darzi, G. N. (2010). Preparation of carbon molecular sieve from lignocellulosic biomass: A review. *Renewable and Sustainable Energy Reviews*, 14(6), 1591–1599. <https://doi.org/10.1016/j.rser.2010.01.024>
- Mohtashami, S. A., Asasian Kolor, N., Kaghazchi, T., Asadi-Kesheh, R., & Soleimani, M. (2018). Optimization of sugarcane bagasse activation to achieve adsorbent with high affinity towards phenol. *Turkish Journal of Chemistry*, 42(6), 1720–1735. <https://doi.org/10.3906/kim-1806-71>
- Nadolny, B., Heineck, R. G., Bazani, H. A. G., Hemmer, J. V., Biavatti, M. L., Radetski, C. M., & Almerindo, G. I. (2020). Use of brewing industry waste to produce carbon-based adsorbents : Paracetamol adsorption study. *Journal of Environmental Science and Health, Part A*, 55(8), 947–956. <https://doi.org/10.1080/10934529.2020.1759320>

- NASA. (2020). Spacecraft Maximum Allowable Concentrations for Airborne Contaminants. *Human Health and Performance Directorate*. Retrieved from [https://www.nasa.gov/sites/default/files/atoms/files/jsc\\_20584\\_signed.pdf](https://www.nasa.gov/sites/default/files/atoms/files/jsc_20584_signed.pdf)
- Nicell, J. A. (2009). Assessment and regulation of odour impacts. *Atmospheric Environment*, 43(1), 196–206. <https://doi.org/10.1016/j.atmosenv.2008.09.033>
- Nudrat, S., Archana, Y., & Hasan, S. S. (2018). A Review Study of Advances in the Science and Technology of Carbon Nanotubes. *Research & Reviews: Journal of Physics*, 5(3), 1–6. <https://doi.org/10.37591/rrjophy.v5i3.421>
- Ok, Y. S., Uchimiya, S. M., Chang, S. X., & Bolan, N. (Eds.). (2016). *Biochar: Production, Characterization, and Applications*. CRC Press.
- Paraná. (2006). Resolução SEMA nº 54, de 22 de dezembro de 2006. Estabelece padrões de emissão e critérios de atendimento para fontes industriais, comerciais e de serviços e metodologias a serem utilizadas para determinação de emissões. *Secretaria do Estado Do Meio Ambiente e Recursos Hídricos (SEMA)*. Retrieved from <https://www.abic.com.br/wp-content/uploads/2018/04/Resolucao-n.-054-2006.pdf>
- Patel, H. (2019). Fixed-bed column adsorption study: a comprehensive review. *Applied Water Science*, 9(45), 1–17. <https://doi.org/10.1007/s13201-019-0927-7>
- Pattara, C., Cappelletti, G. M., & Cichelli, A. (2010). Recovery and use of olive stones: Commodity, environmental and economic assessment. *Renewable and Sustainable Energy Reviews*, 14(5), 1484–1489. <https://doi.org/10.1016/j.rser.2010.01.018>
- Porada, S., Zhao, R., Van Der Wal, A., Presser, V., & Biesheuvel, P. M. (2013). Review on the science and technology of water desalination by capacitive deionization. *Progress in Materials Science*, 58(8), 1388–1442. <https://doi.org/10.1016/j.pmatsci.2013.03.005>
- Portugal. (1993). Portaria nº 286, de 12 de Março de 1993. *Diário da República, I Série-B, Nº 60*. Retrieved from <https://dre.pt/application/conteudo/634909>
- Portugal. (2002). Decreto-Lei nº 89, de 09 de Abril de 2002. *Diário da República, I Série-A, Nº 83*. Retrieved from <https://dre.pt/application/conteudo/302769>
- Portugal. (2004). Decreto-Lei nº 78, de 03 de Abril de 2004. *Diário da República, I Série-A, Nº 80*. Retrieved from <https://dre.pt/application/conteudo/218329>
- Portugal. (2011). Decreto-Lei nº 73, de 17 de Junho de 2011. *Diário da República, Iª Série, Nº 116*. Retrieved from <https://dre.pt/application/conteudo/670034>
- Portugal. (2013a). Declaração de Retificação nº 45-A, de 29 de Outubro de 2013. *Diário da República, Iª Série, Nº 209*. Retrieved from <https://dre.pt/application/conteudo/169457>
- Portugal. (2013b). Decreto-Lei n.º 127, de 30 de agosto de 2013. *Diário da República, Iª Série, Nº 167*. Retrieved from <https://dre.pt/application/conteudo/499546>
- Portugal. (2018a). Decreto-Lei n.º 39, de 11 de junho de 2018. *Diário da República, Iª Série, Nº 111*. Retrieved from <https://dre.pt/application/conteudo/115487878>
- Portugal. (2018b). Decreto-Lei n.º 84, de 23 de outubro de 2018. *Diário da República, Iª Série, Nº 204*. Retrieved from <https://dre.pt/application/conteudo/116747964>
- Rajinipriya, M., Nagalakshmaiah, M., Robert, M., & Elkoun, S. (2018). Importance of Agricultural and Industrial Waste in the Field of Nanocellulose and Recent Industrial Developments of Wood Based Nanocellulose: A Review. *ACS Sustainable Chemistry and Engineering*, 6(3), 2807–2828. <https://doi.org/10.1021/acssuschemeng.7b03437>



- Raut, S. P., Ralegaonkar, R. V., & Mandavgane, S. A. (2011). Development of sustainable construction material using industrial and agricultural solid waste: A review of waste-create bricks. *Construction and Building Materials*, 25(10), 4037–4042. <https://doi.org/10.1016/j.conbuildmat.2011.04.038>
- Razi, M. A. M., Hishammudin, M. N. A. M., Rahim, M. A., & Salleh, N. A. H. M. S. (2018). A review of agricultural waste activated carbon and effect on adsorption parameters. *International Journal of Environmental Engineering*, 9(3–4), 301–323. <https://doi.org/10.1504/IJEE.2018.097516>
- Ren, B., Zhao, Y., Lyczko, N., & Nzihou, A. (2019). Current Status and Outlook of Odor Removal Technologies in Wastewater Treatment Plant. *Waste and Biomass Valorization*, 10, 1443–1458. <https://doi.org/10.1007/s12649-018-0384-9>
- Rincón, C. A., Guardia, A. De, Couvert, A., Le Roux, S., Soutrel, I., Daumoin, M., & Benoist, J. C. (2019). Chemical and odor characterization of gas emissions released during composting of solid wastes and digestates. *Journal of Environmental Management*, 233, 39–53. <https://doi.org/10.1016/j.jenvman.2018.12.009>
- Ro, K. S., Lima, I. M., Reddy, G. B., Jackson, M. A., & Gao, B. (2015). Removing Gaseous NH<sub>3</sub> Using Biochar as an Adsorbent. *Agriculture*, 5, 991–1002. <https://doi.org/10.3390/agriculture5040991>
- Rodrigues, C. C., de Moraes Jr., D. de, da Nóbrega, S. W., & Barboza, M. G. (2007). Ammonia adsorption in a fixed bed of activated carbon. *Bioresource Technology*, 98(4), 886–891. <https://doi.org/10.1016/j.biortech.2006.03.024>
- Ronda, A., Martín-Lara, M. A., Calero, M., & Blázquez, G. (2015). Complete use of an agricultural waste: application of untreated and chemically treated olive stone as biosorbent of lead ions and reuse as fuel. *Chemical Engineering Research and Design*, 104, 740–751. <https://doi.org/10.1016/j.cherd.2015.10.021>
- Rossi, R. (2017). *The EU olive and olive oil sector. Main features, challenges and prospects*. Retrieved from European Parliamentary Research Service website: [http://www.europarl.europa.eu/RegData/etudes/BRIE/2017/608690/EPRS\\_BRI\(2017\)608690\\_EN.pdf](http://www.europarl.europa.eu/RegData/etudes/BRIE/2017/608690/EPRS_BRI(2017)608690_EN.pdf)
- Safarik, I., Baldikova, E., Prochazkova, J., Safarikova, M., & Pospiskova, K. (2018). Magnetically Modified Agricultural and Food Waste: Preparation and Application. *Journal of Agricultural and Food Chemistry*, 66, 2538–2552. <https://doi.org/10.1021/acs.jafc.7b06105>
- Saleem, J., Shahid, U. Bin, Hijab, M., Mackey, H., & McKay, G. (2019). Production and applications of activated carbons as adsorbents from olive stones. *Biomass Conversion and Biorefinery*, 9. <https://doi.org/10.1007/s13399-019-00473-7>
- Sanginés, P., Domínguez, M. P., Sánchez, F., & Miguel, G. S. (2015). Slow pyrolysis of olive stones in a rotary kiln: Chemical and energy characterization of solid, gas, and condensable products. *Journal of Renewable and Sustainable Energy*, 7(043103), 1–13. <https://doi.org/10.1063/1.4923442>
- Sansaniwal, S. K., Pal, K., Rosen, M. A., & Tyagi, S. K. (2017). Recent advances in the development of biomass gasification technology: A comprehensive review. *Renewable and Sustainable Energy Reviews*, 72, 363–384. <https://doi.org/10.1016/j.rser.2017.01.038>
- Saxena, P., & Naik, V. (Eds.). (2019). *Air Pollution: Sources, Impacts and Controls*. CAB International.
- Sevilla, M., & Fuertes, A. B. (2016). A Green Approach to High-Performance Supercapacitor Electrodes: The Chemical Activation of Hydrochar with Potassium Bicarbonate. *ChemSusChem*, 9, 1–10. <https://doi.org/10.1002/cssc.201600426>

- Sevilla, M., & Mokaya, R. (2014). Energy storage applications of activated carbons: supercapacitors and hydrogen storage. *Energy and Environmental Science*, 7, 1250–1280. <https://doi.org/10.1039/c3ee43525c>
- Shen, F., Liu, J., Zhang, Z., Dong, Y., & Gu, C. (2018). Density functional study of hydrogen sulfide adsorption mechanism on activated carbon. *Fuel Processing Technology*, 171, 258–264. <https://doi.org/10.1016/j.fuproc.2017.11.026>
- Shin, H., Park, J., Park, K., & Song, H. (2002). Removal characteristics of trace compounds of landfill gas by activated carbon adsorption. *Environmental Pollution*, 119(2), 227–236. [https://doi.org/10.1016/S0269-7491\(01\)00331-1](https://doi.org/10.1016/S0269-7491(01)00331-1)
- SINDICERV. (2020). O setor da cerveja do Brasil em números. Retrieved from Sindicato Nacional da Indústria da Cerveja (SINDICERV) website: <https://www.sindicerv.com.br/o-setor-em-numeros/>
- Spalvins, K., Zihare, L., & Blumberga, D. (2018). Single cell protein production from waste biomass: comparison of various industrial by-products. *Energy Procedia*, 147, 409–418. <https://doi.org/10.1016/j.egypro.2018.07.111>
- Sun, Y., Zhang, B., Zheng, T., & Wang, P. (2017). Regeneration of activated carbon saturated with chloramphenicol by microwave and ultraviolet irradiation. *Chemical Engineering Journal*, 320, 264–270. <https://doi.org/10.1016/j.cej.2017.03.007>
- Tan, K. L., & Hameed, B. H. (2017). Insight into the adsorption kinetics models for the removal of contaminants from aqueous solutions. *Journal of the Taiwan Institute of Chemical Engineers*, 74, 25–48. <https://doi.org/10.1016/j.jtice.2017.01.024>
- Thommes, M., Kaneko, K., Neimark, A. V., Olivier, J. P., Rodriguez-Reinoso, F., Rouquerol, J., & Sing, K. S. W. (2015). Physisorption of gases, with special reference to the evaluation of surface area and pore size distribution (IUPAC Technical Report). *Pure and Applied Chemistry*, 87(9–10), 1051–1069. <https://doi.org/10.1515/pac-2014-1117>
- Tomczyk, A., Sokołowska, Z., & Boguta, P. (2020). Biochar physicochemical properties: pyrolysis temperature and feedstock kind effects. *Reviews in Environmental Science and Bio/Technology*, 19, 191–215. <https://doi.org/10.1007/s11157-020-09523-3>
- Treuer, T. L. H., Choi, J. J., Janzen, D. H., Hallwachs, W., Pérez-Aviles, D., Dobson, A. P., ... Wilcove, D. S. (2017). Low-cost agricultural waste accelerates tropical forest regeneration. *The Journal of the Society for Ecological Restoration*, 1–9. <https://doi.org/10.1111/rec.12565>
- Uberlândia. (2007). Decreto nº 10.847, de 10 de setembro de 2007. Regulamenta o art. 126, da Lei Complementar nº 017/91, alterado pela Lei Complementar nº 447, de 24 de maio de 2007. *Prefeitura de Uberlândia*. Retrieved from <https://leismunicipais.com.br/a/mg/u/uberlandia/decreto/2007/1085/10847/decreto-n-10847-2007-regulamenta-o-art-126-da-lei-complementar-n-017-91-que-dispoe-sobre-a-politica-de-protecao-controle-e-conservacao-do-meio-ambiente-e-da-outras-providencias-altera>
- Uçar, S., Erdem, M., Tay, T., & Karagöz, S. (2009). Preparation and characterization of activated carbon produced from pomegranate seeds by ZnCl<sub>2</sub> activation. *Applied Surface Science*, 255(21), 8890–8896. <https://doi.org/10.1016/j.apsusc.2009.06.080>
- United Nations. (2015). Transforming Our World: The 2030 Agenda for Sustainable Development. *A/RES/70/1*. Retrieved from <https://sustainabledevelopment.un.org/content/documents/21252030> Agenda for Sustainable Development web.pdf

- US EPA. (2009a). EPA's Guide for Industrial Waste Management. *United States Environmental Protection Agency (US EPA)*. Retrieved from <https://www.epa.gov/sites/production/files/2016-03/documents/industrial-waste-guide.pdf>
- US EPA. (2009b). Terms of Environment: Glossary, Abbreviations, and Acronyms. Retrieved from Office of the Administration/Office of External Affairs and Environmental Education website: [https://ofmpub.epa.gov/sor\\_internet/registry/termreg/searchandretrieve/glossariesandkeywordlists/search.do;jsessionid=CFRBdHwWCYgaE8SdawB0kmrqJ48whIOADPLhN\\_s3flakfBUzh6EMl-1219406376?details=&vocabName=I-BEAM](https://ofmpub.epa.gov/sor_internet/registry/termreg/searchandretrieve/glossariesandkeywordlists/search.do;jsessionid=CFRBdHwWCYgaE8SdawB0kmrqJ48whIOADPLhN_s3flakfBUzh6EMl-1219406376?details=&vocabName=I-BEAM) Glossary of Terms?details=&vocabName=Community
- US EPA. (2019). Our Nation's Air 2018: USA's air quality status and trends through 2018. *United States Environmental Protection Agency (US EPA)*. Retrieved from [https://gispub.epa.gov/air/trendsreport/2019/#air\\_pollution](https://gispub.epa.gov/air/trendsreport/2019/#air_pollution)
- Vallero, D. A. (2019a). Chapter 1 - Introduction. In *Air Pollution Calculations: Quantifying Pollutant Formation, Transport, Transformation, Fate and Risks* (pp. 1–27). <https://doi.org/10.1016/B978-0-12-814934-8.00001-6>
- Vallero, D. A. (2019b). Chapter 3 - Pollutant transformation. In *Air Pollution Calculations: Quantifying Pollutant Formation, Transport, Transformation, Fate and Risks* (pp. 45–72). <https://doi.org/10.1016/B978-0-12-814934-8.00003-X>
- Van Gemert, L. J. (2011). *Odour Thresholds. Compilation of odour threshold values in air, water and other media* (2nd ed.). The Netherlands: Oliemans Punter & Partners BV.
- VDI. (1992a). VDI 3882 Part 1. Olfactometry - Determination of Odour Intensity. *Verein Deutscher Ingenieure (VDI)*. Düsseldorf.
- VDI. (1992b). VDI 3882 Part 2. Olfactometry - Determination of Hedonic Odour Tone. *Verein Deutscher Ingenieure (VDI)*. Düsseldorf.
- VDI. (2010). VDI 3940 Part 3. Measurement of odour impact by field inspection - Determination of odour intensity and hedonic odour tone. *Verein Deutscher Ingenieure (VDI)*. Düsseldorf.
- Vieira, M. M., & Lisboa, H. de M. (2013). *Abordagem de procedimentos legais para o controle de incômodos olfativos*. Universidade Federal de Santa Catarina.
- Volpe, R., Zabaniotou, A. A., & Skoulou, V. k. (2018). Synergistic Effects between Lignin and Cellulose during Pyrolysis of Agricultural Waste. *Energy and Fuels*, 32(8), 8420–8430. <https://doi.org/10.1021/acs.energyfuels.8b00767>
- Wang, J., Nie, P., Ding, B., Dong, S., Hao, X., Dou, H., & Zhang, X. (2016). Biomass derived carbon for energy storage device. *Journal of Materials Chemistry A*, 5(6), 2411–2428. <https://doi.org/10.1039/C6TA08742F>
- Wang, S., Nan, J., Shi, C., Fu, Q., Gao, S., Wang, D., ... Zhou, B. (2015). Atmospheric ammonia and its impacts on regional air quality over the megacity of Shanghai, China. *Scientific Reports*, 5(15842). <https://doi.org/10.1038/srep15842>
- WHO. (2016). Ambient air pollution: A global assessment of exposure and burden of disease. In *Air quality and health, Environment, Climate Change and Health*. Retrieved from World Health Organization website: <https://www.who.int/publications/i/item/9789241511353>
- WHO. (2018). Burden of disease from the joint effects of household and ambient air pollution for 2016. In *Summary of results*. Retrieved from World Health Organization website: <http://apps.who.int/gho/data/node.sdg>.
- Williams, P. T., & Besler, S. (1993). The pyrolysis of rice husks in a thermogravimetric analyser and static batch reactor. *Fuel*, 72(2), 151–159. [https://doi.org/10.1016/0016-2361\(93\)90391-E](https://doi.org/10.1016/0016-2361(93)90391-E)

- Windawi, H., & Truex, T. J. (1988). Suppression of H<sub>2</sub>S Emission in Automotive Exhaust. *Studies in Surface Science and Catalysis*, 38, 601–611. [https://doi.org/10.1016/S0167-2991\(09\)60690-X](https://doi.org/10.1016/S0167-2991(09)60690-X)
- Wu, Y., Gu, B., Erisman, J. W., Reis, S., Fang, Y., Lu, X., & Zhang, X. (2016). PM<sub>2.5</sub> pollution is substantially affected by ammonia emissions in China. *Environmental Pollution*, 218, 86–94. <https://doi.org/10.1016/j.envpol.2016.08.027>
- Yahya, M. A., Al-Qodah, Z., & Ngah, C. W. Z. (2015). Agricultural bio-waste materials as potential sustainable precursors used for activated carbon production: A review. *Renewable and Sustainable Energy Reviews*, 46, 218–235. <https://doi.org/10.1016/j.rser.2015.02.051>
- Yang, T., & Lua, A. C. (2003). Characteristics of activated carbons prepared from pistachio-nut shells by physical activation. *Journal of Colloid and Interface Science*, 267(2), 408–417. [https://doi.org/10.1016/S0021-9797\(03\)00689-1](https://doi.org/10.1016/S0021-9797(03)00689-1)
- Yek, P. N. Y., Liew, R. K., Osman, M. S., Lee, C. L., Chuah, J. H., Park, Y. K., & Lam, S. S. (2019). Microwave steam activation, an innovative pyrolysis approach to convert waste palm shell into highly microporous activated carbon. *Journal of Environmental Management*, 236, 245–253. <https://doi.org/10.1016/j.jenvman.2019.01.010>
- Yeom, C., & Kim, Y. (2017). Adsorption of ammonia using mesoporous alumina prepared by a templating method. *Environmental Engineering Research*, 22(4), 401–406. <https://doi.org/10.4491/eer.2017.045>
- Zhang, X., Gao, B., Creamer, A. E., Cao, C., & Li, Y. (2017). Adsorption of VOCs onto engineered carbon materials: A review. *Journal of Hazardous Materials*, 338, 102–123. <https://doi.org/10.1016/j.jhazmat.2017.05.013>
- Zheng, W., Hu, J., Rappeport, S., Zheng, Z., Wang, Z., Han, Z., ... Economy, J. (2016). Activated carbon fiber composites for gas phase ammonia adsorption. *Microporous and Mesoporous Materials*, 234, 146–154. <https://doi.org/10.1016/j.micromeso.2016.07.011>

APPENDIX A

DATA RECORD SHEET SUBJECTIVE ODOR EVALUATION

Age /Idade: \_\_\_\_\_

☐ Female /Feminino

☐ Male /Masculino

**Data Record Sheet for Odour Hedonic Tone**

Ficha de Registo de Dados para Tónus Hedónico de odor

Please mark your impression of pleasantness/unpleasantness for samples A to E with a single cross, using the following scale. In the “comments” field, write any additional comment whenever pertinent.

Marque, com um “x”, sua impressão de agradabilidade/desagradabilidade das amostras A até E, de acordo com a escala a seguir. No campo “comentários”, escreva qualquer comentário adicional sempre que julgar pertinente.

	Impression /Impressão								
	+4	+3	+2	+1	0	-1	-2	-3	-4
A	<input type="radio"/>	<input type="radio"/>	<input type="radio"/>	<input type="radio"/>	<input type="radio"/>	<input type="radio"/>	<input type="radio"/>	<input type="radio"/>	<input type="radio"/>
B	<input type="radio"/>	<input type="radio"/>	<input type="radio"/>	<input type="radio"/>	<input type="radio"/>	<input type="radio"/>	<input type="radio"/>	<input type="radio"/>	<input type="radio"/>
C	<input type="radio"/>	<input type="radio"/>	<input type="radio"/>	<input type="radio"/>	<input type="radio"/>	<input type="radio"/>	<input type="radio"/>	<input type="radio"/>	<input type="radio"/>
D	<input type="radio"/>	<input type="radio"/>	<input type="radio"/>	<input type="radio"/>	<input type="radio"/>	<input type="radio"/>	<input type="radio"/>	<input type="radio"/>	<input type="radio"/>
E	<input type="radio"/>	<input type="radio"/>	<input type="radio"/>	<input type="radio"/>	<input type="radio"/>	<input type="radio"/>	<input type="radio"/>	<input type="radio"/>	<input type="radio"/>

Extremely Pleasant  
extremamente agradável

Scale /Escala

Extremely Unpleasant  
extremamente desagradável

+4

+3

+2

+1

0

-1

-2

-3

-4

pleasant  
agradável

Neither  
nem agradável nem desagradável

Unpleasant  
desagradável

Comments/Comentários	
A	
B	
C	
D	
E	

Age /Idade: \_\_\_\_\_

☐ Female /Feminino

☐ Male /Masculino

**Data Record Sheet for Odour Intensity**

Ficha de Registo de Dados para Intensidade de Odor

Please mark your impression of intensity for samples A to E with a single cross, using the following scale. In the “comments” field, write any additional comment whenever pertinent.

Marque, com um “x”, sua impressão da intensidade das amostras A até E, de acordo com a escala a seguir. No campo “comentários”, escreva qualquer comentário adicional sempre que julgar pertinente.

	Impression /Impressão						
	6	5	4	3	2	1	0
A	<input type="radio"/>	<input type="radio"/>	<input type="radio"/>	<input type="radio"/>	<input type="radio"/>	<input type="radio"/>	<input type="radio"/>
B	<input type="radio"/>	<input type="radio"/>	<input type="radio"/>	<input type="radio"/>	<input type="radio"/>	<input type="radio"/>	<input type="radio"/>
C	<input type="radio"/>	<input type="radio"/>	<input type="radio"/>	<input type="radio"/>	<input type="radio"/>	<input type="radio"/>	<input type="radio"/>
D	<input type="radio"/>	<input type="radio"/>	<input type="radio"/>	<input type="radio"/>	<input type="radio"/>	<input type="radio"/>	<input type="radio"/>
E	<input type="radio"/>	<input type="radio"/>	<input type="radio"/>	<input type="radio"/>	<input type="radio"/>	<input type="radio"/>	<input type="radio"/>

Scale /Escala

Extremely strong /extremamente forte

Very strong /muito forte

Strong /forte

Distinct /evidente

Weak /fraco

Very weak /muito fraco

Not perceptible /imperceptível

Comments/Comentários	
A	
B	
C	
D	
E	

## APPENDIX B

**RESULTS OF THE EVALUATION OF ODOR HEDONIC TONE AND  
INTENSITY OF SAMPLES OS-M AND OS-M-HTC.**

Results of odor hedonic tone of samples OS-M and OS-M-HTC.

Assessor	OS-M					OS-M-HTC				
	<i>SE<sub>Clean</sub></i>	<i>SE<sub>Break</sub></i>	<i>SE<sub>Stoic</sub></i>	<i>SE<sub>Feed</sub></i>	<i>SE<sub>Satur</sub></i>	<i>SE<sub>Clean</sub></i>	<i>SE<sub>Break</sub></i>	<i>SE<sub>Stoic</sub></i>	<i>SE<sub>Feed</sub></i>	<i>SE<sub>Satur</sub></i>
I	0	-1	-2	-2	-3	2	3	1	-3	3
II	-1	-1	-1	-2	0	2	2	2	-1	-1
III	1	-1	2	-2	-1	-1	0	-2	-3	-3
IV	-1	-1	-1	-2	-1	1	1	0	-3	0
V	0	1	-1	-3	0	-2	-3	-3	-4	-3
VI	-2	-2	-2	-2	-2	-1	0	0	-2	0
VII	-1	-1	-2	-3	-1	1	2	-1	-2	-1
VIII	3	1	-2	-1	-3	-1	-1	-1	-3	-2
IX	-2	0	-1	0	-1	-1	-1	0	-2	-2
X	-1	-	0	-2	0	-1	-2	-1	-3	-2

Results of odor intensity of samples OS-M and OS-M-HTC.

Assessor	OS-M					OS-M-HTC				
	<i>SE<sub>Clean</sub></i>	<i>SE<sub>Break</sub></i>	<i>SE<sub>Stoic</sub></i>	<i>SE<sub>Feed</sub></i>	<i>SE<sub>Satur</sub></i>	<i>SE<sub>Clean</sub></i>	<i>SE<sub>Break</sub></i>	<i>SE<sub>Stoic</sub></i>	<i>SE<sub>Feed</sub></i>	<i>SE<sub>Satur</sub></i>
I	3	3	2	3	2	2	1	3	4	1
II	2	3	2	5	1	2	3	3	4	3
III	4	4	5	5	3	2	2	4	4	3
IV	3	2	1	1	2	4	4	3	4	5
V	3	3	2	2	1	5	3	2	5	3
VI	2	2	3	4	3	2	2	3	3	2
VII	3	2	3	4	3	2	3	4	4	4
VIII	5	3	3	2	4	4	4	3	3	2
IX	3	-	1	1	2	3	2	2	4	3

## APPENDIX C

**ASSESSORS COMMENTS ON THE EVALUATION OF ODOR HEDONIC  
TONE AND INTENSITY OF SAMPLES OS-M-HTC OS-M**

Table C1. OS-M-HTC - Comments on Odor Hedonic.

OS-M-HTC Comments on Odor Hedonic Tone			
Sample label	Comments	Sample label	Comments
$SE_{Clean}$	Mild odor little unpleasant (2x);	$SE_{Feed}$	Smells something rotten (2x)
	It gets unpleasant after a while;		Smells sewage sludge;
	Smell of acid;		Smells sewage;
	Smell of exhaust fumes of a car with malfunctioning catalyst;		Burnt odor, more than $SE_{Stoic}$ ;
	Smells corn chips (2x);		Weak smell of wood decomposition;
	Smell of cleaning product;		Smells animal stable;
	Smell of dentist's office;		Very unpleasant.
$SE_{Break}$	Smells wood.	$SE_{Satur}$	Less unpleasant than $SE_{Feed}$ ;
	Similar to $SE_{Clean}$ (2x);		Less unpleasant than $SE_{Break}$ ;
	Similar to $SE_{Clean}$ , but less unpleasant;		Very similar to $SE_{Clean}$ , but more unpleasant;
	Less unpleasant than $SE_{Clean}$ ;		Smelly feet;
	Little more unpleasant than $SE_{Clean}$ ;		Similar to $SE_{Clean}$ , $SE_{Break}$ and $SE_{Stoic}$ ;
	Slightly unpleasant;		Similar to $SE_{Stoic}$ ;
	Burnt odor (2x);		Smell of chemical product or poison;
	Slightly smell of hay or straw;		Smell of dentist's office.
$SE_{Stoic}$	Smell of grass;		
	Smell of chemical product or poison;		
	Smell of brand-new sneakers.		
	Similar to $SE_{Clean}$		
	Similar to $SE_{Break}$ (2x)		
	Less unpleasant than $SE_{Break}$ ;		
	Little more unpleasant than $SE_{Clean}$ ;		
	Slightly smells like corn chips (2x);		
	Burnt odor, more than $SE_{Break}$ ;		
	Smells polystyrene;		
	Unpleasant but not much;		
	Smells bird food.		

Table C2. OS-M - Comments on Odor Hedonic.

OS-M Comments on Odor Hedonic Tone	
Sample label	Comments
$SE_{Clean}$	Smells something roasted; Known odor, however unidentified.
$SE_{Break}$	Similar to $SE_{Clean}$ (3x); Smells something roasted; Warming sensation.
$SE_{Stoic}$	Similar to $SE_{Clean}$ ; Cooling sensation; Smells rotten wood; Smells products used in water treatment in swimming pools.
$SE_{Feed}$	Characteristic smell, however unidentified; Smell of frying but unpleasant.
$SE_{Satur}$	Similar to $SE_{Feed}$ ; Warming sensation; Smelly feet; Parmesan cheese; Strange odor.



Table C3. OS-M - Comments on Odor Intensity.

OS-M-HTC Comments on Odor Intensity	
Sample label	Comments
$SE_{Clean}$	Intense sour smell
$SE_{Break}$	Little more intense than $SE_{Clean}$ (2x), however same unpleasantness
$SE_{Stoic}$	Little more intense than $SE_{Clean}$ and $SE_{Break}$ ; Little less intense than $SE_{Break}$ .
$SE_{Feed}$	Little more intense than $SE_{Clean}$ , $SE_{Break}$ , and $SE_{Stoic}$ ; The odor is different from $SE_{Clean}$ , $SE_{Break}$ , and $SE_{Stoic}$ ; however, similar intensity.
$SE_{Satur}$	Little less intense than $SE_{Feed}$ .

## COMMUNICATIONS

Lima, T. P.; Saviotti, M. C.; Diaz de Tuesta, J. L.; Gomes, H. T.; Wilken, A. A. P.; Feliciano, M. (2020). *Performance of adsorbents prepared from olive stones on the removal of gaseous ammonia*. In: *VI CIEEMAT - Congresso Ibero-americano de Empreendedorismo, Energia, Meio Ambiente e Tecnologia*, Rio de Janeiro, Brasil. Submitted and accepted for oral presentation.

Lima, T. P.; Saviotti, M. C.; Diaz de Tuesta, J. L.; Gomes, H. T.; Wilken, A. A. P.; Feliciano, M. (2019). *Evaluation of the adsorption capacity of carbonaceous materials prepared from biomass in the removal of air pollutants*. In: *III Congresso Nacional das Escolas Superiores Agrárias*, Viseu, Portugal. Poster presentation.

Lima, T. P.; Diaz de Tuesta, J. L.; Gomes, H. T.; Brianezi, D.; Feliciano, M. (2019). *Avaliação da capacidade de adsorção de poluentes atmosféricos em carvões ativados produzidos a partir de resíduos orgânicos*. In: *2ª Escola de verão e Simpósio de Dupla Diplomação*, Instituto Politécnico de Bragança, Bragança, Portugal. Oral presentation.